Designing Cathodic Protection Systems *for* Marine Structures *and* Vehicles

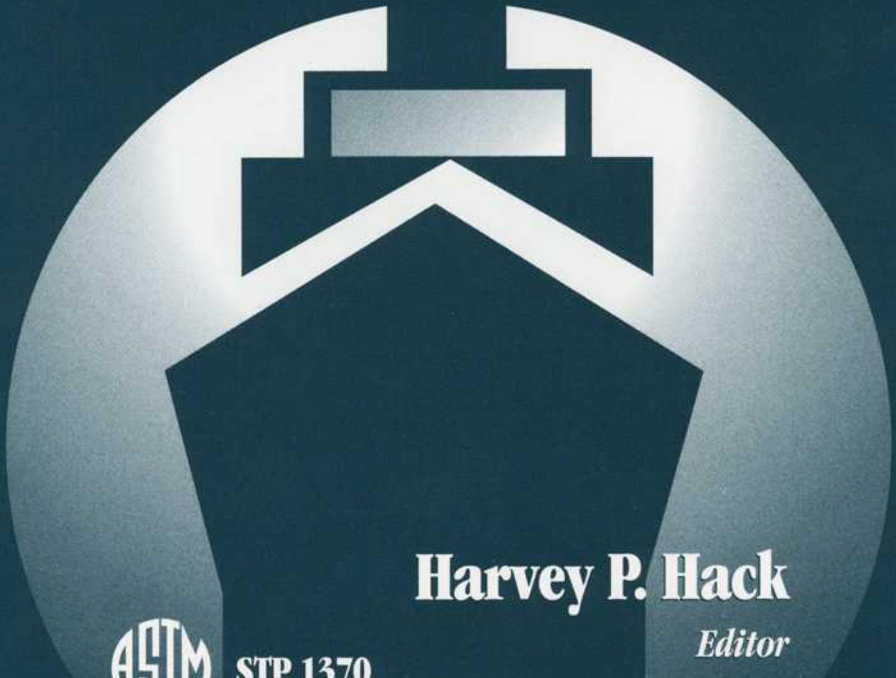

Harvey P. Hack

Editor

ASTM STP 1370

STP 1370

Designing Cathodic Protection Systems for Marine Structures and Vehicles

Harvey P. Hack, editor

ASTM Stock Number: STP1370

ASTM
100 Barr Harbor Drive
West Conshohocken, PA 19428-2959

Printed in the U.S.A.

Library of Congress Cataloging-in-Publication Data

Designing cathodic protection systems for marine structures and vehicles / Harvey P. Hack, editor.
p. cm. -- (STP ; 1370)
"ASTM stock#:STP1370."
Includes bibliographical references.
ISBN 0-8031-2623-9
1. Corrosion and anti-corrosives. 2. Seawater corrosion. 3. Ships--Cathodic protection. 4. Offshore structures--Protection. I. Hack, Harvey P. II. Series. III. ASTM special technical publication ; 1370.

TA462 .D47 1999
620.l'1223--dc21

99-051443

Photocopy Rights

Authorization to photocopy items for internal, personal, or educational classroom use, or the internal, personal, or educational classroom use of specific clients, is granted by the American Society for Testing and Materials (ASTM) provided that the appropriate fee is paid to the Copyright Clearance Center, 222 Rosewood Drive, Danvers, MA 01923, Tel: 508-750-8400; online: http://www.copyright.com/.

Peer Review Policy

Each paper published in this volume was evaluated by two peer reviewers and at least one editor. The authors addressed all of the reviewers' comments to the satisfaction of both the technical editor(s) and the ASTM Committee on Publications.

To make technical information available as quickly as possible, the peer-reviewed papers in this publication were prepared "camera-ready" as submitted by the authors.

The quality of the papers in this publication reflects not only the obvious efforts of the authors and the technical editor(s), but also the work of these peer reviewers. In keeping with long standing publication practices, ASTM maintains the anonymity of the peer reviewers. The ASTM Committee on Publications acknowledges with appreciation their dedication and contribution to time and effort on behalf of ASTM.

Printed in Baltimore, MD
November 1999

Foreword

The Symposium on Designing Cathodic Protection Systems for Marine Structures and Systems was held 3 Nov. 1998 in Norfolk, Virginia. Committee G1 on Corrosion of Metals sponsored the symposium. Harvey P. Hack, Northrop Grumman Corporation, presided as symposium chairman and is editor of this publication.

Contents

Overview

Cathodic protection is an important method of protecting structures and ships from the corrosive effects of seawater. Design of cathodic protection systems can significantly effect the usable lifetime of a structure. Poor designs can be far more costly to implement than optimal designs. Improper design can cause overprotection, with resulting paint blistering and accelerated corrosion of some alloys, underprotection, with resultant structure corrosion, or stray current corrosion of nearby structures. The first ASTM symposium specifically aimed at cathodic protection in seawater was held on 3 November, 1998, in Norfolk, VA. This symposium intended to compile all the criteria and philosophy for designing both sacrificial and impressed current cathodic protection systems for structures and vehicles in seawater. It was not possible to comprehensively cover this topic in a single day, however. The papers which are included in this STP are significant in that they summarize the major seawater cathodic protection system design philosophies.

The first paper, by Hartt, is a summary of the latest approach to determining cathodic protection current requirements for marine structures. This approach, called the Slope Parameter Approach, allows for the formation of calcareous deposits in a more accurate fashion than the older, traditional, methods, and has recently been used as the basis for development of a Standard by NACE International.

The U.S. Navy has probably designed more cathodic protection systems for ships than any other organization. In recent years, the Navy has begun to use physical scale modeling to optimally place reference cells and anodes, and to select the best system size and capacity. The paper by Lucas et al. describes the method that the Navy uses to test scale models, and how this information is translated into actual ship designs.

In the past, zinc was the most common material used for sacrificial cathodic protection anodes. In recent years, aluminum alloys have surpassed zinc in popularity due to their increased efficiency, lower weight, and lower cost. Formulation of aluminum anodes is critical. The paper by Schrieber, a renowned expert in aluminum anode formulations and performance, details how these anodes are properly formulated for various environments.

All cathodic protection design elements are put together in the example of a protection system for a complex wharf structure presented in the paper by Nikolakakos. The complexity of the geometry of this wharf makes for unique challenges to the cathodic protection design.

Providing cathodic protection for structures in deep water, such as offshore oil platforms, **offers** unique challenges. **The paper by Menendez et al. gives the experiences of a company that has done many deep water designs.** These practical experiences are invaluable to anyone considering a design in deep water.

The latest technology for predicting cathodic protection current distribution and magnitude is the use of Boundary Element computer modeling. One of the leaders in this field, the U.S. Navy, shows examples of the utility of this approach in the paper by DeGiorgi et al. In this paper, the results of computer models of shipboard cathodic protection systems are compared to the performance of these systems on ships in service.

The final paper in this volume by Zook discusses a unique application of cathodic protection—preventing corrosion of space shuttle solid rocket boosters during ocean recovery. The challenges of designing a system which is very weight-critical and which must protect a large area for a short time are unique in the corrosion world.

Each of these papers summarizes a particular aspect of marine cathodic protection design. Therefore, this volume will be a valuable reference for designers of marine cathodic protection systems and evaluators of designs performed by others.

Harvey P. Hack
Northrop Grumman Corporation,
Annapolis, MD
symposium chairman and editor.

William H. Hartt[1]

The Slope Parameter Approach to Marine Cathodic Protection Design and Its Application to Impressed Current Systems

Reference: Hartt, W. H., "**The Slope Parameter Approach to Marine Cathodic Protection Design and Its Application to Impressed Current Systems,**" *Designing Cathodic Protection Systems for Marine Structures and Vehicles, ASTM STP 1370*, H. P. Hack, Ed., American Society for Testing and Materials, West Conshohocken, PA, 1999.

Abstract: The recently developed slope parameter approach to design of galvanic anode cathodic protection (cp) systems for marine structures constitutes an advancement in this technology compared to current practice, primarily because the former is first principles based and the latter is an empirical algorithm. In this paper, the slope parameter approach is reviewed; and related applications for which it can be utilized, including 1) design of new and retrofit cp systems, 2) evaluation of potential survey data, and 3) cp system design for complex geometries, are mentioned. The design current density is identified as the single remaining parameter for which values must be projected solely by experience or experimentation. In addition, the slope parameter approach is applied to the results of impressed current cp experiments, and it is shown how parameters for this can be interrelated with those of galvanic anode cp. Advantages of this capability are identified and discussed.

Keywords: cathodic protection, impressed current, galvanic anode, slope parameter, offshore structures, design, marine, seawater.

Introduction

General

Since its inception some 160-plus years ago [*1-3*], cathodic protection (cp) has evolved as the principal means of corrosion control for the submerged portion of metallic structures such as offshore structures, pipelines, and ships. Despite the classical, scientific research of Davy which introduced this technology, its subsequent development has been at best incremental, largely lethargic, and

---

[1] Professor of Ocean Engineering and Director of the Center for Marine Materials, Florida Atlantic University, Boca Raton, Florida 33431

predicated upon trial and error. Presumably this is a consequence, at least in part, of corrosion control not being viewed as directly tied to profit by private sector leadership and to mission accomplishment by the military. Also responsible, however, has been the technical community at large which historically has failed to appreciate and to give adequate priority to structure longevity, even on a justifiable life-cycle cost basis, as a part of the design process.

Irrespective of this, the current recommended practices that address the design of marine cathodic protection systems for fixed offshore structures [*DnV Recommended Practice RP401, "Cathodic Protection Design," Det Norske Veritas Industri Norge AS, 1993; NACE Standard RP 0176-94, "Corrosion Control of Steel-Fixed Offshore Platforms Associated with Petroleum Production", NACE International, Houston, 1994*] are based upon determination of the current output per anode, I_a, as calculated from Ohm's law according to the expression

$$I_a = \frac{\phi_c - \phi_a}{R_a}, \tag{1}$$

where ϕ_c and ϕ_a are the closed circuit cathode and anode potentials, respectively, and R_a is resistance of an individual anode. For three dimensional or spaceframe type structures protected by galvanic cp systems, anode resistance is normally the dominant component of the total circuit resistance; and so it alone need be considered. In most cases, R_a is calculated from standard, closed form numerical relationships which have been reported in the literature [*4-10*] in terms of anode dimensions and electrolyte resistivity. Figure 1 graphically illustrates the

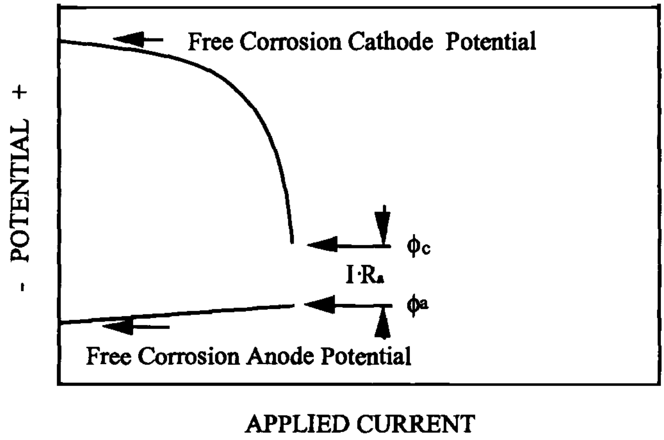

Figure 1 - *SchematicIllustration of Potential, Current, and Resistance Terms for Cathodically Polarized Steel in Sea Water*

principle behind Equation 1 as a schematic polarization curve for both anode and structure. This representation is complicated, however, by the fact that both the anodic and cathodic curves are likely to be a function of time because of progressive corrosion product accumulation and development of local action cells at the anode and calcareous deposits and fouling upon the steel. From the net current for protection (Equation 1) the number of anodes required for protection, N, is determined from the relationship

$$N = \frac{i_c \cdot A_c}{I_a}, \tag{2}$$

where i_c is the cathode current density and A_c is the cathode surface area.

Rapid Polarization

A cornerstone principle of present design practice is the concept of rapid polarization [*11-17*], whereby application of a relatively high current density initially results in a more protective calcareous deposit than if current density were lower. Consequently, the design process [*DnV Recommended Practice RP401, NACE Standard RP 0176-94*] incorporates three current densities, an initial (i_o), mean (i_m), and final (i_f), instead of just one, as was done previously [*NACE Standard RP 0176, "Corrosion Control of Steel-Fixed Offshore Platforms Associated with Petroleum Production", NACE, Houston, 1976*]. Here, i_o and i_f are evaluated using Equations 1 and 2; and respective values of N, N_o, and N_f, respectively, are determined for each. On the other hand, the requisite number of anodes corresponding to i_m is calculated from the mass balance relationship,

$$N_m = \frac{i_m \cdot A_c \cdot T}{C \cdot w}, \tag{3}$$

where T is the design life, C is anode current capacity, and w the weight of a single anode.

Typical values for these three design current densities are listed in Table 1 [*NACE Standard RP 0176-94*]. Ideally, each of the three calculations should yield the same N; however, this is invariably not the case; and so the highest of the three is specified. For uncoated structures, this is normally N_o. Accordingly, the cp system may be overdesigned in terms of the other two current density requirements. This failure of the design procedure to yield a common anode number for each of the three current density criterion arises because the procedure is an empirical algorithm rather than being first principles based.

The predominant reaction which occurs upon cathodic surfaces in natural waters is oxygen reduction or

Table 1 - *Design Current Density Criteria for Marine Cathodic Protection Systems*

Production Area	Typical Design Current Density, mA/m^2 (mA/ft^2)		
	Initial	Mean	Final
Gulf of Mexico	110 (10)	55 (5)	75 (7)
U.S. West Coast	150 (14)	90 (8)	100 (9)
Cook Inlet	430 (40)	380 (35)	380 (35)
Northern North Sea	180 (17)	90 (8)	120 (11)
Southern North Sea	150 (14)	90 (8)	100 (9)
Arabian Gulf	130 (12)	65 (6)	90 (8)
Australia	130 (12)	90 (8)	90 (8)
Brazil	180 (17)	65 (6)	90 (8)
West Africa	130 (12)	65 (6)	90 (8)
Indonesia	110 (10)	55 (5)	75 (7)

$$\frac{1}{2}O_2 + H_2O + 2e^- \rightarrow 2OH^-; \qquad (4)$$

however, at potentials negative to that of the reversible hydrogen electrode,* water dissociation or the reaction

$$H_2O + e^- \rightarrow \frac{1}{2}H_2 + OH^- \qquad (5)$$

also transpires. Figure 2 presents data from a series of experiments where steel specimens were galvanically coupled in natural seawater to an aluminum anode ring through an external resistor, the size of which varied for each test [*18*]. By interconnecting the resultant data points at 24 hours exposure, a polarization curve, the slope of which is negative at all potentials and which is indicative of relatively limited oxygen concentration polarization, was identified. However, similar curves for progressively greater exposure times reveal development of a sigmoidal trend. Figure 3, which shows the 3200 hours and additional longer-term data, illustrates in greater detail the steady-state potential-current density *(ϕ-i)* relationship that results from this type of experiment. These results and the data representation which has been employed here render apparent the basis, if not the mechanism, for rapid polarization in that the current density that ultimately

---

* The pH at the surface of cathodically protected steel in sea water is thought to be about 9.5, in which case the reversible hydrogen electrode potential is about -0.78v (Ag/AgCl).

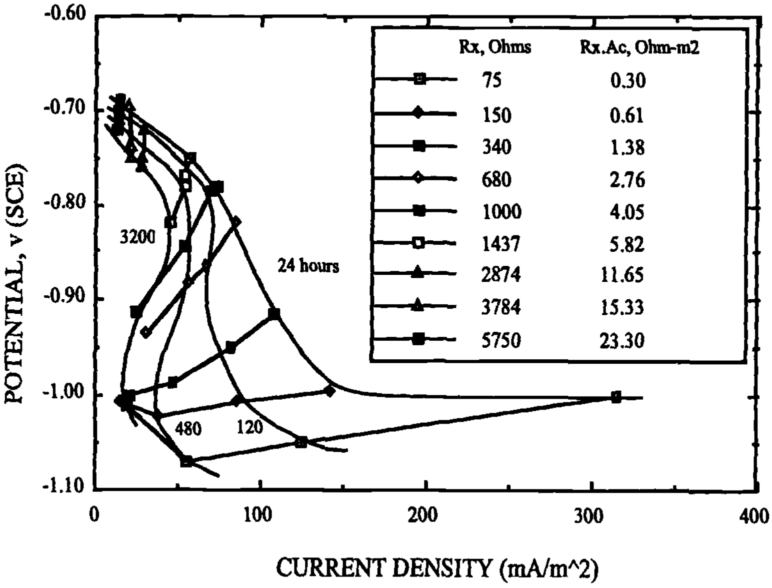

Figure 2 - *Cathodic Potential versus Current Density for Representative Laboratory Experiments at Different Exposure Times*

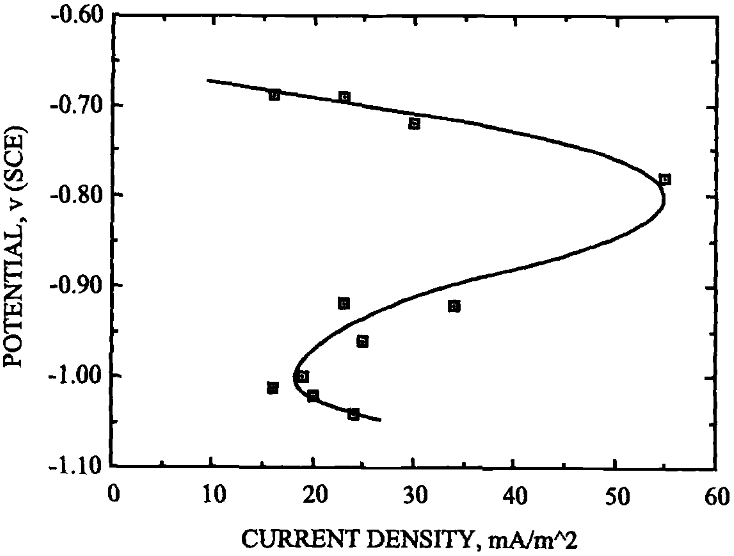

Figure 3 - *Long-Term ϕ-I Relationship for Steel in Sea Water as Determined from Laboratory Experiment*

resulted from modest cathodic polarization, such that the least (most positive) protection potential (-0.80 v (Ag/AgCl)) was achieved only in the long-term, is about 2.5 times greater than if the long-term potential were near -1.00 v*. The trend in Figures 2 and 3, where current density increases with increasing cathodic polarization for potentials below about -1.00 v, was attributed to the hydrogen reaction (Equation 5). Thus, the optimum situation is one where the steady-state potential of protected structures is in the range -0.90 to -1.05 v.

Any comprehensive effort to advance marine cathodic protection practice must include an improved understanding of the long-term ϕ-i relationship (Figure 3), the variables upon which it depends, and how and why it evolves. To this end, it is generally recognized that the minimum maintenance current density that results in the potential range -0.90 to -1.05 v reflects establishment of a particularly protective calcareous deposit [*18-24*]. Such deposits form as a consequence of reactions 3 and 4 displacing the inorganic carbon equilibria, as expressed by the reactions

$$CO_2 + H_2O \rightarrow H_2CO_3, \qquad (6)$$

$$H_2CO_3 \rightarrow HCO_3^- + H^+, \text{ and} \qquad (7)$$

$$HCO_3^- \rightarrow CO_3^{2-} + H^+, \qquad (8)$$

to the right such that pH in the vicinity of the cathode is increased and calcium and magnesium rich compounds precipitate according to

$$Ca^{2+} + CO_3^{2-} \rightarrow CaCO_3 \downarrow \text{ and} \qquad (9)$$

$$Mg^{2+} + 2OH^- \rightarrow Mg(OH)_2 \downarrow. \qquad (10)$$

Presumably, the finding that deposits which formed in the potential range from -0.90 to -1.05 v were the most protective (that is, these were most impermeable to oxygen ingress such that current density was minimum) resulted because those that formed at more positive potentials were thinner or less dense (or both) and those at more negative potentials became dislodged by hydrogen gas generation (Equation 5). It is also possible that deposits which formed outside this optimum potential range have a different composition or microstructure (or both) and less protective properties.

---

*The difference in reference electrode for Figures 2 and 3 (saturated calomel) and the potential criterion from recommended practices [*DnV Recommended Practice RP401, NACE Standard RP 0176-94*] (Ag/AgCl) is expected to be negligible and has not been considered.

Slope Parameter Method of Galvanic Anode Cathodic Protection Design

Analytical Representation of Polarization Data - In an attempt to quantify the above polarization behavior, Fischer et al. [*14*] considered the interrelationship between ϕ_a and ϕ_c in terms of the anodic or cathodic current (I_a or I_c, respectively) according to Ohm's law as

$$I_c = I_a = \frac{\phi_c - \phi_a}{R_a + R_c + R_x}, \tag{11}$$

where R_x and R_c are the external (metallic path) and cathode resistances, respectively. In effect, this is a generalization from which Equation 1 was developed (see Figure 1 also). Upon rearranging, expressing I_c in terms of current density, and substituting a total resistance term, R_t, for the sum of the different components,

$$\phi_c = (R_t \cdot A_c) \cdot i_c + \phi_a. \tag{12}$$

Thus, a linear interdependence between cathode potential and current density is projected, the slope of which equals the product of the total circuit resistance and cathode area with the vertical axis intercept corresponding to the anode potential, assuming R_t, A_c, and ϕ_a are constant with time. Several recent investigations have substantiated this relationship [*18,25-28*] for various conditions ranging from small laboratory specimens to actual offshore structures. In this regard, Figure 4 presents ϕ-i data for the cp system upon a Gulf of Mexico structure deployed in 162 m deep water during the initial 7,000 hours [*29*] in comparison to a laboratory specimen of identical slope parameter (R_x = 450 Ohms). This reveals excellent correlation between the two, thereby indicating how results from vastly different structures and components can be compared directly. Other areas of applicability include interpretation of potential survey data [*25*], design of retrofit cp systems [*26*], design of cp for systems which include components of different geometries [*28*], and cp system design itself [*25*].

A Unified Design Equation – The slope term in Equation 12, $R_t \cdot A_c$, (also designated as the slope parameter, *S*) becomes, for a structure with multiple galvanic anodes of identical geometry [*18, 25-27*],

$$S = \frac{R_a \cdot A_c}{N}. \tag{13}$$

Combining this with Equation 3 yields

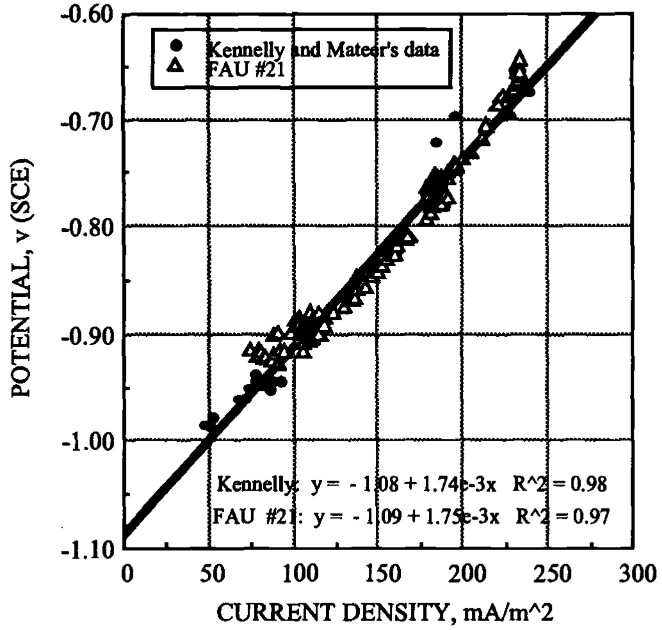

Figure 4 - *Comparison of Polarization Trend from an Offshore Structure and Laboratory Specimen where the Slope Parameter was the Same in the Two Cases*

$$R_a \cdot w = i_m \cdot T \cdot K \cdot S, \tag{14}$$

where w is the weight of an individual anode, and K is anode consumption rate or inverse of capacity, C *[25-27]*. Application of Equation 14 to a particular design situation requires that a value for S be specified, as discussed below. Once this is done, all terms on the right side are known from the design choices; and so the process is reduced to determination of the optimum combination of R_a and w. Figure 5 presents a schematic illustration of four design alternatives (choices for S) in relation to the dynamic and steady-state polarization curves. Thus, design according to S_1 results in underprotection and S_2 in protection but at a relatively high current density. Designs in the range from S_3 to S_4, on the other hand, yield the optimum situation (adequate protection and minimum current density). The value of this approach compared to current practice [*DnV Recommended Practice RP401, NACE Standard RP 0176-94*] is that both i_o and i_m are represented in Equation 14, the latter explicitly and the former implicitly in S. Consequently, the design can be optimized in terms of both parameters. However, a residual limitation of cp design is that S (alternately, i_o and i_m) must still be specified based upon experience or experimentation (or both).

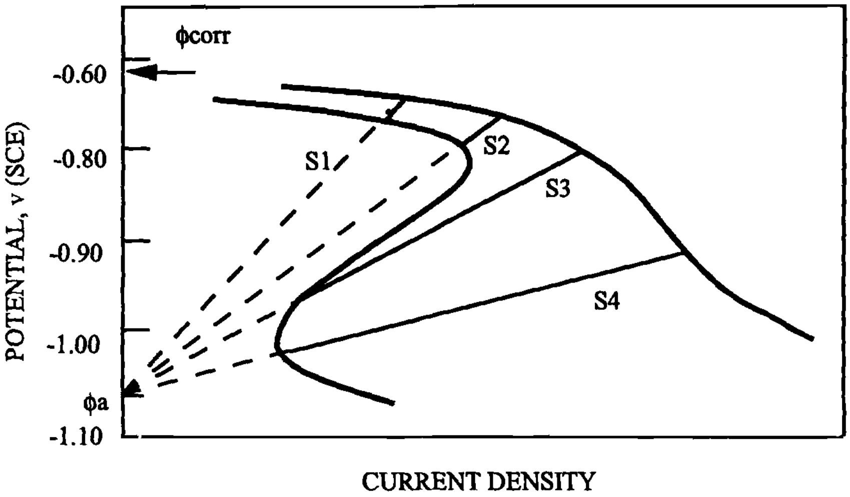

Figure 5 - *Schematic representation of alternative design slopes in perspective to the long-term ϕ-i curve*

Research Objective

The objective of the present research was to evaluate applicability of the slope parameter approach, as this has been developed for galvanic anode cathodic protection, to design of impressed current cp systems. In accomplishing this, laboratory experiments were performed upon cathodically polarized steel specimens in seawater and the results analyzed in terms of the *ϕ-i* relationship (Equation 12). This paper reports the results of the findings.

Experimental Procedure

The experiments involved cathodic polarization of a 0.560 m wide by 0.333 m high by 3.2 mm thick UNS-G10150 carbon steel plate. Specimen preparation consisted of 1) degreasing with acetone, 2) sand blasting, 3) bolting and soldering an electrical lead wire at the top center of the plate, 4) degreasing a second time, and 5) coating the back side and the electrical connection with Pilgrim Plastics EM5 epoxy. For each experiment, a new steel plate was placed fully submerged in a 0.61 m wide by 0.30 m deep by 0.42 m high glass tank with nylon spacer supports at each corner. Natural seawater, as is available to the laboratory on a once-through basis via a wellpoint located offshore and pump and plastic piping system [*30*], flowed through the tank at a rate of 0.75 l/min. Cathodic polarization was initiated after approximately ten minutes of free corrosion by energizing a Tektronics PS 280 direct current power supply at either 2.00, 2.50, or 3.00 v. A 152 by 95 mm section of Elgard 210 mixed metal oxide mesh positioned at the top of the tank opposite the steel plate served as the counter electrode. Two commercial saturated calomel reference electrodes (SCE) were employed to independently measure the anode and steel potentials. In each case, this was done in conjunction with a Luggin probe, the tip of which was positioned approximately one mm from the electrode of interest (anode or cathode). Current through the cp circuit was determined from the voltage drop across a ten Ohm resistor in series between the power supply and steel cathode. Potentials and voltages were recorded using a pc based data acquisition system. Figure 6 shows a schematic illustration of the experimental arrangement.

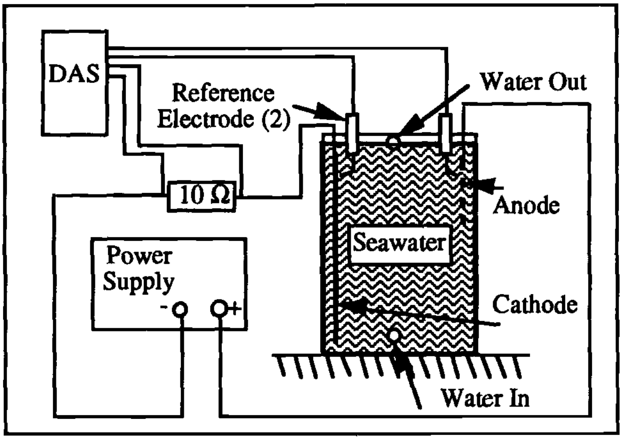

Figure 6 - *Schematic Illustration of the Experimental Set-Up*

Results and Discussion

Figure 7 shows a typical plot of cathode and anode potential as a function of time and indicates that, in this case, the cathode polarized within a relatively brief period to approximately –1.10 v, after which potential remained essentially constant. Anode potential was relatively invariant at near 1.12 v for the entire duration of the experiment. Correspondingly, Figure 8 shows that current density also decreased with time and stabilize near 125 mA/m^2 after about 50 hours.* Figure 9, in turn, shows a ϕ-i plot for experiments at each of the three applied voltages. Consistent with both R_t and anode potential being constant during the experiments, a linear trend between these two parameters is apparent in accordance with Equation 12. However, for the impressed current case, Equation

---

*Duration of the present experiments was from one to several weeks, and so the current densities referred to do not reflect truly long-term or maintenance values.

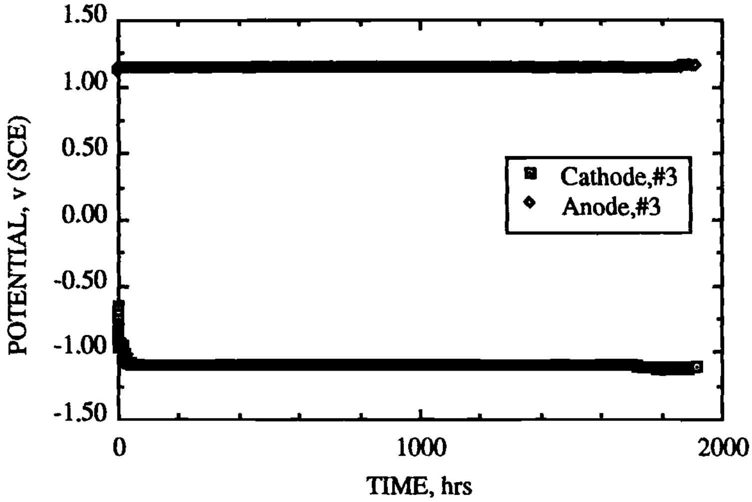

Figure 7 - *Anode and Cathode Potential as a Function of Time under Polarization for Experiment 3 (2.50 v Applied)*

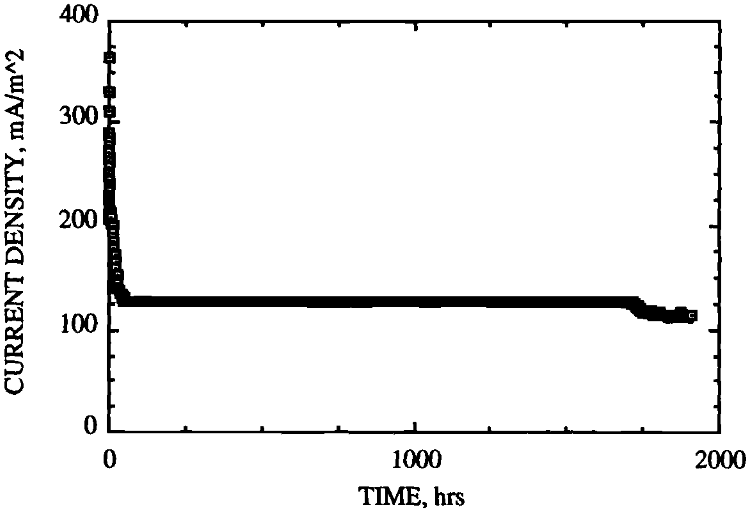

Figure 8 - *Cathode Current Density as a Function of Time under Polarization for Experiment 3 (2.50 v Applied)*

12 must be rewritten as

$$\phi_c = (R_t \cdot A_c) \cdot i_c + \phi_a(eq), \tag{14}$$

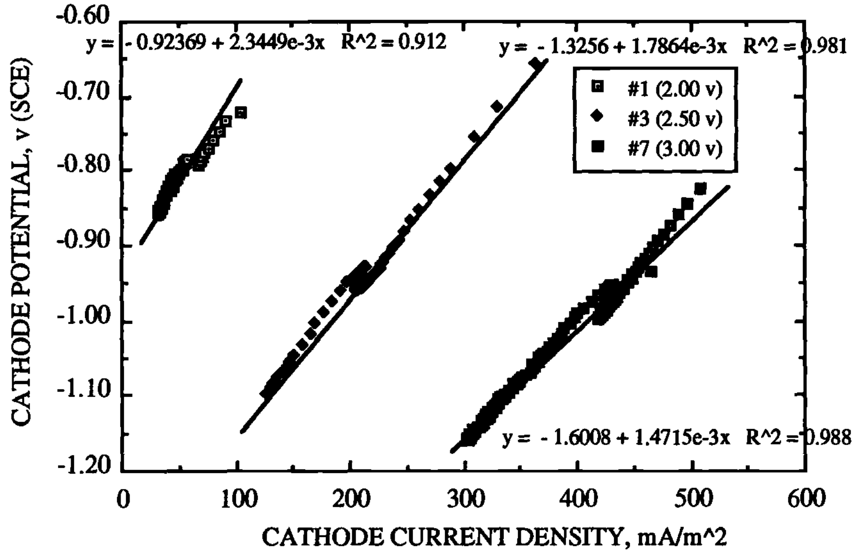

Figure 9 - *Plot of Cathode Potential versus Cathode Current Density for Impressed Current Experiments Performed at 2.00, 2.50, and 3.00 v*

where $\phi_a(eq)$ is an equivalent anode potential; that is, the anode potential on the basis of this electrode being galvanic, and not the measured value of the impressed current anode, which is designated below as $\phi_a(ic)$. The three best fit lines in Figure 9 have slopes of 2.34, 1.79, and 1.47 $\Omega \cdot m^2$ for the 2.00, 2.50, and 3.00 v applied voltage cases, respectively. By comparison, the product $R_t \cdot A_c$ (Equation 14) based upon the experimental parameters (R_t = 10 Ω and A_c = 0.186 m^2) is 1.86 $\Omega \cdot m^2$, thus indicating general agreement between the two. Alternatively, the vertical intercept (-0.92, -1.33, and –1.60 v for the 2.00, 2.50, and 3.00 v experiments, respectively) corresponds to the equivalent galvanic anode potential, designated $\phi_a(eq)$, which provides the same polarization as achieved via impressed current.

Bazzoni and Lazzari [*31*] proposed a relationship between polarized anode and cathode potentials and applied voltage for the specific case of impressed current (ic) cathodic protection of prestressing steel in concrete as

$$E = \phi_a(ic) + (-\phi_c) + E_m + E_{concr}, \qquad (15)$$

where E is the rectifier voltage, which is assumed to be constant, $\phi_a(ic)$ is the potential of the ic anode, and E_m and E_{concr} are the lead wire (metallic) and concrete path Ohmic drops, respectively. For an iccp system on an offshore structure, the latter term is replaced by the anode Ohmic drop, E_a. Thus,

$$E = \phi_a(ic) + (-\phi_c) + E_m + E_a. \tag{16}$$

For the present experiments, the Ohmic drop associated with the external ten Ohm resistor, E_x, alone was present; and so

$$E = \phi_a(ic) + (-\phi_c) + E_x. \tag{17}$$

Substitution of the measured values for ϕ_a, ϕ_c, and E_x from each of the three experiments into the latter expression indicated that the average value for E in the case of Experiment #1 (2.00 v applied voltage) was 2.00 v, for Experiment #3 (2.50 v applied voltage) 2.48 v, and for Experiment #7 (3.00 v applied voltage) 2.93 v. This constitutes excellent agreement between theory and experiment. It follows that for situations where hydrogen embrittlement is a concern, an iccp system can be designed to avoid excessive polarization by substituting Equation 14 into Equation 16 to give

$$E = \phi_a(ic) - \phi_a(eq). \tag{18}$$

Then, by setting $\phi_a(eq)$ equal to some lower potential limit (-1.05 v (Ag/AgCl), for example) and knowing the anode polarization characteristics (ϕ_a), the corresponding rectifier voltage can be calculated.*

Conclusions

Although the slope parameter approach to cathodic protection design was developed specifically for galvanic anode systems, it also has utility for design and analysis of impressed current ones. In the latter case, the governing expression is

$$\phi_c = (R_t \cdot A_c) \cdot i_c + \phi_a(eq).$$

where ϕ_c is the polarized cathode potential, R_t is the total circuit resistance, A_c is the cathode area, i_c is cathode current density, and $\phi_a(eq)$ is the potential a galvanic anode would have to exhibit to affect polarization equivalent to that of the impressed current system. On the other hand, rectifier voltage, E, polarized

---

* Potential attenuation normally occurs along pipelines, risers, tendons, and even tubular members on fixed structures, in which case ϕ_c is spatially variable. How this can best be accommodated into Equations 16 and 17 is beyond the scope of the present paper.

impressed current anode and cathode potentials ($\phi_a(ic)$ and ϕ_c, respectively), and lead wire and anode Ohmic drops (E_m and E_a, respectively) are interrelated through the expression

$$E = \phi_a(ic) + (-\phi_c) + E_m + E_a.$$

Combining these two equations to eliminate ϕ_c yields

$$E = \phi_a(ic) - \phi_a(eq).$$

Excessive polarization can then be avoided by defining a minimum value for $\phi_a(eq)$, knowing the anode polarization characteristics ($\phi_a(ic)$), and solving for E.

Acknowledgements

The author is indebted to Mr. George Jones for conducting the experimental portions of this research. Also appreciated is the financial and technical support provided by past and present Joint Industry Projects whose membership includes Amoco, British Petroleum, Chevron, Elf Aquataine, Exxon, Marathon, Minerals Management Service, Mobil, Shell, and Texaco.

References

[1] Davy, H., *Phil. Trans. Royal Soc. London*, Vol. 114, 1824, p.151.

[2] Davy, H., ibid, Vol. 114, 1824, p.242.

[3] Davy, H., ibid, Vol. 115, 1825, p.328.

[4] Dwight, H. B., "Calculations of Resistance to Ground," *Electrical Engineering*, Vol. 55, 1936, pp. 1319-1328.

[5] Sunde, E. D., *Earth Conduction Effects in Transmission Systems*, Dover Publications, Inc., New York, 1968.

[6] McCoy, J. E., "Corrosion Control by Cathodic Protection – Theoretical and Design Concepts for Marine Applications," *Transactions Institute of Marine Engineers*, Vol. 82, 1970, pp. 210-214.

[7] Cochran, J. C., "A Correlation of Anode-to-Electrolyte Resistance Equations Used in Cathodic Protection," paper no. 169 presented at CORROSION/82, March 22-26, 1982, Houston.

[8] Strommen, R., "Evaluation of Anode Resistance Formulas by Computer Analysis," *Materials Performance*, Vol. 24(3), 1985, pp. 9-15.

[9] Sunde, E. D., *Earth Conduction Effects in Transmission Systems*, Dover Publications, Inc., New York, 1968, p. 72.

[10] Cochran, J. C., "Additional Anode-to-Electrolyte Resistance Equations Useful in Offshore Cathodic Protection," paper no. 254 presented at CORROSION/84, April 2-6, 1984, New Orleans.

[11] Cox, G. C., U.S. Patent 2,200,469, May 14, 1940.

[12] Foster, T., and Moores, V. G., "Cathodic Protection Current Demand of Various Alloys in Seawater," paper no. 295 presented at CORROSION/86, March 17-21, 1986, Houston.

[13] Mollan, R. and Anderson, T. R., "Design of Cathodic Protection Systems," paper no. 286 presented at CORROSION/86, March 17-21, 1986, Houston.

[14] Fischer, K. P., Sydberger, T., and Lye, R., "Field Testing of Deep Water Cathodic Protection on the Norwegian Continental Shelf," paper no. 67 presented at CORROSION/87, March 9-13, 1987, San Francisco.

[15] Evans S., "Use of Initial Current Density in Cathodic Protection Design", *Material Performance*, Feb. 1988, Vol. 27(2), pp. 9-11.

[16] Fischer, K. P. and Finnegan, J. E., "Cathodic Protection Behavior of Steel in Sea Water and the Protective Properties of the Calcareous Deposits," paper no. 582 presented at CORROSION/89, April 17-21, 1989, New Orleans.

[17] Schrieber, C. F. and Reding, J., "Application Methods for Rapid Polarization of Offshore Structures," paper no. 381 presented at CORROSION/90, April 23-27, 1990, Las Vegas.

[18] Wang, W., Hartt, W. H., and Chen, S., "Sacrificial Anode Cathodic Polarization of Steel in Seawater," *Corrosion*, Vol. 52, 1996, pp. 419-427.

[19] Wolfson, S. L. and Hartt, W. H., "An Initial Investigation of Calcareous Deposits upon Cathodic Steel Surfaces in Seawater," *Corrosion*, Vol. 37, 1981, pp. 70-75.

[20] Hartt, W. H., Culberson, C. H., and Smith, S. W., "Calcareous Deposits on Metal Surfaces in Seawater – A Critical Review," *Corrosion*, Vol. 40, 1994, pp. 609-618.

[21] Lin, S-H and Dexter, S. C., "Effects of Temperature and Magnesium Ions on Calcareous Deposition," *Corrosion*, Vol. 44, 1988, pp. 615-622.

[22] Finnegan, J. E. and Fischer, K. P., "Calcareous Deposits: Calcium and Magnesium Ion Concentrations," paper no. 581 presented at CORROSION/89, April 17-21, 1989, New Orleans.

[23] Luo, J. S., Lee, R. U., Chen, T. Y., Hartt, W. H. and Smith, S. W., "Formation of Calcareous Deposits under Different Modes of Cathodic Polarization," *Corrosion*, Vol. 47, 1991, pp. 189-196.

[24] Mantel, K. E., Hartt, W. H., and Chen, T. Y., "Substrate, Surface Finish, and Flow Rate Influences on Calcareous Deposit Structure," *Corrosion*, Vol. 48, 1992, pp. 489-500.

[25] W. H. Hartt, Chen, S., and Townley, D. W., "Sacrificial Anode Cathodic Polarization of Steel in Sea Water - Part II: Design and Data Analysis," Corrosion, Vol. 54, 1998, pp. 317-322.

[26] Hartt, W. H. and Chen, S., "Sacrificial Anode Cathodic Polarization of Steel in Sea Water - Part III: Retrofit Cathodic Protection of Offshore Structures," accepted for publication in *Corrosion.*

[27] Townley, D. W., "Unified Design Equation for Offshore Cathodic Protection," paper no. 97473 presented at CORROSION/97, March 9-14, 1997, New Orleans.

[28] Pierson, P. and Hartt, W. H., "Galvanic Anode Cathodic Polarization of Steel in Sea Water – Part IV: Conductor Arrays on Offshore Petroleum Production Platforms," accepted for publication in *Corrosion.*

[29] Kennelley, K. J. and Mateer, M. W., "Evaluation of the Performance of Bi-Metallic Anodes on Deep Water Production Platforms," paper no. 523 presented at CORROSION/93, March 8-12, 1993, New Orleans.

[30] Hartt, W. H., "Fatigue of Welded Structural Steel in Seawater," paper no. 3962, Proc. Offshore Technology Conference, Society of Petroleum Engrs., Richardson, TX, 1980, pp. 87-104.

[31] Bazzoni, B. and Lazzari, L., "A New Approach for Automatic Control and Monitoring of Cathodically Protected Reinforced Concrete Structures," *Materials Performance*, Vol. 31(12), 1992, pp. 13-18.

Keith E. Lucas[1], E. Dail Thomas[2], Alexis I. Kaznoff[3], and Elizabeth A. Hogan[4]

Design of Impressed Current Cathodic Protection (ICCP) Systems for U.S. Navy Hulls

Reference: Lucas, K. E., Thomas, E. D., Kaznoff, A. I., and Hogan, E. A., **"Design of Impressed Current Cathodic Protection (ICCP) Systems for U.S. Navy Hulls,"** *Designing Cathodic Protection Systems for Marine Structures and Vehicles, ASTM STP 1370*, H. P. Hack, Ed., American Society for Testing and Materials, West Conshohocken, PA, 1999.

Abstract: The goal of impressed current cathodic protection (ICCP) design for ship hulls, under the Navy Ship's Technical Manual (NSTM, Chapter 633), is to provide a uniform potential distribution at -0.85 V, ± 0.05 V, versus a silver/silver chloride (Ag/AgCl) reference cell, over the wetted hull surface during all operational aspects of an active ship. To accomplish this, the physical scale modeling (PSM) technique, combined with a rigid design protocol, has been used extensively by the U. S. Navy to provide optimal and retrofit upgrade designs of ICCP systems for hulls. The ICCP design guidance, provided by the protocol, defines the hull properties, hull damage and general power supply requirements. PSM is utilized to determine optimal placement of ICCP components (anodes and reference cells) and to evaluate performance for up to a 15% wetted hull coatings loss under static (pierside) and dynamic (underway) conditions. Data are provided which illustrate the use of the design protocol criteria, along with the integrated PSM technique, to determine ICCP system design and evaluate performance.

Keywords: cathodic protection, impressed current, physical scale modeling, Navy, design criteria

Introduction

ICCP is the standard method utilized by the Navy for the corrosion protection of fleet ship hulls in seawater. These systems, when used in conjunction with good hull coatings, provide for complete life-cycle protection and typically require little maintenance during the life of the ship. The control feature of ICCP uses a reference cell to provide continual

---

[1] Corrosion Engineering Section Head, Naval Research Laboratory, PO Box 1739, Key West, FL 30041
[2] Environmental Effects Branch Head, Naval Research Laboratory, 4555 Overlook Ave, Washington, DC 20375-5343
[3] Director of Materials Engineering, Naval Sea Systems Command, Washington, DC
[4] Corrosion Engineer, Geo-Centers, Inc., PO Box 1739, Key West, FL 33041

monitoring and feed-back of the hull potential to a controller and enables the establishment of self-regulating "set" potential levels for operation, normally at -0.85 V versus the Ag/AgCl reference cell for surface ships.

The design capacity of an ICCP system is estimated by determining the amount of wetted metallic surface that will require protection, incorporating both coated metallic areas and anticipated bare metallic area into the initial assessment. By further utilizing an allowance for coatings deterioration over the life-cycle, a design capacity can be established which will insure rapid initial polarization of the system from a freely corroding "off" state. Beyond this initial assessment of capacity, the design of an ICCP system requires knowledge of the geometry involved and insight into the protection current requirements. The correct placement of ICCP components is the critical factor for balanced system operation and, accordingly, is necessary in order to provide uniform current distribution and sufficient current density to all wetted hull areas throughout the life-cycle.

On large hulls, it has become common practice to divide the ICCP system into geometric jurisdictions, each having independent control and potential monitoring capability, defined as multiple-"zone" systems. These systems protect the hull more effectively, whereby the potential is sensed from a number of control points, rather than one, and each correspondingly regulates local anode current, rather than an entire hull system. A good zone design typically provides more uniform polarization over the hull and enables additional protection current to be supplied to specific geometric areas as required. The determination of the optimal zone configuration is a function of factors such as: hull geometry, wetted surface area, operational design criteria, uncoated non-ferrous components, economics and effective interpretation of model data.

Because of concerns for fleet longevity, reduced maintenance and inherent operational complexities, the Naval Sea Systems Command (NAVSEA) and the Naval Research Laboratory (NRL) have developed a comprehensive methodology for rigorous ICCP design. This methodology utilizes a design "protocol" to first define the corrosion protection requirements for each ship class and currently calls for system engineering to be performed using the physical scale modeling (PSM) technique. The basic technique of PSM uses near-exact scale models to provide the representative geometry needed for design, along with the use of scaled electrolyte, to provide the equivalent ohmic paths.

The basic aspects of potential and current distribution in scaled electrochemical systems were originally discussed in terms of plating and electrodeposition, but apply directly to cathodic protection as well. Initial works by Kasper [1], Agar and Hoar [2] and Waber [3] established the relationship between scaled size and solution conductivity necessary for the physical scale modeling of ICCP systems.

For ICCP, it is the cathodic surfaces that define the behavior, rather than the anodic surface, because the system power supplies can easily overwhelm any anodic resistance and will polarize the cathodic surfaces in response to the reference cell feedback to the controller. Cathodic protection behaves in accordance with Ohm's Law

$$E = I\,(R_P + R_{OHMIC}) \qquad (1)$$

where, E = potential (V), I = current (A), R_P = polarization resistance and R_{OHMIC} = electrolyte ohmic resistance = $\rho L/A$, and where, ρ = electrolyte resistivity, L = length of ship or model and A = area. For exact scaling, it is desired for potential relationships to exist, such that $E_{SHIP} = E_{MODEL}$ and for current density (i) behavior, such that $i_{SHIP} = i_{MODEL}$, where $i = A/m^2$. For a relationship where:

$$E_{SHIP} = I_S(\rho_S L_S/A_S) = i_S(\rho_S L_S) \text{ and } E_{MODEL} = I_M(\rho_M L_M/A_M) = i_M(\rho_M L_M) \qquad (2)$$

it is necessary that $R_{P\,(SHIP)} = R_{P\,(MODEL)}$ for the model to scale exactly, by definition. For scaled models $L_S / L_M = k$ and $\rho_M = \rho_S\,(k)$, where k = scale factor, the relationship becomes:

$$E_{SHIP} = E_{MODEL} = i_S(\rho_S L_M)\,(k) = i_M(\rho_S L_M)\,(k) \qquad (3)$$
$$i_S = i_M$$

For current measurement on the model, it follows from (2) and (3) that:

$$I_S = I_M\,(k)^2 \qquad (4)$$

These relationships are consistent with the Wagner similarity law [4,5] and with scaling relationships for cathodic protection design described by other investigators [6,7,8,9]. The present work is based on this theoretical framework of exact scale geometries, scaled conductivity seawater and representative surface polarization behavior that satisfy these relationships [10,11,12,13,14]. Typically, physical models are scaled to 1/96th, 1/40th or 1/2 size [13], while the seawater electrolyte is correspondingly diluted to an equivalent scaled resistivity.

Using PSM, each ship configuration can be evaluated to determine the best ICCP component placement, life-cycle performance, zone interaction behavior and various failure modes, such as loss of anodes or defective reference cells, under both static (dockside) and dynamic (underway) operational conditions. Special consideration can likewise be given to: 1) complex geometry, 2) restricted areas, 3) coatings degradation and 4) evaluation of new computerized ICCP design technology. This paper will provide information pertaining to this design methodology and will include: 1) ICCP design engineering and protocol, 2) PSM design technique and 3) Navy ship hull ICCP design criteria.

Experimental

NAVSEA Design Protocol

For each ship class, there is a design protocol, which defines the basic ship attributes and protection requirements. Included in this guidance are general hull wetted surface areas, specific areas to emphasize during design and anticipated coatings damage scenarios for up to 15% loss (including propeller area). This information is utilized in the physical model for the layout of specific cathodic areas, for special geometric problems and to provide a sequential procedure for investigating ICCP performance over a life-cycle coatings deterioration scenario. This "coatings damage scenario" establishes the damage (cathodic area) percentages which are anticipated over time and forms the basis for the performance evaluation from a new condition state through a worst case 15% coatings loss. The basic assumptions and requirements of the protocol for the modeling are as follows:

1. ICCP Engineering and Performance:
    a) Navy power supplies are usually 150 A or 300 A or multiple units and use multiple 37.5 A, 75 A and 150 A hull anodes. Basic requirements are based on wetted hull area and cathodic current demand.
    b) Cathodic protection goal of –0.85 V ± 0.05 V (vs. Ag/AgCl) for all surface ship hull areas, using a –0.85 V controller set potential.
    c) Cathodic current demand (average of cathodic surfaces) for protection of bare metal and paint loss areas: (experimental control requirement)
        0.27 A/m^2 (25 mA/ft^2) "Static" state
        0.81 – 1.35 A/m^2 (75 - 125 mA/ft^2) "Dynamic" state
    d) Each zone consists of a controller, reference cell (and auxiliary), power supply(s) and associated anodes (basic configuration scheme)
2. Operational Criteria:
    a) ICCP system should have the minimum number of "zones" to effectively protect the wetted hull, unless special military requirements are specified
    b) All non-bare hull area is considered to be coated with MIL-P-24441 Polyamide Epoxy system or equivalent (plus antifoulant coating)
    c) The propeller is considered to be bare nickel-aluminum-bronze (NAB) material
    d) System performance and capacity should provide protection for up to a 15% coatings deterioration on steel/non-ferrous materials (including propeller area)
3. Model Layout Data:
    a) Wetted hull area
    b) Coatings damage distribution for cathode layout (See Table 1)
    c) Special problem areas and location of other hull components
    d) Coatings Damage Test Scenario procedure

Wetted hull area is defined as the effective metallic surface area below the waterline and includes all steel and non-steel hull surfaces, struts, bilge keel, skeg and propeller surface area. The ICCP performance is based on the capability of the system to protect bare metallic area, rather than that for the entire coated hull surface. Well-coated surfaces typically require 2-3 orders of magnitude less initial current to polarize than a non-protected bare area, thus, a well designed ICCP system will provide protection to all painted surfaces as a consequence of protecting the bare areas.

While the theory provides guidelines to insure scalability, the operating ICCP system on the model should duplicate the natural dynamic response and react directly to the changing cathodic demands of the surfaces. Experimental control and repeatability is accomplished by closely monitoring the cathodic current demand on the model and by collecting data only when the average static current density values of 0.27 A/m^2 (25 mA/ft^2) and dynamic values of 0.81-1.35 A/m^2 (75-125 mA/ft^2) are observed. These values, represent sufficient current densities to rapidly protect a bare steel surface under static and dynamic conditions and are a good compromise between initial very high current requirements for polarization and low maintenance current densities observed for well protected surfaces with calcareous deposition.

A basic ICCP zone is defined as an independent region of the hull ICCP system having a controlling Ag/AgCl reference cell (CRC), controller electronics, power supply(s) and associated hull anodes controlled by the system. Most often a zone configuration is established by the overall changes in geometric shape along the length of the hull, areas of coatings deterioration and the corresponding relationship of the associated hull features, such as rudder, prop, struts, etc. Each zone operates independently, but has the ability to influence the behavior of surrounding zones through the common hull cathode. Zone interaction is commonly seen in poorly designed systems and often results in a system "shut-down" from overpolarization of the CRC by an adjacent zone. Once system shut-down occurs, other areas of the hull may either become underpolarized or over polarized as a result of the unbalanced operation. It is thus necessary to provide correct anode and reference cell placement for each zone in order to insure uniform current distribution and balanced zone behavior.

Table 1 shows a typical design protocol layout for a three zone system, having forward (fwd), middle (mid) and aft independent zone control. The protocol specifies areas where cathodic damage should be placed, (i.e. docking block, general hull, etc.) and defines the percentage of bare area assigned to each region or component. This information is based on shipyard overhaul information or maintenance log documentation and represents known areas which receive routine corrosion damage, mechanical abuse or those which will require special attention to insure protection. From these damage locations and percentages, the coatings damage scenario provides for the sequential testing of coatings degradation from the original new hull state. In terms of model operation, this sequence constitutes an algebraic addition of cathodic surface area by electrically connecting cathode area to the total hull working electrode circuit.

Physical Scale Modeling

The PSM program at NRL was established with the objective of designing ICCP systems for Navy ships without relying on empirical design data and the arbitrary placement of components, as was the hallmark of prior designs. With this technique, it has been possible to consider problems relating to both the optimal design and geometric placement of components, as well as, the physical response of the ICCP system to life cycle changes, velocity conditions and inter-zone relationships. In conjunction with the NAVSEA protocol, the basic parameters for a model class are established at the onset of a design. These include:

a) basic scale of the model (large enough to allow interior instrumentation)
b) an initial multi-zone ICCP design for preliminary tests
c) calculation of wetted hull area to estimate power supply requirements
d) basic propulsion design
e) anode and reference cell array configuration and location

Precision scale fiberglass hull models are fabricated from specification drawings to provide realistic hull geometries for the attachment of hull steel surfaces and propulsion components. Steel is placed on the models so as to segment the wetted hull surface into specific bare metal areas which add up to the cathode percentages defined in the design protocol. Segmentation of the cathodic area provides for an effective method to add and subtract surface area requiring protection and allows for evaluation of the hull from a minimal damage percentage to a maximum 15% coatings deterioration state.

Table 1 - *NAVSEA Hull Damage Protocol for Model Large Carrier Hull*[1]
Initial Hull Cathode Layout

Damage Location	**Damage (%)**	**Full Scale Area (m^2)**	**1/96 Model Area (cm^2)**
Fwd Zone (frame 0-85)			
General fwd hull	1.42	210	3.29
Fwd waterline	0.63	93	1.45
Fwd docking blocks	0.58	86	1.34
Subtotal:	2.62	389	6.08
Mid Zone (frame 85 173)			
General mid hull	2.83	421	6.58
Mid waterline	0.63	93	1.45
Mid docking blocks	1.17	174	2.72
Bilge Keels	1.10	164	2.55
Subtotal:	5.73	852	13.31
Stern Zone (frame 173-260)			
General stern hull	2.83	421	6.57
Aft waterline	0.50	74	1.16
Aft docking blocks	0.30	45	0.70
Struts	0.75	111	1.74
Rudders	0.65	97	1.51
Propellers	1.62	241	3.76
Subtotal:	6.65	988	15.44
Total Damage	**15.00**	**2 229**	**34.83**

[1] Total wetted hull area = 14 863 m^2

The steel hull segments, shown in Figure 1, were cut to fit the prescribed locations and bare hull metal percentages outlined previously in the NAVSEA protocol given in Table 1. Each steel segment is installed with an internal electrical lead to allow for independent electrical connection, necessary for the sequential aging. Each section thus can be electrically isolated or added to the system with individual cathodic current demand monitored through a 1 ohm shunt resistor at a remote shunt box. Each segment fraction can be added and subtracted from the whole hull total, thus providing the multiple damage scenarios.

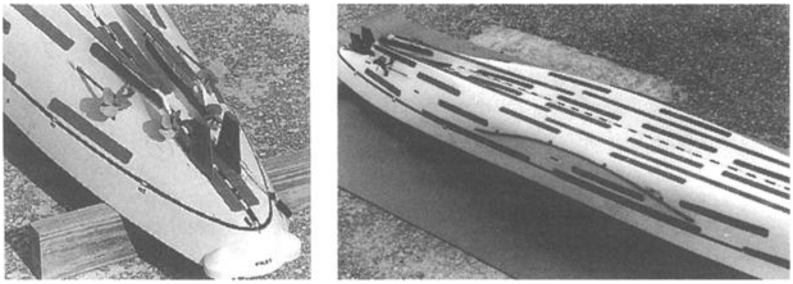

Figure 1 - *Photograph of Physical Model Showing Cathode Area, Basic Layout and Precise Hull Geometry.*

An array of Ag/AgCl reference cells are installed on the hull to enable the 3-dimensional sensing of protection potential around the hull and especially in areas of complex geometry. More specifically, hull reference cells are located linearly along both port/starboard waterline, along the bottom centerline, at distal locations for comparison to hull potential surveys, and at all areas of special interest (i.e., struts, propeller, rudders, bilge keels, etc.). Each zone CRC is installed at a selected location, although during the modeling process, any array reference cell has the ability to be utilized for control purposes if desired.

The electrolyte used in the modeling is a combination of natural seawater from the circulation system at the Naval Research Laboratory, Marine Corrosion Facility, Key West, FL and deionized tap water. The seawater typically has a pH in the range of 8.1 - 8.3 with an initial resistivity of 18 ohm·cm. From equation (3) the electrolyte is prepared to satisfy the relationship, $\rho_M = \rho_S$ (k), thus for seawater, a scaled electrolyte is 1728 ohm·cm at 25°C for 1/96th scale. Dissolved oxygen levels are maintained near saturation in the tank by air injection and mixing prior to testing.

Models are prepared for use before each set of tests to remove any corrosion product or previous calcareous deposition and to renew the cathodic surfaces to a clean bare state. All metallic surfaces are grit blasted and masked to provide the exact surface areas, as given by the NAVSEA protocol. Areas without masking are coated with MIL-P-24441 polyamide epoxy and allowed to dry before removal of the masking material and immersion. Once surfaces are prepared, the model is pre-conditioned in natural full-strength seawater for two hours while under cathodic protection to -0.85 V vs. Ag/AgCl. This step enables the adsorption of a natural calcareous film to the cathodic surfaces and modifies the R_P behavior to that of a full-scale system. Immediately following pre-conditioning, the model is rinsed briefly with fresh water and transferred to the modeling electrolyte, taking care not to damage or dry the surface films during the transfer. Following transfer to the modeling electrolyte, the model (with all cathode areas electrically in-circuit) is immediately re-polarized to -0.85 V and is then monitored until the average cathodic current density decreases to the static demand of 0.27 A/m^2 (25 mA/ft^2) before a modeling sequence is started.

Dynamic mode consists of: a) rapid bubbling of the water adjacent to the hull to achieve the 3-5X increase in current density at the cathodic surfaces and occasionally b) rotation of the propeller for the same effect along the NAB blades. Movement of the water is not intended to simulate hydrodynamic conditions, but only to increase the oxygen delivery to the cathodic sites, as a primary cathodic reaction in seawater is oxygen reduction and is characteristically diffusion limited. Only a moderate agitation of the water is required to achieve the 3-5X increase in current density. Any further increase in water movement has relatively little effect on the current demand.

The PSM technique utilizes an interative approach to improve and optimize ICCP system performance and component locations. Figure 2 is a schematic representation of a typical modeling scenario, where the model is first prepared, then pre-conditioned in seawater to allow the growth of a natural calcareous film and finally relocated into the modeling electrolyte for stabilization and performance of experimental static/dynamic design scenarios. As discussed previously in the NAVSEA design protocol section, modeling is only performed while the cathodic areas are still active, but within the required current density design ranges. Once the cathodic current demand naturally stabilizes below acceptable control limits, the model is removed from test and the process repeated, as required until the ICCP design is completed.

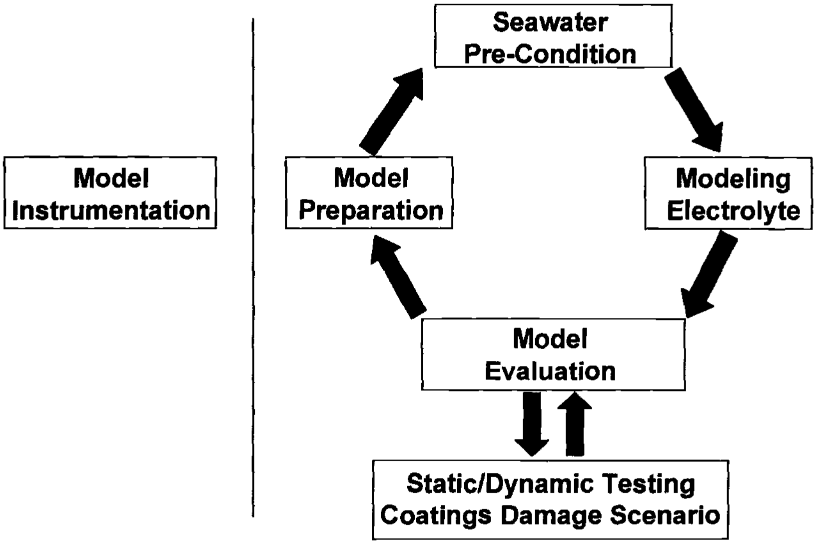

Figure 2 - *Iterative Modeling Process*

Results and Discussion

In the derivation of equations for modeling there are basic assumptions, which when satisfied, provide for precision measurement of potential and current on the model with a direct mathematical relationship between the model and full scale system. These assumptions are as follows:

1) $R_P = \Delta E/i_C$ must be same for the model and full scale system, where ΔE represents the polarization from E_{CORR} to the cathodic protection set potential of –0.85 V. This value in the full scale is the instrument set potential on the ship controller and is set identically in the modeling, thus $\Delta E_{SHIP} = \Delta E_{MODEL}$ is preserved in all work. As defined in equation (3), the resistance of the model circuit, in accordance with Ohm's law, must have an equivalent scaled ohmic component $(R_{OHMIC})(k)$ and an equivalent polarization resistance (R_p) component consistent with that of the material polarization behavior in full strength seawater. To preserve the $R_{P\,(SHIP)} = R_{P\,(MODEL)}$ for direct scaling, NRL established a pre-conditioning sequence whereby the models were first cathodically protected in full scale seawater (to -0.85 V), to allow the deposition and adsorption of natural calcareous films on the model surfaces prior to testing. Thus, it was experimentally shown that once a calcareous film was deposited, prior to placement in the scaled electrolyte, the R_p component of the metallic surface would behave in a manner very similar to natural seawater behavior and that the scaling equation was correct. Comparisons of static and dynamic polarization curves between model hulls (pre-conditioned), actual ship ICCP data, full conductivity seawater exposures and computer simulations have shown very good correlation [15,16]. Additionally, electrostatic analysis of the modeling setup, using a simple scale dipole configuration, showed very close approximation of electric field current distribution with that predicted from theoretical calculations.
2) The current density relationship, $i_{SHIP} = i_{MODEL}$ is true, by definition, when the model size, electrolyte dilution and polarization resistance components obey the scaling law. Further, current density as previously discussed, is rigorously controlled on the model and data are collected only when cathodic demand is stable and within the sampling ranges defined by the protocol. Values for the total current output (I) in the model system are used routinely as a performance check because by conservation of energy, the anode output and cathode demand must sum to zero.
3) The surface areas and geometry are exact and scaled such that $A_{SHIP} = A_{MODEL}\,(k)^2$. Using a precisely scaled model, the current pathways, distances and electric field distribution are can be directly related. This relationship is closely controlled in the PSM process.

The evolution of an ICCP design for each class of ship is essentially the same, with only minor modifications in the layout to enable incorporation of special geometry or operational/design restrictions. Comparisons with actual hulls, as discussed previously, have been very consistent where the actual state of the real hull is well determined. In most cases, the unknown variables come from indeterminate knowledge of the actual ship hull coatings condition.

The design of an ICCP system can take on three distinct forms: 1) an examination of an existing hull ICCP design, often used as a baseline for further improvement, 2) a "low cost upgrade" of an existing design to improve performance with minimal component addition or relocation and 3) an "optimal design" where few system design restrictions are imposed.

Data were collected for various physical scale model hull damage scenarios, under both static and dynamic conditions. Figure 3 shows a comparison between static and dynamic performance for a modeled two-zone system in minimum damage condition (2-3%) state. In most cases, static system performance is more uniform and balanced near the set potential of -0.85 V, while the dynamic data often typify operational behavior and highlight system deficiencies. In this illustration, even at minimal hull damages, there is a difference in behavior between static and dynamic operation. Statically, the system

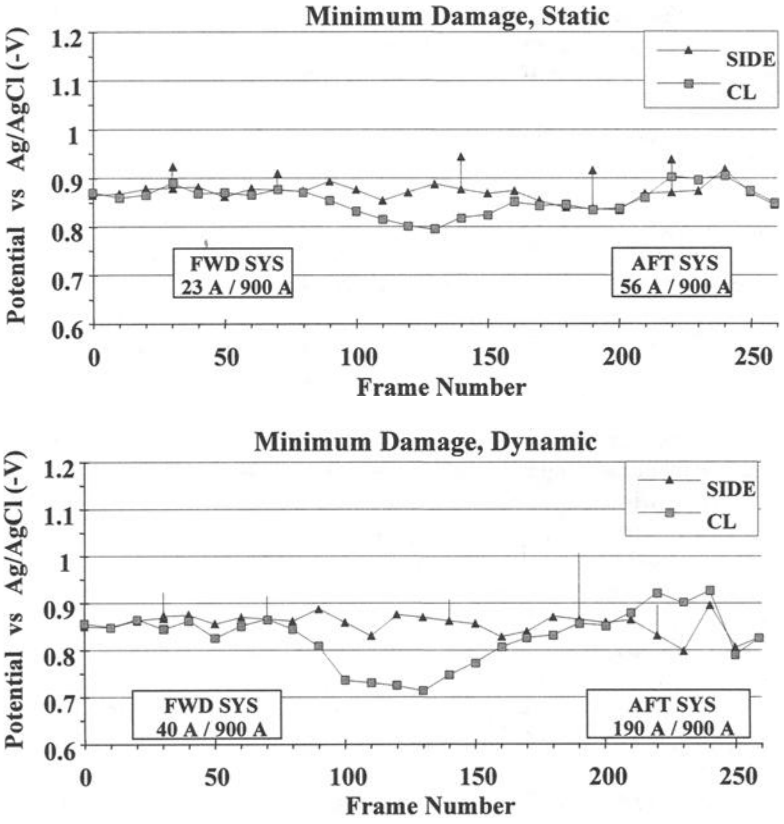

Figure 3 - *Comparison of "Static" (top) Versus "Dynamic" (bottom) Hull Potential for a 2-3% Minimum Damage Scenario. A 2 Zone System is Shown with Potential Profiles Along Centerline and the Starboard Side. Fwd and Aft System Current Output (left) and Zone Capacity (right) are Provided in the Boxes.*

potentials are nearly uniform, with all data well within the design range of -0.85 V ± 0.05 V, except for those readings indicated by a sharp spike near an anode. These spikes illustrate the close proximity of the reference cell to an anode and vary in magnitude and quantity depending on ICCP system output and configuration. Anode spikes are not intended to identify anode location, but to illustrate the net polarization behavior near adjacent anode surfaces. The frames used in the figures represent hull distances from the bow and equal 8 feet per frame for the described ship class. Under dynamic conditions, the ICCP system shows an increased current output, corresponding to the enhanced cathodic activity and, as a consequence of ICCP system design, there is an area of under protection amidships along the centerline and slight overprotection in the aft. While static data are useful during modeling, the dynamic condition highlights features better and will be used in the following illustrations.

Figure 4 shows an example of some results for an "existing" carrier model ICCP design layout. The plots illustrate a hull potential profile measured on the model at distinct locations along the side waterline and along the hull centerline bottom. Frame 0 represents the bow region, while frame 250 represents the stern region around the rudders and propellers. The existing ICCP layout is a 2 zone system having 900 A capacity in the forward zone and 900 capacity in the aft zone (shown as the right current output value for each zone). The actual current output values for each zone, as measured during the data run, are shown as the left hand number. The CRCs are located at frame 50 for the forward zone and at frame 210 in the aft. Typically the anodes on a hull of this size are 75 A or 150 A apiece and are generally located symmetrically port and starboard. The modeling conditions shown are for three different hull damage scenarios, in dynamic conditions, representing approximately 3%, 6% and 15% hull cathode area. On large hulls, anodes are always located on the hull sides, rather than the bottom, to prevent the possibility of having an anode buried in the mud while in port.

For older class ships, the ICCP systems installed were designed empirically, without detailed analysis and with little attention given to zone relationships. In Figure 4, the modeled ICCP system is deficient at controlling potential along the mid-centerline and in the stern. As the damage percentage increases to the mid-damage state (5-6%), the system performance further exhibits both over- and under-polarization in both the mid and aft regions. In the maximum 15% damage state, much of the mid section of the hull and far aft is under-polarized, while there is a possibility for over-polarization in the bow and along the aft centerline. The ICCP system outputs increase correspondingly with the introduction of cathodic area from Figure 4a to 4c. At the maximum damage state, the ICCP system is operating at full output in both zones and still cannot provide enough current to sufficiently polarize all areas along the hull. To improve an existing ICCP system, an "upgrade" system can be designed which provides better performance without significant component modification. Figure 5 shows an example of an upgrade to the system, where the two zone layout is split into three zones and adds one power supply, controller and reference cell pair. With just this change, which better reflects the natural geometric contour of the hull, the ICCP system operates more uniformly and performance is improved in each damage state. Overall, the potential extremes seen previously are reduced and a greater percentage of the hulls potential lies within the 100 mV design window. At the maximum damage state, in Figure 5c, the aft zone is operating at

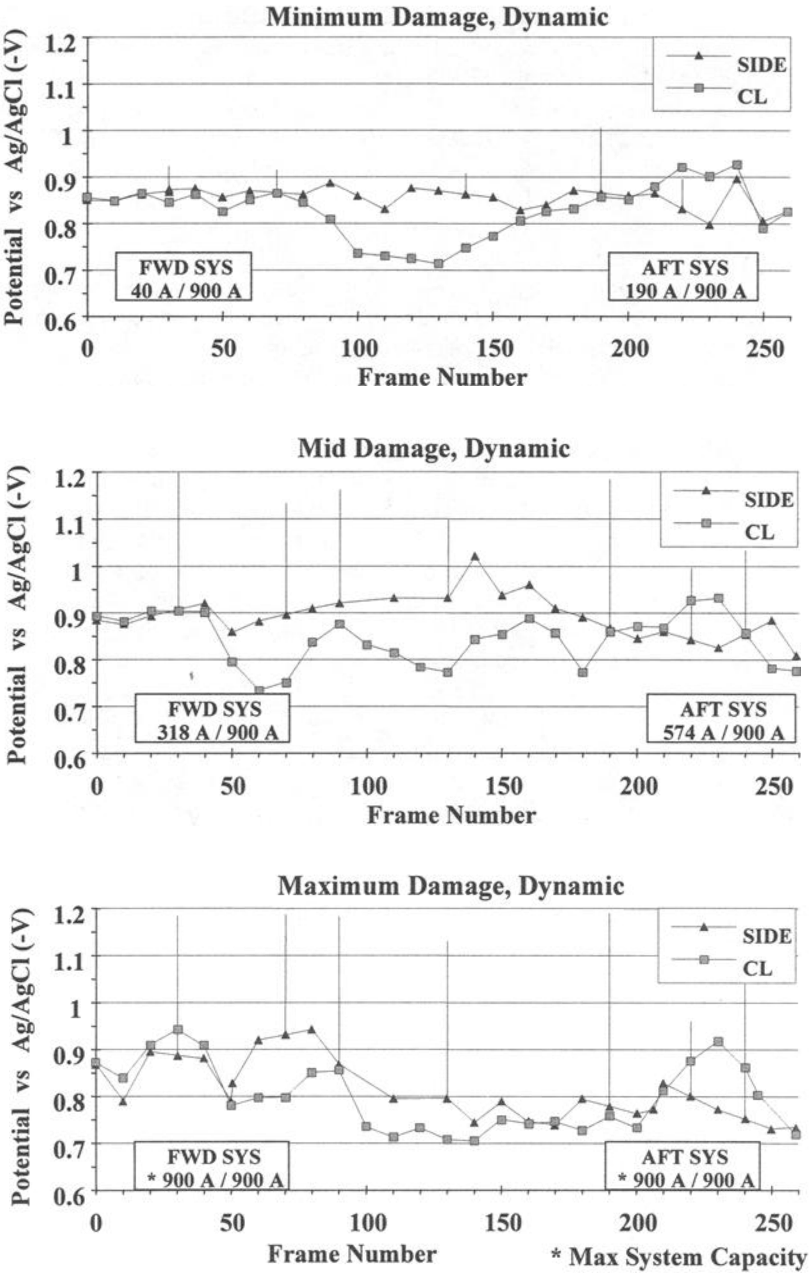

Figure 4 - *"Existing" 1800 A ICCP System - Dynamic Conditions. (a) Top Graph Shows Minimum Damage Scenario, (b) Middle Graph Shows a Mid Damage State and (c) Bottom Graph Gives a Maximum Damage "Worst Case Scenario".*

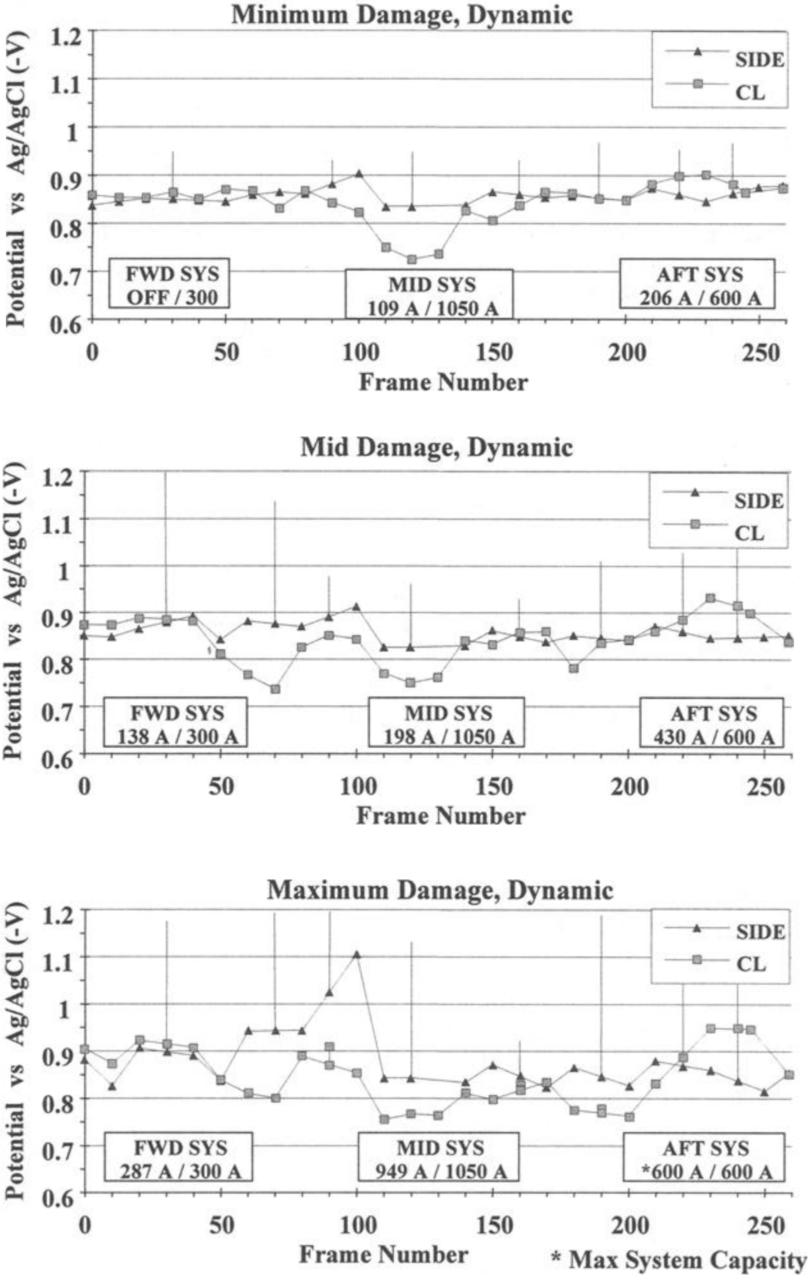

Figure 5 - *"Upgrade" 1950 A ICCP System - Dynamic Condition. (a) Top Graph Shows Minimum Damage Scenario, (b) Middle Graph Shows a Mid Damage State and (c) Bottom Graphs Gives a Maximum Damage "Worst Case Scenario".*

maximum output with the other two zones near maximum levels. An "optimum" ICCP design provides significantly more freedom to layout components for maximum performance and efficiency. An optimal system design, shown in Figure 6, is a three zone design with a 2025 A current output capability. The zone layout is optimized for the large flat-bottomed mid section of the ship, but provides sufficient capacity and response to enable good current distribution to both the forward and aft zones. In the minimum damage state, the ICCP system provides uniform protection along the hull and operates in a balanced manner. As hull damage is added in Figure 6b, the system responds uniformly and even potential distribution is maintained along both the centerline and waterline. At the maximum hull damage state, the ICCP system continues to remain balanced even where anode output is at or near full current.

The optimization of component locations is accomplished using the iterative process. Relocation and repositioning is based on results of prior data runs and from observation of the ICCP system behavior during testing. The basic power requirements for a given hull are defined by the protocol, but are fine-tuned and modified as needed during the modeling. The future for ICCP system design will likely incorporate computer efforts along with physical scale modeling to support the iterative data collection process. Data obtained from physical modeling is particularly suited for the computer modeling boundary element mesh (BEM) layout [16] and for the verification of potential and current requirements calculated from polarization data input fed into the model parameters. Where calculations are necessary for potential/current distribution, the computer is particularly beneficial, but reliant on the correct polarization curve to support the result. Additionally, zone interaction and system balancing are not well defined theoretically, but can be studied using a combination of both techniques.

Some ongoing and future efforts are designed to integrate the computer modeling results to support related physical modeling analysis. With experience, computer efforts can remove much of the iterative procedure necessary in the PSM and may provide combined flexibility for continued effective ICCP engineering system design.

Conclusions

The cathodic protection design criteria for the U. S. Navy utilizes a rigid design protocol and system engineering using PSM. The design protocol establishes the basic cathodic protection requirements and defines the areas of the hull which require the greatest attention to detail and model layout criteria. Using the protocol, the modeling provides the engineering tools to test cathodic protection performance and to optimize the necessary placement of components for near-ideal current distribution. When completed, the model provides for ICCP system sizing, anode/reference cell placement, anode output, and "zone" electrical differentiation. Results from modeling data provide a picture of overall hull potential, current output, cathodic demand and system voltage requirements. Performance data are available for ICCP operation over the maintenance life-cycle from a hull "new state" through a maximum "worst case" 15% hull damage.

From a ship design standpoint, the specification of an ICCP system, which has quantitative support and hull specific design methodology, is advantageous for both the ship-builder and ultimately the customer. In addition, in instances where an empirical

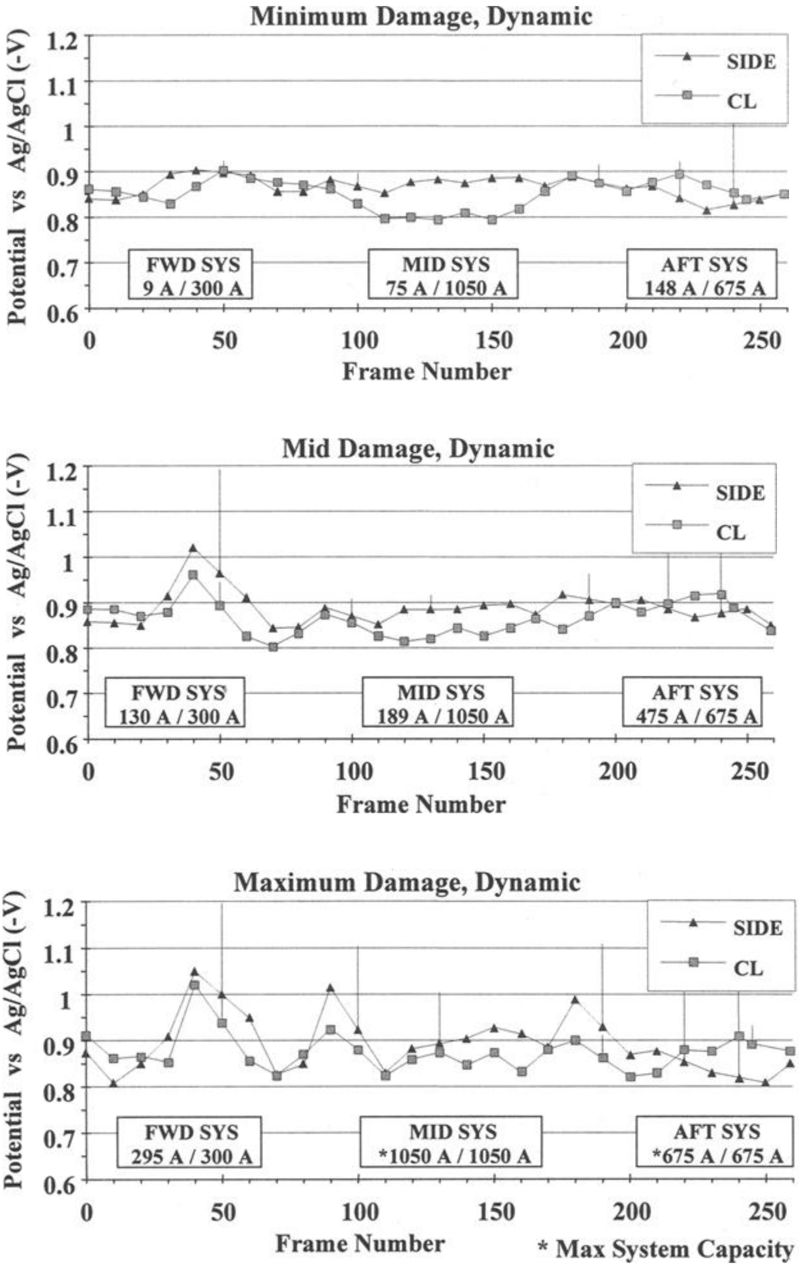

Figure 6 - *"Optimum" 2025 A ICCP System - Dynamic Conditions. (a) Top Graph Shows Minimum Damage Scenario, (b) Middle Graph Shows a Mid Damage State and (c) Bottom Graphs Gives a Maximum Damage "Worst Case Scenario".*

ICCP system does not perform well, it is very difficult to document the ICCP performance and to substantiate the necessary changes to improve the system operation. With modeling data, systems can be life-cycle analyzed before installation or reanalyzed after the fact to facilitate modification, support hull improvements, or used for failure analysis testing/evaluation scenarios.

References

[1] Kasper, C., "The Theory of the Potential and the Technical Practice of Electrodeposition, Papers I-IV", *Transactions of the Electrochemical Society*, Vols. 77 and 78, 1940.

[2] Agar, J. N., and Hoar, T. P, "The Influence of the Change of Size in Electrochemical Systems" *Discussions of Faraday Society*, No. 1, pp. 162-168, 1947.

[3] Waber, J. T., and Fagen, B., "Mathematical Studies on Galvanic Corrosion", *Journal of the Electrochemical Society*, Vol. 103, No. 1, pp. 64-72, 1956.

[4] Wagner, C., "Contribution to the Theory of Cathodic Protection II", *Journal of the Electrochemical Society*, Vol. 104, No. 10, 1957.

[5] Wagner, C., "Distribution of Potential and Current with Cathodic Corrosion Protection", *Werkstoffe u. Korrosion*, Vol. 11, No. 11, 1960.

[6] Iossel, Y.Y., Kochanov, E. S. and Strunskil, M. G., "Questions Concerned with the Design and Modeling of Electrochemical Anticorrosion Protection for Ships", Sudostroyeniye (shipbuilding) Publishing House, Leningrad, 1965. (translation)

[7] Clerbois, L., Heita, E., Ijsseling, F. P., Rowlands, J. C., and Simpson, J. P., "Principles for Scaling of Corrosion Tests", *British Corrosion Journal*, Vol. 20, No. 3, 1985.

[8] Nelson, E. E., "A Study of Current Distribution in Cathodic Protection", Naval Research Memorandum Report #4868, 1957.

[9] Waldron, L. J., Nelson, E.E., and Peterson, M. H., "Major Factors in the Cathodic Protection of Steel in Sea Water", NRL Memorandum Report #4596, 1955.

[10] Tighe-Ford, D. J. and Ramaswamy, S., "The Use of Stylised Physical Scale Models for Studying the Impressed Current Cathodic Protection of Ships", Royal Naval Engineering College, RNEC-RP-88024, 1988.

[11] Mc Grath, Tighe-Ford and Hodgkiss, "Scale Modeling of Impressed Current Cathodic Protection Systems for Ships", *Journal of Naval Engineering*, Vol. 29, No. 2, pp. 314-322, 1986

[12] Thomas, E. D., Lucas K. E., Foster, R. L., Parks, A. R., and Kaznoff, A. I., "Physical Scale Modeling of Impressed Current Cathodic Protection Systems" NACE Corrosion '89, Paper # 274, New Orleans, LA, April 1989.

[13] Lucas, K. E., Evans, M. A., Hogan, E. A., Thomas, E. D., and Seelinger, A., "Criteria for the Design of Impressed Current Cathodic Protection (ICCP) Systems for Seawater Ballast Tanks" *Tri-Services Conference Proceedings*, Nov 1997

[14] Hack, H, "Scale Modeling for Corrosion Studies", *Corrosion*, Vol. 45, No. 7, pp. 314-322, July 1989.

[15] Parks, A. R., Thomas, E. D., and Lucas, K. E., "Verification of Physical Scale Modeling with Shipboard Trials", NACE Corrosion '90, Paper #370, April 1990.

[16] DiGiorgi, V., Kee, A., Thomas, E. D., and Lucas, K. E., "Verification of Scale Effects for Modeling of Shipboard Impressed Current Cathodic Systems" ASME Applied Mechanics and Materials Mtg., Johns Hopkins Univ., Baltimore MD, *Journal of Computers and Structures*, June 1996.

Charles F. Schrieber[1]

Relationship of Chemical Components and Impurities of Aluminum Galvanic Anodes Upon the Cathodic Protection of Marine Structures

Reference: Schrieber, C. F., **"Relationship of Chemical Components and Impurities of Aluminum Galvanic Anodes Upon the Cathodic Protection of Marine Structures,"** *Designing Cathodic Protection Systems for Marine Structures and Vehicles, ASTM STP 1370*, H. P. Hack, Ed., American Society for Testing and Materials, West Conshohocken, PA, 1999.

Abstract: Aluminum galvanic anodes form the principal basis for cathodic protection of offshore structures and marine vehicles. A satisfactory cathodic protection (CP) design using the galvanic mode must employ a valid anode. It follows, therefore, that highly responsible compositional consideration be associated with such anodes. Since applications extend from very low temperature to above ambient seawaters, this factor is addressed in the paper. Applications in sea muds and its effect upon anode behavior is also considered. Primary emphasis will be given the indium-activated alloys with occasional comparisons to the mercury-activated aluminum anodes. The grounds for this emphasis lies in the fact that the indium-activated anodes constitute the great majority of use. The data and observations discussed are based primarily on low temperature, ambient and higher temperature laboratory and pilot tests supplemented by user field applications over the last 25-30 years.

Dependable aluminum anode performance in the subject waters and muds point to careful control of iron and copper impurities, coupled with the correct balance of indium, zinc and silicon. Generalized recommendations are presented with regard to composition. The future challenges of cathodic protection at greater seawater depths are also addressed. Possible effects upon anode current capacity and voltage are so related.

Keywords: aluminum galvanic anodes, compositional components, activation mechanisms, chemical impurities

---

[1] Consultant, Oronzio De Nora S.A. (Italy, USA). 219 Narcissus Street, Lake Jackson, Texas, USA 77566.

Introduction

Since 1975, aluminum anode technology in the marine environment has emphasized the indium and mercury-activated alloy chemistry. During the last 5 years the predominant alloy has been the generic indium-containing alloy. The increasing use of this alloy stems in a large measure from the fact that the composition does not contain a controversial component. Generically, this alloy contains 0.01 - 0.025% indium, 0.08 - 0.20silicon and 3.5-6.5% zinc. The mercury-activated aluminum anode contains 0.035 - 0.048% mercury, 0.3 - 0.48% zinc and approximately 0.2% silicon. Both anodes suffer serious voltage and current capacity (anode life) problems when chemical impurities of iron, copper and lead exceed certain limits. Interactions of impurities with major alloy constituents are critical. The user of aluminum galvanic anodes for normal and low temperature seawater applications generally has sufficient information at his/her disposal to affect a workable and dependable design [*1-5*]. However, a majority of anode applicators have not had the opportunity or time to review in a simply stated manner what the anode components contribute or take away from the design performance. The purpose of this paper is to provide technical information in this area.

Experimental Methods

Performance or behavior of aluminum anodes is determined largely by their chemical composition. Thus, it can be expected that specific anode compositions will behave differently with changing marine environments. Also, changes within an alloy's range of chemical specifications can be varied, based on observations to optimize performance.

Galvanostatic Anode Testing

This is the principal mode of testing aluminum anodes. This procedure presets the anode current density at a specific level or series of levels in turn. Current capacity is determined by integrating current-time product and knowledge of anode weight loss.

NACE TM0190-98

NACE TM0190-98, "Impressed Current Test Method for Laboratory Testing of Aluminum Anodes," NACE International, Houston, Texas, 1998, is the accepted standard for evaluating aluminum anodes in most global locations. The purpose of this standard is that of comparing the current capacity and potential of anodes from a continued line of production heats or melts. The procedure employs the galvanostatic testing mode. Ambient temperature testing is specified. The procedure is adaptable and can be used over a broad range of temperatures. With such modification, however, the test standard title must not be used.

Other Electrochemical Testing Techniques

Testing of aluminum galvanic alloys involves the possibility of anode passivation. This is especially true when trials are carried out in low temperature (<10-12°C) seawater or sea muds. Galvanostatic modes of test provide anode potential data under operating load, but a resulting reduction of current due to passivation will not be indicated, since the current is preset at a steady level. The following two procedures should also be considered to supplement galvanostatic methods when a new alloy is being considered for low temperature service.

Free Running - The anode current and potential are not preset. These values become a function of the electrolyte and circuit resistances. Anode current capacity is determined by knowledge of cumulative ampere-hours of operation and weight lost by the anode. Anode potential is measured directly.

Potentiostatic - This technique employs a potentiostat to preset 3 or 4 samples from the same anode or heat at differing voltages less negative than the open potential. Resulting anode current (current density) at each set potential is determined over several time intervals. An anode polarization curve can be evolved from the data. Anode passivation tendencies may be noted from the polarization curve. Passivation may be suspected when the resulting current density on the anode fails to rise with greater potential differences between anode open circuit and the set potential.

Elevated Temperature Testing: Saline Waters and Muds

Figure 1 is a laboratory test assembly used for determination of aluminum anode current capacity and potential [2]. As-cast anode rods, 1.6 cm diameter by 15.0 cm length constituted the test samples. Ten cm of anode length was exposed in the electrolyte. Steel pots used as cathodes were prepared from 16.5 cm lengths of standard 7.6 cm diameter pipe. These cells were immersed in a non-conducting heating medium (tetra-ethylene glycol) to a depth at least equal to the mud or seawater level in the pots. The heating medium was slowly circulated and temperature controlled. Heavy rubber stoppers fitted into the steel cells accommodated the anode, a portable reference electrode and a stainless steel tube condenser for return of condensed vapor to the electrolyte. Galvanostatic and potentiostatic trials were used to characterize anode performance with respect to anodic properties [*7*].

Low Temperature Testing: Saline Waters and Muds

The test assembly shown in Figure 1 was also modified for low temperature trials. In this case, the bath container was insulated and the circulating medium was cooled by a refrigeration loop. As with the high temperature tests, each test pot was fitted with temperature monitors. The condenser remained in each pot to permit the chilled seawater and mud to dissolve additional oxygen at lower temperatures.

Larger test equipment was designed and used for deep ocean depth simulation. This testing necessarily involved lower temperatures. This unit was a high pressure pilot

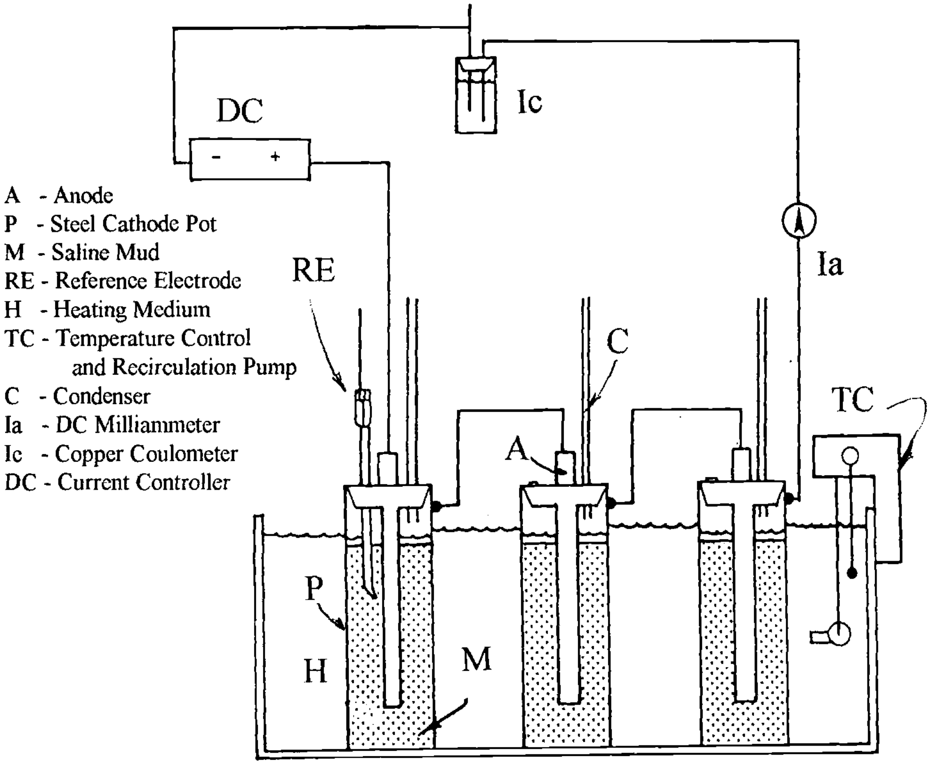

Figure 1 - *Schematic of Elevated Temperature Test Assembly: Seawater and Saline Muds* [1]

plant which incorporated a 4-16 liter per minute natural seawater intake with capability to cool the water to the temperature associated with the test depth [*2*]. Refreshed seawater continually entered the plant to compensate for a blowdown within the above range. Anodes for trial were as-cast and weighed approximately 400 g with a diameter of 3.8 cm.

High purity zinc served as controls for all testing described. Elevated and low temperature studies primarily employed the galvanostatic testing procedure.

Long Term Exposures

Aluminum anode behavior for periods through 6 years was assessed in the seawater flumes and intake bays of the Dow Chemical Company at Freeport, Texas. Necessarily, these exposures only considered waters in the temperature range attendant with that area (12-30°C). These results were very useful, since this enabled the more rapid laboratory findings to be compared in the field with commercial-size anodes. Cooperative user studies from 6-8 areas of the world further enhanced the temperature sector of information.

Aluminum Activation

Activation of the aluminum surface is the process of transition from the naturally passive state to the active state by removal or weakening of the passivating film. Activation may be achieved by cathodic currents, by a reduced substance in the adjacent solution, or by an alloying element added at a low quantity having a suitably negative potential [*3*].

Unalloyed aluminum adopts a relatively noble solution potential in saline media as a result of its protective oxide film. The oxide is the cause of polarization when aluminum is placed under anodic load in a cathodic protection circuit. Numerous alloying combinations have been made to aluminum to reduce anodic polarization traits. With a few exceptions, the alloying approaches used to eliminate passivation, and hence promote surface activation, have been largely empirical. Unfortunately, it is not clear why these activating materials are successful or how they work.

Nonetheless, the success of the aluminum anode is dependent upon the alloying of certain metals whose surface role is, ultimately, to prevent the formation of a continuous, adherent and protective oxide film on the alloy, thus permitting continued galvanic activity of the aluminum.

The physical form of the oxide barrier on aluminum is important when activation is considered. This is important because behavior in the presence of an orderly crystalline film can be explained by a conductor-type theory [*3*].

The inorganic premise would state that aluminum oxide can transmit cations but not electrons. This would be an ideal situation, because high anodic efficiency would result. Supporting this is the evidence that high purity aluminum is very efficient [*3*]. A theory can be set up by turning the oxide into a good cation conductor and a poor electron conductor:

Assume a crystalline, rate controlling film somewhere on the aluminum anode surface. Normally, Al_2O_3 is considered an n-type semi-conductor. Interstitial metal ions (nickel, copper, iron, for example) cause this type of oxide to transmit ions and electrons along the interstitial sites [*4*].

The oxidation rate can be increased by dissolving metal oxides of lower valence than aluminum or including elements that form a much smaller oxide, thus putting thin spots in the oxide layer. Thus, the addition of zinc would increase conductivity in the oxide and that of mercury should greatly enhance conduction.

For a good anode, the combination of elements must provide an oxide that will transmit metal ions to the solution surface and hinder the passage of electrons through the same oxide [*4*].

All the pieces fit semi-conductor theory. Why aluminum is improved by certain elements, and why magnesium is not, can be explained but not demonstrated.

If the oxide is amorphous, many directions are available. An easy explanation of why Cu, Ni, Fe, and Pb, destroy efficiency or raise electrode potential is available. These metals dissolve and then plate out at a cathodic site. The crystal grows until it protrudes through the aluminum oxide. Now an unprotected, short circuited cathode is available, and H^+ is easily reduced at the surface. Any use of the electrons for this purpose represents inefficiency.

According to Deltombe and Pourbaix [*5*], a reasonable reaction involving aluminum oxidation can be expressed by the following:

$$2Al + 3H_2O = Al_2O_3 + 6H^+ + 6e^-$$

One H+ is formed for each electron. If the hydrogen ions accumulate, the pH becomes very low and the protective oxide film could be dissolved. A pH of four would have to be reached before this would occur. The other alternative is that the hydrogen ion must be removed. This must occur in practice because containers used in the laboratory come to a constant pH above four [*5*].

Whatever the means of hydrogen ion removal, there are many such ions around to be removed. Reduction of this hydrogen ion at cathode sites would cause efficiency losses.

If the hydrogen ion is to be neutralized, this must also be caused by base being generated at a local cathodic site. Once again, a loss of efficiency would be expected. How can a small amount of material do a large amount of work? The type of work that must be done can best be done by hydrogen species. Hydrogen ions can move through an oxide film either as a cation or as a series of oxygen compounds. The driving force is a negative potential on the metal surface. Once it arrives, several things may happen. If it is reduced to a hydrogen atom, hydrogen gas will be formed and two atoms will then have caused a disproportionate change in the situation. The bubble of hydrogen formed fractures the oxide coating, an anodic reaction occurs, etc.; the aluminum surface would be a mass of tiny reactions. A paper by Draley and Ruther [*6*] describes this phenomenon. Observation in the Dow laboratories have shown evidence that, as the anode is driven, new anodic areas become available, thus maintaining the potential.

Although it is not essential to the theory, the attack probably occurs through pores in the oxide. These pores have been studied in reasonable detail by Dow and exist in fact. Some resistance to H+ flow is desirable or poor efficiencies would result. High overvoltage would also discourage the flow of ions. Heavy ion flow would result in low efficiencies.

Metals Accounting for Activation

The most widely accepted aluminum anode alloys contain mercury or indium as elements responsible for surface activation. Indium is second to mercury in this application followed by tin, magnesium, cadmium, and bismuth, with the latter elements not necessarily listed in their order of importance.

The primary reason that a certain group of metals are beneficial is because they come into intimate contact with aluminum but are not dissolved in it enough to affect the potential. Textbooks on electrochemistry [*7*] describe the morphology of these metals and aluminum. Mercury would be expected to be very finely associated with aluminum. Zinc aids in this contact and is generally used with mercury in aluminum sacrificial anodes.

In order for these elements to be effective over any period, sufficient amounts must be present. That is, they must not be leached away faster than the aluminum. Once again, mercury heads the list. Through its calomel reaction, it is easily replated, $2Hg + 2Cl^- \leftrightarrow Hg_2Cl_2$. As it is easy to have too much mercury on the surface, this reaction is fortuitous.

The activating elements must not be adversely affected by metallic impurities. Indium also has significant merit here.

An additional requirement is that the metals, if they accumulate at the local cathode, must 'stay low' so that they do not protrude through the oxide film.

Also of importance, the concentration of the activating metal in the anode should be relatively low so that H_2 absorption does not occur. This would have the tendency to cause weakening of the anode oxide as well as loss of the necessary hydrogen gas.

The solid solubility of mercury in aluminum is on the order of 350 ppm. Structural studies on a mercury-containing anode indicate that additional mercury may be present as several intermetallic compounds, usually incorporating iron, silicon and aluminum [*4*].

Employing the 'mixed potential' theory, it can be concluded that the potential of any anode is the result of anodic and cathodic contributions of the metals involved. The contributions will be increased by depolarization or, conversely, decreased by polarization of the reactions. Studies indicate that anodic depolarization is necessary and that it occurs with almost every low melting point addition to about the same extent. Improved potentials are the result of this anodic depolarization coupled with polarization of the cathodic reactions [*3*].

Cathodic polarization is caused by adding elements with a high hydrogen overvoltage. They are also metals with low melting points. The effective elements must be resistant to poisoning by other elements, notably iron, and remain in the proper place and an appropriate concentration. In other words, it must not be readily depleted by dissolution or precipitation nor must it be related to a harmful effect on the cathodic areas. It has been demonstrated that an active aluminum anode has areas that are sufficiently cathodic to plate both copper and mercury [*3*].

Anode efficiency (or current capacity) cannot be readily explained by the above, since the explanation pertains, primarily, to voltage.

Activation by Mercury

Microscopic studies show that mercury in solid solution is primarily responsible for points that displace the potential toward more active values. These active points propagate within themselves to form additional or continued pits which eventually develop into shallow crevices. As the pits continue to propagate, their activity further prevents formation of a protective oxide layer. The activation of this anode followed by continued attack is, therefore, slightly more heterogeneous than uniform.

Mercury in solid solution produces a number of amalgams which are highly reactive electro-chemically with little tendency to passivate. As noted above, this reactivity is not confined to grain boundary regions. During continued activation, the mercury does not agglomerate into droplets on the surface or interior grains. There is no evidence of increased mercury concentration with anode depletion. Instead, mercury is thought to be lost mechanically as electrolyte salts. Resolution of polarization data also show no indication of mercury agglomeration on the anode surface.

Activation by Indium

Indium is the second most reliable activator of aluminum. Alloy developers, however, view indium as a distant second to mercury. The point remains, however, that mercury is controversial as a component in aluminum anodes because of environmental concerns. Indium does not have this problem and has come to the application foreground as an additive to aluminum anodes. However, numerous problems have been associated with indium activation. These are listed in a later section on Indium.

Aluminum activation by indium proceeds in the presence of chloride ions which produce localized active sites upon the alloyed aluminum. This is the same mechanism which is responsible for the pitting of aluminum and its alloys [*8*].

Other Activators

Other activators of aluminum have included tin, gallium, bismuth, and magnesium. Of these, tin has been used to the greater extent. Longevity of activation of aluminum by tin addition requires an exacting solution heat treatment. The use of tin has diminished significantly since the entrance of indium into this technology. An environmental concern also exists regarding the possibility of tin discharge into estuary and harbor waters.

Commentary on Chemical Components and Impurities: Their Effect on Anodic Behavior

Performance of aluminum anodes is dependent upon chemical composition. Composition is more critical in low temperature (<10-12°C) seawater. Tables 1 through 4 provide information on the principal components in the alloys under discussion.

Tables 5 through 6 provide information on copper and iron, which make up the principal impurities in these anodes. Table 7 is a summary of recommended compositions for the indium and mercury-activated aluminum anodes.

Mercury

Mercury is ideally suited for the activation of aluminum. It is a good electronic conductor having a suitable negative potential. Mercury comes into intimate contact with aluminum, but it is not dissolved in it enough to affect the potential. Mercury is also very finely distributed with aluminum. The presence of zinc aids in this distribution. Also, mercury is not leached away faster than aluminum. Mercury is not affected by metallic impurities present in aluminum. Low amounts of mercury are required for activation.

Table 1 - *Mercury in Aluminum Anodes*

Metal Characteristics	Comment
Component type	Principal addition
Function	Activation of aluminum
Desirable properties	Best known activator, lab and field tests pose no problems. *NACE TM0190-98* procedure is an adequate test. Capacity of anodes with mercury are superior to other aluminum anodes.
Concentration range	350-400 ppm ambient seawater (see Table 7) 400-480 ppm cold seawater (see Table 7)
Limitations	a. Not recommended for seamuds b. Anodes with mercury may air oxidize in storage (initially). c. Analysis for mercury remains at ±20-30 ppm (accuracy). d. Environmental concern e. Special safety practice is required in the foundry.

Performance of mercury-activated anodes is highly acceptable in low temperature and ambient seawater. Activation is virtually instantaneous in both waters. This anode has no activation limitations regarding sample size or surface treatment. Activation is almost instantaneous regardless of current density (10-15000 mA/m^2). This anode has no reported loss of activation potential from commercial field applications since introduction in 1965.

The anode will also activate promptly in seamuds; however, 4-6 percent zinc in the alloy is required for acceptable efficiencies. Since residues of mercury salts accumulate in the muds as the anode is expended, its use has been curtailed in this environment.

Indium

Indium has many of the activation characteristics of mercury. It is not affected by normal impurities in aluminum. The low melting point of indium is beneficial. At room temperature, indium is a solid. It is easily and safely handled in the foundry. In many foundries, it is initially alloyed with zinc at a 10:1 ratio prior to addition into the aluminum melt. Alloying is routine using standard foundry practice. The use of indium in aluminum does not require post heat treatment.

Indium-activated alloys, of the compositions shown in Table 7, are the most versatile of the aluminum anodes. Performance has been acceptable in the broad range of seawater applications as well as in sea bottom muds [*9,10*].

The indium-activation process is not as reliable as aluminum anodes activated by mercury. Several factors may affect this process and are listed as follows with brief comments:

a. *Anode or Test Sample Size* - Test pieces which have been cast or cut from the same melt (and composition) have shown unpredictable activation with sample sizes less than 10 cm^2. Larger anode or sample sizes activate reproducibly.
b. *Test Sample Surface Characteristics* - In general, surfaces having an as-cast finish will activate more reliably than saw-cut or machined samples. This factor is less important as the sample size is increased.
c. *Seawater or Sea-mud Temperature* - Temperatures above 15-20°C favor predictable and satisfactory activation.
d. *Time in the Electrolyte (ambient temperature and below)* - In general, all recommended compositions will ultimately activate. Very small test samples (2-3 cm^2) in cold seawater may require 24-48 hours before full activation. A small commercial anode (500 cm^2) of the same composition in the same seawater may activate in less than one minute.

Slow activation is rarely attributable to a single variable. Explanations to the above factors are inadequate, since not all specimens (or anodes) in a given heat show the same response to activation.

Table 2 summarizes indium characteristics in aluminum anodes.

Table 2 - *Indium in Aluminum Anodes*

Metal Characteristics	Comment
Component type	Principal addition
Function	Activating element
Desirable properties	a. Ranks second to mercury as an activator. Anodes perform well in seawater and seamuds b. Indium is a non-controversial additive. c. Indium-activated anodes provide 150 mV more negative potential than mercury-activated aluminum.
Concentration range (See Table 7)	Ambient seawater (15-35°C): 100-180 ppm Cold seawater (<10-15°C): 160-200 ppm Ambient seamud (15-35°C): 140-200 ppm Cold seamud (<10-15°C): 180-230 ppm
Limitations	Lab testing in low temperature seawater and mud may pose problems of activation. Sample size and surface finish can be critical. Problems have occurred with NACE TM0190-98

Figure 2 shows the performance relationship of indium and zinc upon the indium-activated anode. The data was obtained by laboratory testing over 30-day periods in synthetic seawater at 24-26°C. Anode current density averaged 2690 mA/m^2 (250 mA/ft^2).

Figure 2 indicates improved current capacity as the indium concentration is reduced. Continued trials run between 0-100 ppm indium showed slightly improved capacities to 65-70 ppm indium. Capacity and anode potential, however, were reduced below this concentration. Anode activation becomes less predictable below 90 ppm indium.

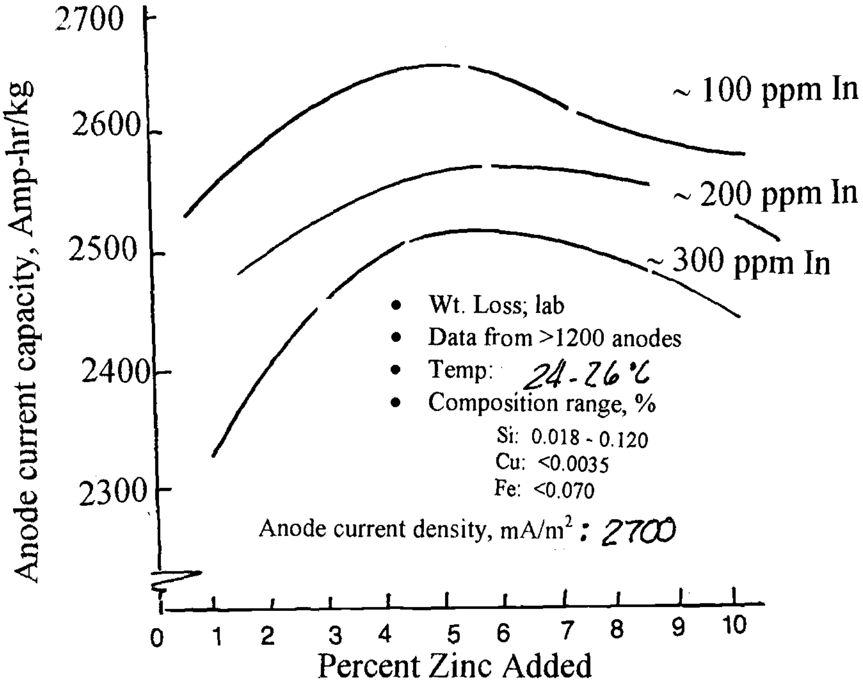

Figure 2 - *Effect of Zinc and Indium on Al-In-0.1% Si Alloys*

The Aluminum Company of America has stated that the solid solubility of indium in aluminum is 170 ppm at room temperature [*11*]. Approximately 25 weight percent is soluble at the general casting temperature of 750°C. The lower current capacities shown by Figure 2 for higher indium concentrations may be related to indium not in solid solution. Pockets or particulate of indium were not observed by Dow investigations when the concentration exceeded 200 ppm. However, it must be pointed out that the Dow work was commercial in nature and emphasized the range of 100-200 ppm indium (close to the recognized solid solubility value of 170 ppm) [*11*].

Zinc

Zinc as a single additive to aluminum sacrificial alloys has very limited activation properties. Zinc has a high solid solubility with aluminum and use is made of this property with the addition of indium or mercury. Its low melting point makes zinc an ideal pre-alloying metal for indium and mercury. The foundry handling of mercury becomes much safer and more reproducible when pre-alloyed with zinc.

Electrochemically, zinc has a combination effect upon anode current capacity when alloyed with indium in aluminum. This characteristic is shown by Figure 2. As indicated by the curve, the target zinc concentration for indium-activated aluminum is 3.5-6.5%.

Table 3 summarizes zinc characteristics in aluminum anodes.

Table 3 - *Zinc in Aluminum Anodes*

Metal Characteristics	Comment
Component type	Major additive
Function	Used as a master alloy additive with mercury and indium. Zinc provides a weight advantage to aluminum anodes in the commercial sense.
Desirable properties	a. Improves castability of mercury and indium-activated aluminum anodes. b. Provides resistance to anaerobic bacteria in sediments, thus permitting improved anode behavior.
Concentration range	Concentration varies with alloy and manufacturer. Hg alloys: 0.35 - 0.40% In alloys: 3.5 - 6.5%
Limitations and problems	On a theoretical basis, zinc lowers the current capacity of the alloy on a constant weight basis. Zinc has approximately one-third the electrochemical equivalent of aluminum.

Silicon

Silicon is added to aluminum anodes in order to form silicon-iron compounds which are less cathodic as an impurity than iron alone. Such compounds formed upon silicon addition permits less pure ingot aluminum to be used as a highly effective anode. Ultimately, anode current capacity is improved for a given concentration of iron. Figure 3 points out this effect for the mercury-activated anode. Silicon addition to the indium - activated anode shows the same behavior pattern at current capacities attendant with this anode.

Table 4 is a summary of silicon characteristics in aluminum anodes.

Copper

When aluminum anodes demonstrate low voltage or decreased life, the cause can generally be traced to the presence of high copper, iron or combinations thereof. Copper, in excess of specification, can devastate the anode by voltage passivation or more positive influences in potential Copper is also soluble in some activators of aluminum, thus making them ineffective. Mercury and indium, fortunately, have low copper solubility. Care must

Table 4 - *Silicon in Aluminum Anodes*

Metal Characteristics	Comment
Component type	Alloying addition to that already present in aluminum.
Function	Added to reduce the cathodic effect of iron by the formation of less cathodic silicon-iron compounds. Resulting anode current capacity is improved.
Concentration ranges	Hg alloys: 0.14 - 0.21% (ambient seawater) Hg alloys: 0.085 - 0.15% (cold seawater: In alloys: 0.08 - 0.20% (ambient seawater) In alloys: 0.08 - 0.12% (cold seawater) In alloys: 0.08 - 0.20% (ambient seamud) In alloys: 0.08 - 0.11% (cold seamud)
Limitations	a. Higher concentration will slightly reduce potential of the anode. b. Concentrations above 0.10% may retard activation of indium-activated aluminum in low temperature environments.

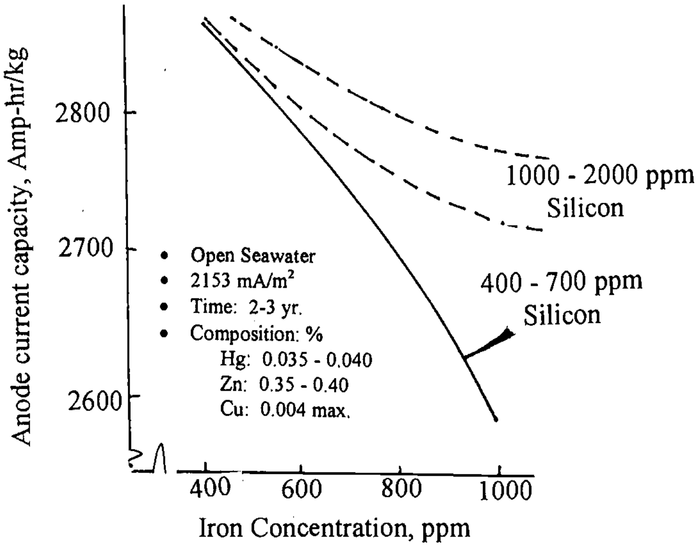

Figure 3 - *Effect of Added Silicon to the Mercury-Activated Anode*

be taken in foundry operation such that copper does not enter the melt. The level of copper, therefore, is an important factor on the acquisition of anode grade ingot.

Table 5 summarizes the effect of copper.

Table 5 - *Copper in Aluminum Anodes*

Metal Characteristics	Comment
Impurity type	Inherent impurity in aluminum ingot. High purity aluminum used as an anode will contain 5-40 ppm.
Function or effect	a. Retards activation of indium-aluminum anodes. b. Lowers potential of all aluminum anodes. c. Stifles anodic site activity by interference. d. All deleterious effects of copper are enhanced in low temperature environments.
Recommended maximum impurity limit	Hg-alloys: (See Table 7) In-alloys: (See Table 7)
Desirable properties	a. Can be selectively added to Hg-activated aluminum to control air-oxidation. b. Copper should not be totally absent in anodes. In the rare but observed case where less than 1 - 2 ppm Cu was present in the ingot, the anode became overactive with normal indium or mercury additions. This circumstance will result in reduced anode current capacity.

Iron

Iron, copper, nickel and lead all reduce or destroy efficiency of anodes to some extent. Iron is the most pronounced of this group. It was pointed out earlier that copper primarily raised the electrode potential (made the potential less negative with respect to a reference electrode). Since the oxide of the aluminum anode is amorphous, an explanation of this behavior is possible. The metals dissolve and then plate out at a cathodic site. The crystal grows until it protrudes through the aluminum oxide. Now, an unprotected, short-circuited cathode is available and hydrogen ion is easily reduced at the surface. Any use of the electrons for this purpose represents inefficiency [3]. Table 6 is a summary of iron characteristics when present in aluminum anodes. Discussion earlier has shown that iron-silicon intermetallics, rather than iron, is beneficial regarding anode efficiency. Electrochemically, the iron-silicon cathodic site provides a lower driving force with aluminum. This is favorable with respect to anode efficiency.

Figure 4 illustrates the effect of iron content in indium-activated anodes. This figure considers the seawater environment (laboratory and field applications). The same trend curves hold for seamud applications; however, the current capacity values are lower.

Lead

Lead as an impurity in aluminum anodes generally enters the alloy through the introduction of low purity zinc. When present, lead acts in much the same way as iron,

Table 6 - *Iron in Aluminum Anodes*

Metal Characteristics	Comment
Impurity type	Inherent impurity in aluminum ingot. Aluminum designated for sacrificial anodes nominally contains 600 ppm or less. Aluminum anode grade ingot is readily available with 200 ppm Fe.
Function or effect	a. Promoter of local cathodic sites. b. Slightly deleterious effect on potential. c. Broad effect of lowering anode current capacity with consequence of reduced anode life
Recommended maximum impurity limit	Hg-alloys: (See Table 7) In-alloys: (See Table 7)
Desirable Properties	The presence of iron in aluminum sacrificial anodes provides no electrochemical or casting merits

resulting in reduced anode current capacity. Use of high purity zinc will eliminate the possibility of lead contamination. Dow studies indicate that the concentration of lead should not exceed 15-20 ppm [*1*].

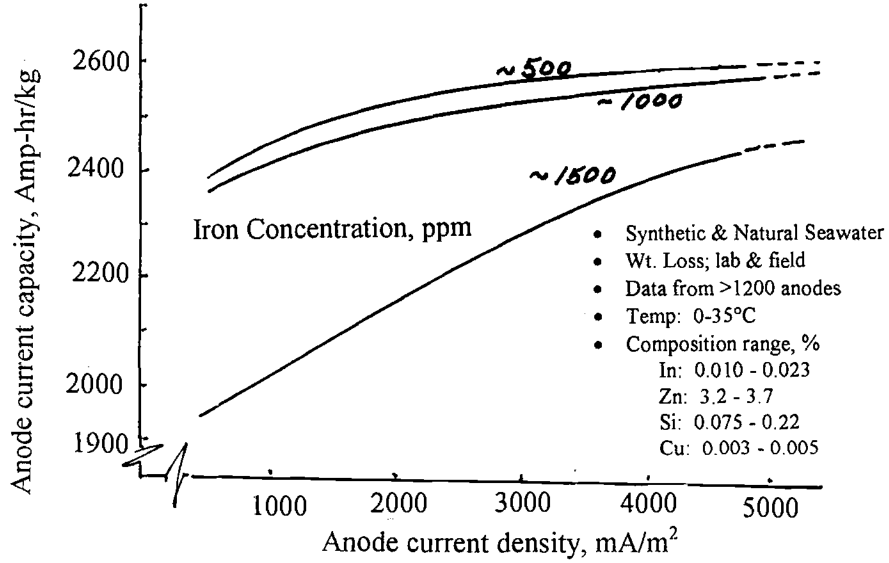

Figure 4 - *Effect of Iron on Current Capacity: Indium-Activated Anodes in Seawater*

Current Density Effects

Aluminum anodes in seawater generally operate in the 1600-2700 mA/m^2 current density range. Bracelet anodes on well-coated lines in cold seamud will operate in the 270-650 mA/m^2 density range.

Figure 5 is a summary curve of a widely used indium-activated aluminum anode. As indicated by the data, current capacity is reduced as current density on the anode is lowered. Low temperature behavior of the indium-containing anode is essentially identical to those anodes in ambient water. Field information in the North Sea and Alaskan area confirms the laboratory curve within the figure. This observation is known to be valid from 23°C to -5°C [*1*,*3*].

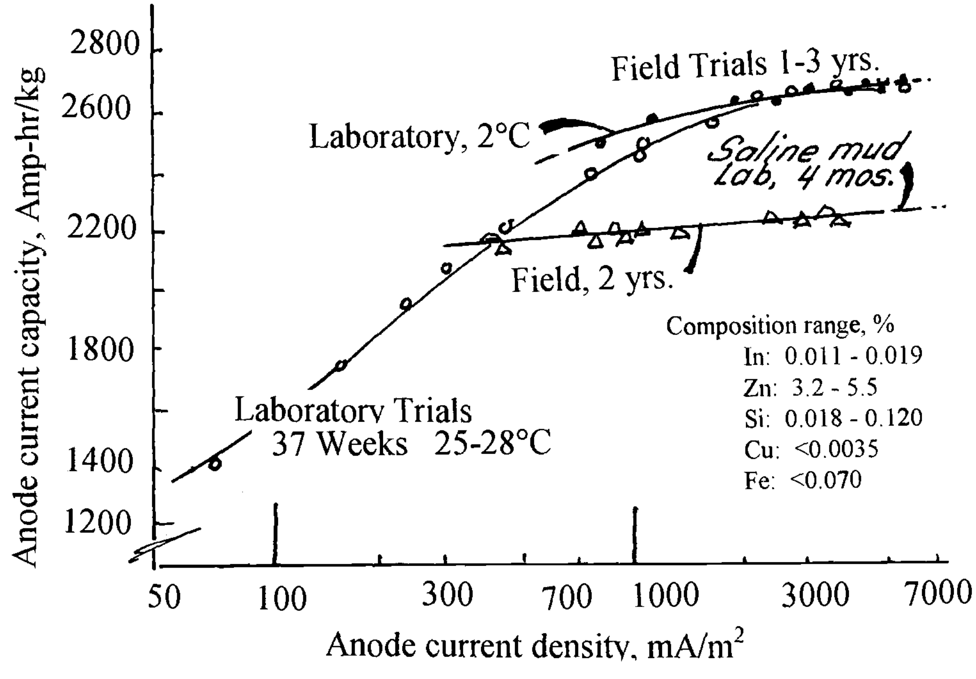

Figure 5 - *Combined Use of Laboratory and Field Data for an Indium-zinc-silicon-aluminum Anode [5]*

Recommended Compositions

Table 7 lists recommended chemical compositions for a mercury and indium-activated aluminum anode. Both anodes are actively applied in the marine cathodic protection industry. The use of mercury-activated anodes is not recommended for seamud application. Therefore, a composition is not given for this environment.

Table 7 - *Chemical Compositions of Two Prominent Mercury and Indium-Activated Aluminum Anodes, (weight percent)*

Anode	Mercury	Indium	Zinc	Silicon	Iron	Copper	Aluminum
Al-In-Si-Zn (ambient seawater)	----	0.010 - 0.018	3.5-6.5	0.08- 0.20	0.12 max.	0.006 max.	Balance
Al-In-Si-Zn (cold seawater)	----	0.016 - 0.020	5.0 - 6.5	0.08 - 0.12	<0.070	0.003 - 0.004	Balance
Al-In-Si-Zn (ambient seamud)	----	0.014 - 0.020	3.5 - 6.5	0.08 - 0.20	0.12 max.	0.003 - 0.004	Balance
Al-In-Si-Zn (cold seamud)	----	0.018 - 0.023	5.0 - 6.5	0.08 - 0.11	<0.070	0.003 - 0.004	Balance
Al-Hg-Si-Zn (ambient seawater)	0.035 - 0.040	----	0.35 - 0.40	0.14 - 0.21	0.10 max.	0.004 max.	Balance
Al-Hg-Si-Zn (cold seawater)	0.040 - 0.048	----	0.40 - 0.48	0.085 - 0.150	0.10 max.	0.004 max.	Balance

Notes: (a) Cold seawater and seamud denotes temperatures less than 10-12°C.
(b) Ambient seawater and seamud denotes temperatures in the range 12-40°C.

Concluding Remarks

1. The indium-activated alloy constitutes the predominant marine aluminum anode.
2. The mercury-activated anode, while being the most electrochemically efficient, is continually subject to environmental concerns.
3. The indium-activated anode can be chemically tailored to a broad range of seawater and seamud applications. This includes application in elevated temperature seawater and brines, which are not discussed in this paper.

4. Both anode chemical types have demonstrated excellent pilot and in-service performance in deep ocean applications.
5. Future deep ocean applications requiring cathodic protection should rely on the indium-activated alloys. The effect of ocean depth (pressure) does not appear to be a significant factor. Decreasing temperature and changes in water chemistry will be more of a factor on performance. Anodes destined for these environments must be tested at the ocean site largely because of complex seawater chemistries.

References

[1] Schrieber, C. F. and Murray, R. W., "Effect of Hostile Marine Environments on the Al-Zn-In-Si Sacrificial Anode," *Materials Protection,* National Association of Corrosion Engineers, July 1994.

[2] Schrieber, C. F., "The Aluminum Anode in Deep Ocean Environments," Paper No. 580, NACE Corrosion 1989, New Orleans, LA, 1989.

[3] Chaverin, J. U., "Electrochemical Investigations of the Activation Mechanism of Aluminum," *Corrosion*, 47, June 1991.

[4] Bessone, J. B., Ph.D., Thesis, University of Manchester Institute of Science and Technology, 1983.

[5] Deltombe, E. and Pourbaix, M., *Corrosion*, 14, 496t, 1958.

[6] Draley, J. E. and Ruther, W. E., *Corrosion*, 12, 480t, 1956.

[7] Kortum, G. and Bockris, J. O'M., *Textbook of Electrochemistry,* Elsevier Publishing Company, New York, 1951.

[8] Binger, W. W., Hollingsworth, E. H. and Sprowls, O. O., *Aluminum Properties, Metallurgy and Phase Diagrams*, American Society of Metals, K. R. Van Horn, Ed., Metals Park, Ohio, 1971, pp. 209-276.

[9] Lucas, K. E., Peterson, M. H., and Guanti, R. J., "Long Term Performance of Aluminum Anodes in Seawater," Paper No. 277, NACE Corrosion 1989, New Orleans, LA, 1989.

[10] Murray, J. N., Hays, R. A., and Lucas, K. E., "Testing Indium-Activated Aluminum Alloys Using NACE TM0190-90 and Long Term Exposures," Paper No. 534, NACE Corrosion 1993, New Orleans, LA, 1993.

[11] Willey, L. A., *Aluminum Properties, Metallurgy and Phase Diagrams.* American Society of Metals, K. R. Van Horn, Ed., Metals Park, Ohio, 1971, pp. 359-396.

Steve Nikolakakos[1]

Cathodic Protection System Design for Steel Pilings of a Wharf Structure

Reference: Nikolakakos, S., **"Cathodic Protection System Design for Steel Pilings of a Wharf Structure,"** *Designing Cathodic Protection for Marine Structures and Vehicles, ASTM STP 1370*, H. P. Hack, Ed., American Society for Testing and Materials, West Conshohocken, PA, 1999.

Abstract: Corrosion of steel pilings in sea and brackish water is mostly due to the establishment of localized corrosion cells and the effects of the tidal changes. The most frequently used corrosion protection systems are coatings and/or cathodic protection. These protective systems when properly designed, installed and operated are very effective in preventing corrosion problems. The design of a cathodic protection system, in order to be effective and reliable, must take into consideration all technical design criteria, the type of materials used, the geometric shape of the structure, environmental conditions, site restrictions, and any outside interferences. These design considerations, as well as the use of design data and an overall design methodology for a cathodic protection system for pipe and sheet piling used in a wharf structure, are discussed in this paper.

Keywords: wharf structure, pipe piles, sheet pilings, cathodic protection, galvanic anode system, impressed current system, corrosion of steel piles, corrosion control

Corrosion of Steel Piles

Corrosion of steel in marine environments, especially in the submerged/soil zones, is mostly electrochemical in nature. In evaluating corrosion of steel piles in a marine environment, it is necessary to examine each area/zone of the pile exposed to different environmental conditions. These areas/zones are: (1) Atmospheric Zone: The area of the top of the pile which is always exposed to the atmosphere. (2) Splash Zone: The area of the pile from the bottom of the atmospheric zone to the mean high water level.

---

[1] Manager Corrosion Engineering, Raytheon Engineers and Constructors, Inc., Princeton, New Jersey

Tidal Zone: The area of the pile between mean low water and high water level. (4) Submerged Zone: The area of the pile which is always submerged from the mud line to mean low water level. (5) Soil Zone: The area of the pile in the mud and/or soil.

The corrosion rate in each of the zones can vary considerably. The lowest corrosion rate is in the soil zone (25 to 114.3 μ (microns) per year) while the highest rate is found in the splash zone (101.6 to 355.6 μ per year). Corrosion normally occurs in the presence of moisture and oxygen. The rate of corrosion is affected by many environmental factors, of which the most important are:

- Different aeration (variations in oxygen concentration at the steel surfaces). The oxygen concentrations near the piling, below the mud line, are normally low and, therefore, the differential aeration cells in this area are very weak or do not develop at all. This is one of the reasons why the corrosion rate in the soil is small.
- Soil/water resistivity (the ability of soil/water to conduct electric current). The lower the resistivity the more corrosive the environment.
- pH (indicator of acidity or alkalinity). The pH of sea water, normally is in the range of 7 to 8. The pH values, however, can be affected by pollutants in the water. Low pH values (below 4) indicate acidic conditions which can dissolve protective films on steel surfaces and therefore accelerate corrosion. High pH values (above 9.5) indicate high alkalinity which promotes the formation of corrosion protective films on the metal surfaces.
- Marine organisms. Organisms such as barnacles can normally accelerate corrosion by creating a differential aeration condition. Another organism, anaerobic bacteria (found in oxygen-free environments), increases corrosion by changing sulfate to sulfides which attack steel.
- Stray Currents. (Currents flowing through paths other than the intended circuit). In the corrosion industry, such currents are normally direct and generated by d.c. powered rail systems, cathodic protection and high voltage direct current ground electrodes.

In general, an assessment of the overall corrosion of piles can be summarized as follows:

- Corrosion of piles in undisturbed soil is absent or insignificant.
- Corrosion of piles in disturbed fill soil can be significant.
- Corrosion of piles in the water and atmosphere can vary depending on the corrosion characteristics of the environmental factors.
- Corrosion of piles due to stray currents can be very significant, and therefore when such a condition is present, a careful and detailed evaluation must be conducted.

Corrosion Control

Optimum corrosion control is achieved by a combination of methods. There are normally four basic methods that can be utilized to effectively control corrosion. These methods are:

- *Material Selection.* Material selected must perform adequately in the environment to be installed and must be economically justifiable.
- *Design/Fabrication Practices.* The practices used in this phase of the work must be such as to reduce the formation of galvanic cells. Combination of two or more metals should be avoided if possible.
- *Coatings.* Coatings are used to insulate the steel from the environment. Coatings are very effective in controlling corrosion in the splash/tidal and atmospheric zones. They are also very effective in reducing the cathodic protection current requirements, when used in buried/submerged structures.
- *Cathodic Protection.* Cathodic protection is used to provide corrosion prevention of metallic structures in the soil and/or water. It is very effective in the soil and water zones and partially effective in the tidal zones. This method of corrosion control is based on the observation that when a metallic structure collects current (becomes cathode) does not corrode. The reasoning is that if all points on the surface of a structure in contact with a corrosive environment collect current from that environment corrosion would stop. Therefore, if the entire structure can be made to act as a cathode in relation to the surrounding environment, corrosion will be controlled.

Cathodic Protection System Design

General

Once a decision has been made to design and install a cathodic protection system, the engineer must determine the type of the system to be used, galvanic or impressed current. In many case the system is already defined and no such determination is required.

The main factors that must be considered in the evaluation of the system selection are:

Availability of A-C Power

- Satisfying design criteria such as, protective current, and life expectancy.
- System maintainability.
- Stray current effects, if any.
- Cost effectiveness.

Design Requirements - The initial information required for the design of a cathodic protection system must consider the following:

- The design/construction details and specifications of the structure to be protected.
- The identification of any materials that may be adversely affected by high cathodic polarized potentials. Such materials may be high strength steels, certain stainless steels, aluminum, lead, etc.
- Soil/water resistivity, pH and pollutants in the water.
- Coating system(s) to be used. If certain areas of the piles are to remain bare, they should be identified and considered in the design.
- Selection of cathodic protection current densities (Table 1) to be utilized in the design that are appropriate for the site.
- Determination of stray currents, if any. Are there any subways or light rail systems near the site? Are there any other structures in the proximity that have an impressed current cathodic protection system?
- Determination of the surface area of the piles to be cathodically protected. Separate calculations must be made for bare, coated surfaces and for the areas of the piles in the tidal, water and soil zones.
- Determination of the total protective current requirements using the calculated surface areas of the piles and the selected current densities for the specific site.

Table 1 - *Protective Current Density (mA/m^2)*

Environment	Bare Steel	Coated Steel
Soil	0.093-0.465	0.046-0.095
Sea Water		
Stagnant	0.093-1.4	0.046-0.279
Moving	0.465-2.8	0.093-0.465

Once the basic design data has been collected and evaluated then the detail design of the cathodic protection system can start. A design system approach for galvanic and impressed current systems are presented below.

Galvanic Anode System Design - General

Galvanic anode systems utilize the potential difference between active metals such as aluminum, magnesium and zinc and the metal of the structure to be protected, to provide the driving voltage to force cathodic protection current to flow. When the galvanic anodes are electrically "connected" to the structure to be protected, current will then flow through the conducting environment (soil/water) from the anode to the structure to be protected. A galvanic anode system has certain advantages and limitations especially when compared to an impressed current system. The advantages are: reliability; long life (in most cases); anodes are available in many sizes and shapes; low maintenance; low cost (for certain applications).

The limitations are: limited driving voltage (in the range of 0.9 to 1.5 volts); normally restricted to low resistivity environments; normally restricted (due to cost considerations) to low current output installations.

Galvanic Anode Materials

There are basically three materials that are used as galvanic anodes in cathodic protection system designs, magnesium, zinc and aluminum.
The material characteristics for these anodes are shown on Table 2.

Table 2 - *Some Properties of Galvanic Anodes*

Anode Material	Density Kilograms Per Cubic m	Current Efficiency %	Consumption Rate Actual (Kg/Amp.-Yr.)	Potential to $CuSO_4$ Electrode (Volts)
Magnesium:	1936	50	7.9	
Standard Alloy				-1.55
High Potential Alloy				-1.80
Aluminum	2720	95	3.1	-1.1
Zinc	7040	90-95	11.8	-1.1

Design Calculations (Galvanic Anodes)

The design calculations for a galvanic anode system must include:

- *Protection Current Requirements* - In order to calculate the protection current, the surface areas of the structure in the tidal, water and soil zones must first be calculated. The current is then determined using the following formula:

$$I_p = SA \times CD$$

where

I_p = Required protection current (milliamps)
SA = Surface area of structure (ft^2)
CD = Protective current density (mA/ft^2)

The I_p for each zone of pile must be calculated. The total current must be the summation of all "zone" currents.

The protective current densities to be utilized are given in Table 1. Other current densities could be utilized if specific information is available for that site.

Normally the initial current densities required to polarize (develop a protective film) the structure is much higher than the current required to maintain the polarization once it is formed.

- *Anode Life Expectancy (Galvanic Anodes)* - Cathodic protection systems are normally designed to perform for a 15 to 30 year life. In some special situations, however, it is not feasible nor economical to design a system for long performance. In such cases the anodes are replaced frequently or an impressed current system is used (if possible). The general formula to calculate the life of a galvanic anode is:

$$Life(Years) = \frac{Constant \times Anode\ Weight\ (Kg) \times Efficiency \times Utilization\ Factor}{Current Output\ (Amps)}$$

The constants vary with the anode material and are based on the length of time in years that one kilogram of material would last when discharging one ampere. These constants are:

For Magnesium	0.052
For Zinc	0.0192
For Aluminum	0.0696

The efficiency for each of the anodes is 0.5 (50%) for magnesium, and 0.95 (95%) for zinc and aluminum.

The utilization factor is based on the assumption that the anode has reached its useful life at .85 (85%) consumption.

The number of anodes required for the system can be calculated by dividing the total anode weight to the weight of a single anode.

It should be noted that the actual number of anodes used in a system may have to be increased to take into consideration other factors such as non-uniform current distribution and avoid current shielding effects due to the shape of the structure.

- *Resistance-to-Earth/Water of Anode System* -The resistance calculations are required for determining the anode current output of the system.
  The formulas that can be used are:

$$R_V = \frac{0.522}{L} \rho \left[2.3 \, Log_{10} \, \frac{8L}{d} - 1 \right]$$

$$R_S = \frac{0.522}{L} \rho \left[2.3 \, Log_{10} \, \frac{8L}{d} - 1 + \frac{2L}{S} 2.3 \log_{10} \, 0.656 \, N \right]$$

where:

R_v = Resistance of one vertical anode (ohm)
R_s = Resistance of anode system (ohm)
N = Number of anodes
L = Length of each anode (m)
ρ = Water/soil resistivity (ohm-m)
d = Diameter of anode (m)
s = Spacing of anodes (m)

Where more than one anode is in the circuit then the resistance formula (R_s) is used.

- *Current Output of the Anode System* - The current output of the system can be calculated as follows:

  $$I_o = \frac{V(Driving\ Voltage)}{R_S(Resistance\ of\ Anode\ System)}$$

  The current of a galvanic anode system will vary depending on the potential of the structure. Initially, the potential of the structure will be less negative than the potential after polarization has been achieved. The driving voltage of a non-cathodically polarized structure and a magnesium anode could be in the order of 1.2 volts, whether the driving voltage of a cathodically polarized structure could be in the order of 0.7 volts. The anode life expectancy calculations should be made utilizing the system current that is calculated using the polarized potential of the structure.

- *Design Drawings and Specifications* - The development of design/installation drawings and specifications must be as explicit as possible. In many cases the contractors installing the systems have no functional knowledge of the system and therefore could take shortcuts that can be proven to be detrimental to the integrity and overall operating efficiency of the system.
  System maintainability is another important factor that must be considered in the design. The system must be easily maintained (anodes, test wires, reference electrodes, etc. should be easily replaced).
  A constructability review of the system should also be performed to insure proper installation techniques.

Impressed Current Systems Design - General

This system utilizes an external source of d.c. power between the structure to be protected and a "ground connection" which is normally comprised of inert (low corrosion rate material) anodes.

An impressed current system has certain advantages and disadvantages when compared to a galvanic anode system. The advantages are: adjustable voltage output and current capacity; economical for large current output requirements; long life; anodes are manufactured in many sizes and shapes.

The disadvantages are: requires a power or fuel supply; partial or entire system failure due to wire installation failure; requires more maintenance than galvanic anodes.

Impressed Current Anode Material

The most frequently used materials for impressed current anodes are:

- High silicon cast iron
- Graphite
- Platinized titanium or niobium
- Mixed metal oxide

The material characteristics for these anodes are shown on Table 3.

Table 3 - *Some Properties of Impressed Current Anodes*

Material	Anode Current Density (Amps/ m^2)	Consumption Rate (Kg/Amp.-Yr.)	Form Available	Special Operating Requirements
Graphite	2.7-10.7	0.176-4.84	rods/slabs	
High Silicon Cast Iron	10.7-53.5	0.66-2.42	rods/cast shapes	
Platinized Anodes	267-1070	6-10 Mg./Amp-Yr.	rods, wires, mesh	Pt-Ti: Voltage <12V
Mixed Metal Oxide	267-1070			Pt-Ni: Voltage <90V

- *Impressed Current Power Sources.* The most common power source used is the rectifier, a commercial device for converting an a.c. power to low voltage d.c. power. These devices are commercially available in a wide range of voltage and current outputs.
- *Design Calculations.* The design calculations for an impressed current system are similar to those of a galvanic anode system with the exceptions of the calculations for life expectancy, and current output of the system. The protection current requirement (I_p) and the resistance-

to-earth of the anode system calculations are similar to those discussed under the galvanic anode system design calculations.

- *Anode Life Expectancy* - Impressed current cathodic protection systems are also designed for 15 to 30 year life.
  The formula for calculating the life of the anode system is:

$$Life\ (Years) = \frac{W(Kg)\ x\ Utilization}{ACR\ (Kg/Amp.-Yr.)\ x\ I\ (Amps)}$$

where:

ACR = Anode Consumption Rate (Kg/Amp.-Yr.)
W = Total Anode Weight (Kg)
I = Total Current (Amps)

The efficiency factor of an impressed current system is 100%. The utilization factor can be as low as 50%. The consumption rate varies considerably depending on the type of anode used. Table 3 lists the consumption rates of the anodes.

The minimum number of impressed current anodes to be used is calculated by dividing the total anode weight by the weight of a single anode. The total number of system anodes however, may have to be increased in order to provide better current distribution to the structure and also avoid possible shielding effects due to the shape of the structure.

- *Current Output of the Anode System* - The current output of the system is normally equal to the protective current required to cathodically polarize the structure.
  It is calculated by multiplying the surface area of the structure by the current density required to polarize the structure (Table 1). Sometimes a safety factor of 10 to 20% is added to the total current.

D.C. Power Source (Rectifier) Voltage Calculation. A.C. Power Input: The a.c. power input requirements are normally 120 volts/220 volts and 15 amps (single phase air or oil cooled). Higher A.C. voltages and currents can be used.

D.C. Output: The voltage required is equal to total current times the total circuit resistance plus two volts.

$$V_{Rectifier} = (I_{Total}\ x\ R_{Circuit}) + 2\ volts$$

The total current is the protective current (surface area x current density). The circuit resistance is calculated by adding, a) the anodes-to-earth, b) the Circuit cable resistance (the resistance in ohms of all the cables used in the circuit) and c) the structure to electrolyte resistance (in most cases this resistance is very small and therefore not considered in the calculations).

The two volts is the anode back voltage. The total design rectifier voltage is normally increased by 10%, 20% or more (safety factor).

Design Drawings and Specifications. Similar to the galvanic anode system, the design/installation drawings and specifications of an impressed current system must be as explicit as possible. In addition to the considerations stated in the galvanic anode system section, the following precautions must be taken.

- Insure that all piles and any other metallic components of the structure are electrically connected.
- Insure that all cable to cable and cable to anode splices are well insulated.
- Insure that cable insulation is not damaged, and that no copper strands are exposed.
- Insure that no anode is placed near a metal component that may be damaged due to high cathodic polarized potentials.

The design of the system must allow for system maintenance and provide test stations and/or computerized equipment for manual and/or remote monitoring of the system. Permanent reference electrodes (silver/silver chloride (Ag/AgCl) or copper sulfate ($CuSO_4$)) must also be included in the design to facilitate monitoring of the system. The reference electrodes must be protected from mechanical damage. They should therefore be directly buried or suspended in perforated plastic piping.

An Example of An Impressed Current System Design

General

The structure that the cathodic protection system is designed for is a reconstructed wharf located in New York City along a river with brackish water. The wharf structure is of an “L” shape with approximate dimensions of 97.5 m x 36.6 m. The wharf is supported by 37 pipe piles and 39 H piles. On one side there is a sheet piling retaining wall (30.48 m wide x 13.41 m long). The new sheet piling is installed approximately 51 cm away from an existing sheet piling wall.

Design Requirements

- The material of the piles and sheet piling are carbon steel. There are high strength steel tie rods connected to the top of the sheet piling.
- The water resistivity is 40 ohm-cm.
- The coating of the structure was specified to be "Flake Glass Polyester" (35-45 mils or 889-1143 microns), to be applied in two coats.
- The current densities to be used, based on the site of the structure were selected to be: 1) For coated surfaces: 43 mA/m^2 for water zone and 10.75 mA/m^2 for the soil zone; 2) For bare surfaces: 322.5 mA/m^2 for the water zone and 10.75 mA/m^2 for the soil zone. For safety purposes we assumed that 25% of the coating in the water and 50% of the coating in the soil area will be damaged during installation. These areas were assumed to be bare.
- A stray current condition may be present due to the electrified rail systems near the wharf and due to a cathodic protection system that is used to protect a pipeline near the wharf.
- The total surface area of all piles were calculated to be in the order of 3,258 m^2.
- The total current required to protect the 3,258 m^2 area of piles was calculated to be 160 amperes. This current was calculated based on the current densities indicated above. An average current density of 49 mA/m^2 was calculated by dividing the total current in milliamperes to the total surface areas.

Design Calculations

- *Protective Current.* The protective current of 160 amperes was calculated based on data and assumptions discussed above.
- *Anode Material.* Mixed metal oxide anodes were selected for this application, because of the long life (low rate of consumption) and small diameter (0.95 cm) shapes. This was necessary because the space (51 cm) between the two sheet piles was very small to accommodate bigger diameter anodes. The anodes were installed inside a perforated plastic pipe for mechanical protection and to avoid accidental shorting to the piles.
- *Anode Life Expectancy.* A total of 43 mixed metal anodes (0.95 cm x 6 m) were used in the design. The life of the anode based on the design current of 160 amperes (3.7 amperes/anode) was calculated to be higher than thirty years.
- *Anode Resistance Calculations.* The cathodic protection system was divided into four subsystems, each one with its own power source and approximately 10 to 11 anodes each. The overall circuit resistance was calculated to be in the order of 0.1 ohm.
- *D. C. Power Source (Rectifier).* The rectifier a.c. input was selected to be sixty (60) cycles, 115/230 volts. The d.c. current output was selected to be 160 amps and 12 volts. In order to better control the output of the anode current output in the different areas of the structure, the power source was

supplied in four smaller, independently adjustable power units. All units are automatic potential control units, and can be adjustable remotely, utilizing a computerized remote monitoring system.

- *Rectifier Voltage.* The voltage of each rectifier unit was calculated to be 6 volts. A 12 volt rectifier unit, however, was specified.

Design Drawings and Specifications

Detail design/installation drawings and specifications were issued for the project. The following items were specially detailed and emphasized.

- Avoid cable splicing; other than the anode cable to rectifier header cable.
- Mechanical protection of anodes and cables during installation procedure.
- Electrical continuity of all components of the structure.
- Measures for detecting and resolving stray current problems.
- Location of anodes to minimize high polarized potentials on the high strength steel tie rods.
- Remote monitoring units for frequent computerized monitoring and flexibility of rectifier current adjustment from remote locations.
- Individual anode monitoring for easy maintenance and troubleshooting.

Some details of the design drawings are shown on Figures 1 through 6.

Summary

Corrosion of steel pilings in sea and brackish water is well documented and is mostly concentrated in the tidal zone and the areas where the piles were installed in disturbed soils. In general, the corrosion rate of a pile varies depending on environmental conditions. Corrosion protection of piles in the form of protective coatings and/or cathodic protection is the most frequently used method of corrosion control. The selection of the system to be used is normally based on cost and maintenance conditions.

In the evaluation process, items such as, life expectancy, maintainability and specific design materials and structure requirements must be considered.

The design of a cathodic protection system must be based on accurate environmental and structure design data. The most critical items to consider in the design of a are: selection and location of anodes for complete coverage of the structure; electrical continuity of all structure components; identification of stray currents; identification of materials that may be affected by high polarized potentials; system maintainability; provisions for monitoring and frequency of monitoring.

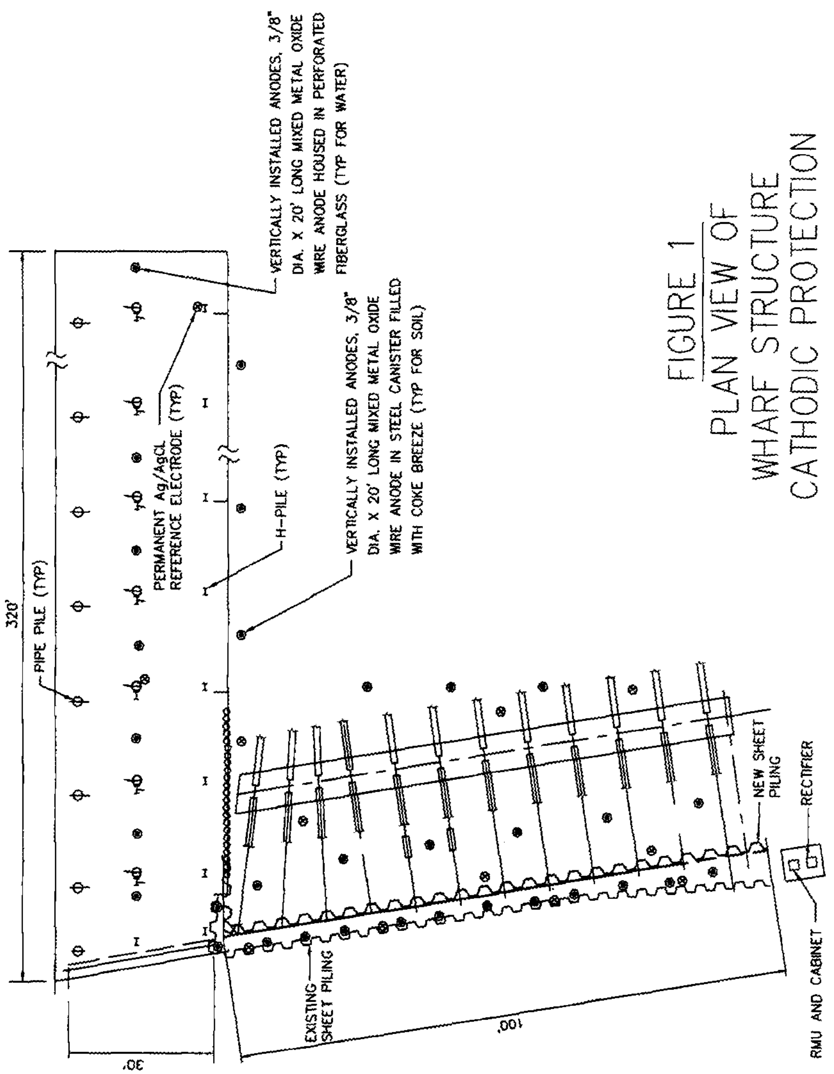

FIGURE 1
PLAN VIEW OF
WHARF STRUCTURE
CATHODIC PROTECTION

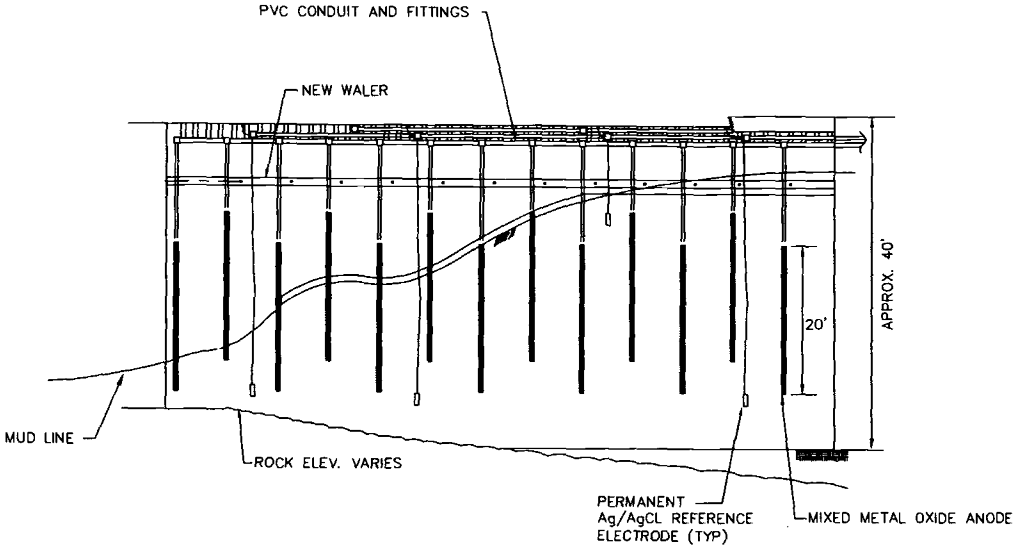

FIGURE 2
ELEVATION VIEW OF SHEET PILING SIDE ANODE LOCATION

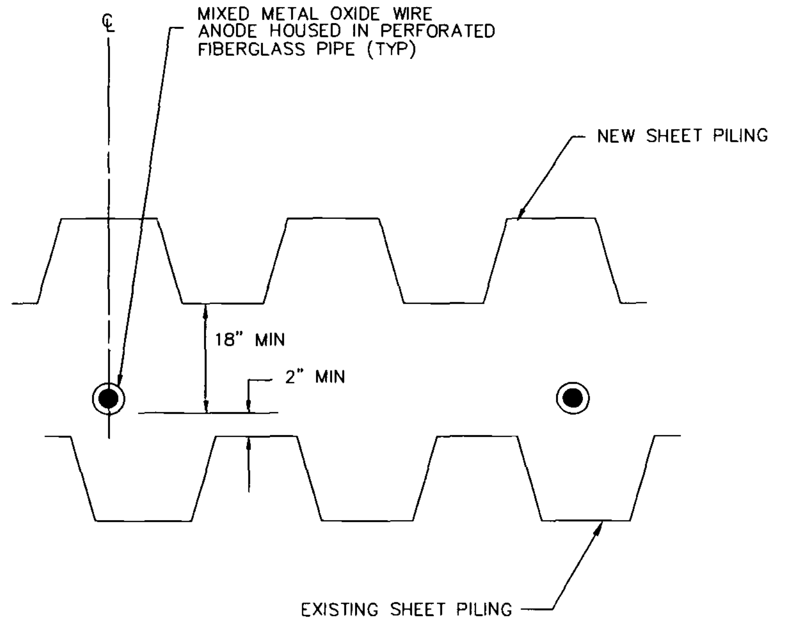

FIGURE 3
ANODE PLACEMENT BETWEEN SHEET PILING

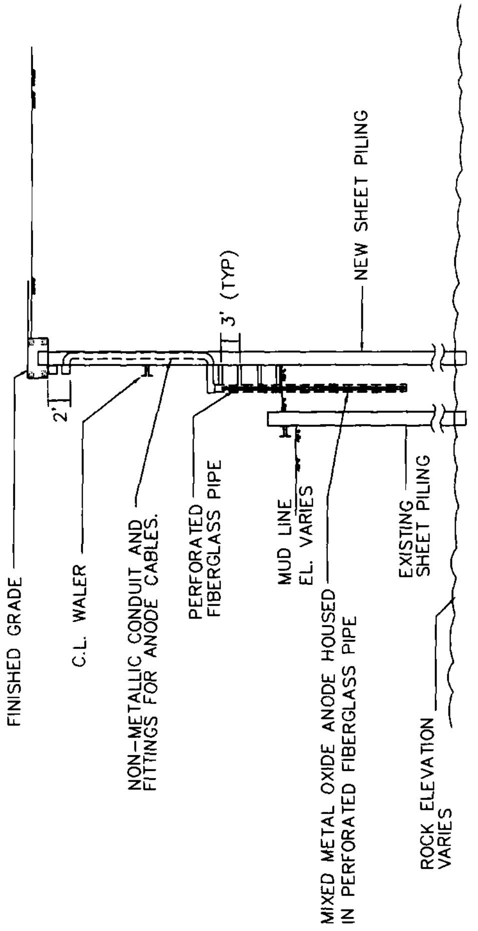

FIGURE 4
SIDE VIEW OF
ANODE INSTALLATION BETWEEN TWO SHEET PILINGS

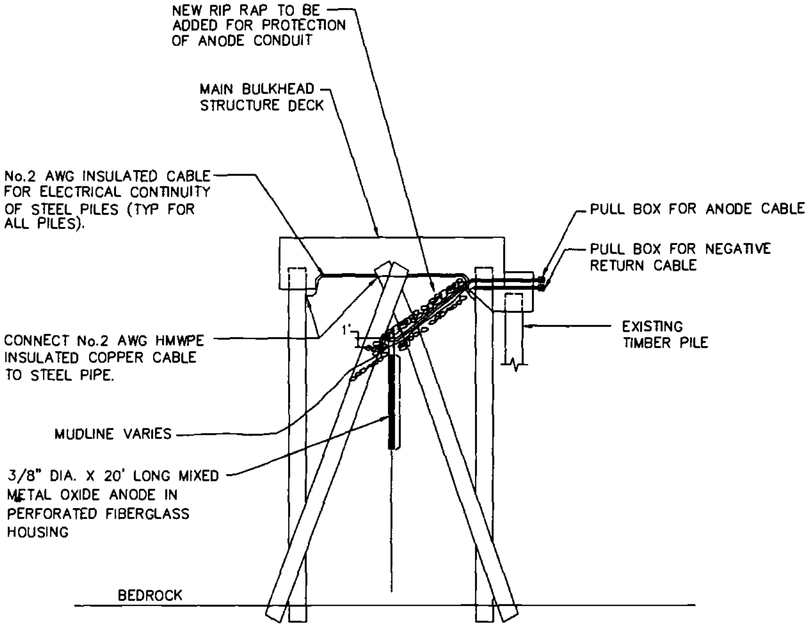

FIGURE 5
MAIN BULKHEAD
SIDE VIEW OF
ANODE INSTALLATION BETWEEN PIPE PILES

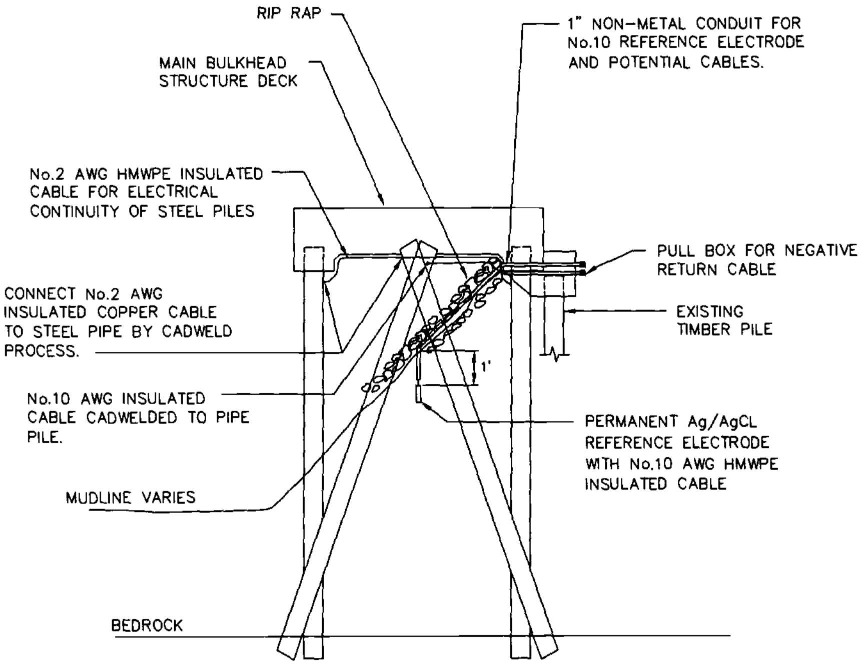

FIGURE 6

MAIN BULKHEAD
SIDE VIEW OF
REFERENCE ELECTRODE INSTALLATION BETWEEN PIPE PILES

References

[1] Romanoff, Melvin, "Results of National Bureau of Standards Corrosion Investigations in Disturbed and undisturbed Soils", Proceedings of the Ninth Annual Appalachian Underground Corrosion Short Course, 1964.

[2] J. A. Beavers and C. L. Durr, "Corrosion of Steel Piling in Nonmarine Applications", National Cooperative Highway Research Program Report 408, 1998.

[3] American Iron and Steel Institute, "Handbook of Corrosion Protection For Steel Pile Structures In Marine Environments", 1981.

[4] Sunde, E. C., "Earth Conduction Effects in Transmission Systems", D. Van Nonstrant Company, Inc., 1949.

[5] Uhlig, H. H., "Corrosion and Corrosion Control", John Wilen and Sons, Inc., 1963.

Carlos M. Menendez,[1] Harry R. Hanson,[1] Russell D. Kane,[1] and Gale B. Farquhar[2]

Cathodic Protection Requirements for Deepwater Systems

Reference: Menendez, C. M., Hanson, H. R., Kane, R. D., and Farquhar G. B., "**Cathodic Protection Requirements for Deepwater Systems,**" *Designing Cathodic Protection Systems for Marine Structures and Vehicles, ASTM STP 1370,* H. P. Hack, Ed., American Society for Testing and Materials, West Conshohocken, PA, 1999.

Abstract: Field and laboratory experience related to requirements for cathodic protection (CP) in deep water are reviewed with emphasis on identification of the major variables that need to be specified for successful deepwater CP designs for offshore structures. The subject is addressed based on the historical development of cathodic protection design methodologies for offshore structures focusing on sacrificial anode systems and trends that have resulted in specific changes in design requirements. Three main subjects are discussed: (1) application of existing industry standards such as NACE RP0176; (2) environmental factors - dissolved oxygen, temperature, salinity, pH, water velocity and fouling; and (3) calcareous deposits - difference between shallow and deep waters. Current practice of design criteria and systems for deepwater applications is assessed, including initial polarization, use of coatings and anode materials. The results from laboratory tests are compared with available documented service experiences and field tests results.

Keywords: cathodic protection, deep waters, sacrificial anodes, offshore structures, design requirements, industry standards, environmental factors, calcareous deposits, initial polarization, field experience, laboratory simulation

---

[1] Research Scientist, Consultant and President, respectively, *InterCorr* International, Inc.,14503 Bammel-N. Houston, Suite 300, Houston, Texas 77014.

[2] Texaco, GED, 4800 Fournace Place, Bellaire, Texas 77401.

Introduction

The 1990's have been significant for deepwater (CP) systems, for two major reasons. First, during this period there has been substantial development of offshore facilities in waters with depths greater than 1000 ft (305 m) in several areas of the world. Secondly, research conducted by various organizations has been performed specifically to ensure corrosion protection of facilities in this environment.

The present paper focuses on the following:

- A review of field and laboratory experience identifying the major variables that need to be specified in designing sacrificial anode CP systems for deepwater structures.
- An analysis of the applicability of existing industry standards such as NACE RP0176, accepted design criteria and the new slope parameter concept for deep water systems given in NACE International Publication 7L198[*1*].
- Comparison of laboratory tests results obtained in this investigation with available documented field experiences.

Historical Background

The oil industry first began building platforms in offshore waters in significant quantities in the late 1940's and the 1950's. Most of the structures were in shallow waters at a depth of approximately 50 ft (15 m) deep or less. Cathodic protection of these structures was accomplished by using impressed current systems or by using magnesium anodes. Beginning in 1962, when the Federal Government opened additional tracts for bid and development, the industry first moved into waters that were up to 200 ft (61 m) deep.

Earlier systems in these "deeper" waters required frequent (every two years) replacement of anodes and maintenance was no longer practical. Longer lasting, cathodic protection systems were needed. As a result of this need, the first systems using aluminum (Al) or zinc (Zn) anodes that would provide protection for 10 to 20-years were designed and installed. Some major oil companies spearheaded this effort designing several systems having a ten-year life using Zn anodes and others designing several 20-year systems using an Al anode that was alloyed with Zn and tin (Sn). The Al anodes were less costly than Zn anodes but were not as reliable.

Much of the work performed in the 1960's was to find an Al anode material that was both reliable and economical. This work led to the development of the aluminum-mercury (Al-Hg) anodes and the aluminum-indium (Al-In) alloy anodes that are still in use today. As the industry continued to move into still deeper waters, another threshold was found to exist at depths of over 1000 ft (305 m). The design criteria that had been used in more shallow waters were not completely effective in waters at these greater depths.

Providing corrosion protection to the deepwater structures is more important than ever before since the cost of these mammoth structures are often 100 to 1000 times those of the earlier platforms. Additionally, due to their depths, repair and retrofitting of the anode systems is very costly.

Current Practice in Design of Cathodic Protection Systems

Recommended Practice for Corrosion Control of Steel Fixed Offshore Platforms Associated with Petroleum Production (NACE RP0176)

In this standard, three independent criteria are listed that must each be satisfied to design a successful cathodic protection system: (1) the current criteria, (2) the weight criteria and (3) the polarization criteria.

For the ***current criteria***, the design uses a calculation method that specifies the amount of anode area that must be available at all times during the life of the system to produce the current that is needed to maintain the structure at a protection potential level. The arbitrary choices that are left to the designer are to determine what the average current density should be and what weight and shape anode should be used.

For the ***weight criteria***, the life of the system must be selected. Knowing the required life of the system, the weight of anode material needed to ensure current for the life of the system can be calculated. Again, the designer can choose the anode shape and the core size to ensure that the most efficient shape and size are used.

For ***polarization criteria***, the designer must initially provide enough anode area when the structure is first placed in the water to ensure that adequate current is available to polarize the structure. Based on experience, the polarization current is usually about three to five times the maintenance current density.

Application of the above mentioned criteria will strongly depend on the specific environmental conditions that apply for the projected location of the structure. In deep waters, CP designers have encountered very cold waters[*2,3*]. In very cold waters, calcium carbonate is more soluble and a higher CP current is required to cause the structure to polarize adequately to insure corrosion protection.

In warm waters, calcium carbonate is nearly insoluble, and a heavy, protective calcareous deposit (calcium carbonate) forms easily during CP. Structures are readily protected with very low current densities. Other environmental factors such as pH, salinity, dissolved oxygen, water velocity and fouling can directly affect the quality of the calcareous deposits and will be discussed in detail in the following sections.

Designs with High Initial Polarization Currents

The idea of the high initial polarization current was developed as one of the cardinal concepts in cathodic protection designs for offshore petroleum production. It clearly defines that, in order to generate a more protective calcareous deposit, high initial current densities are required, but current demand decreases as the protective calcareous deposit is formed. The standard NACE RP0176 gives a general guide to the design of cathodic protection systems in ten major offshore petroleum producing areas based on service experience. The guide, shown in Table 1, may be used as a starting point for investigation prior to selection of final design parameters for a particular application.

Several papers indicate that if a high initial polarization current is used, the required maintenance current levels will be much lower[*2,4,5,6,7*]. This concept was first reported in the literature during the 1940s[*8,9*]. For cold waters near freezing, a value of 300 mA/m^2 has been used and field tests have shown it to cause the structure to polarize quickly, usually in one day. In some areas like in the Barents Sea, adequate CP can be achieved only if high initial current densities are applied (>300 mA/m^2)[7].

There are experiences using bi-metallic anodes[*10*] in order to achieve high initial current densities. These anodes consist of a thin layer of high potential magnesium cast onto one face of an Al based anode and are a cost effective means to achieve the high initial current densities[*10*]. High current from the magnesium enables rapid polarization of the structure.

Design Criteria For Cathodic Protection Systems

			Environmental Factors (A)		**Typical Design Current Density (C)mA/M^2 (mA/ft^2**		
Production Area	**Water Resistivity(B)(ohm-cm)**	**Water Temp. (ºC)**	**Turbulence Factor (Wave Action)**	**Lateral Water Flow**	**Initial (E)**	**Mean (F)**	**Final (G)**
Gulf of Mexico	20	22	Moderate	Moderate	110 (10)	55 (5)	75 (7)
US West Coast	24	15	Moderate	Moderate	150 (14)	90 (8)	100 (9)
Cook Inlet	50	2	Low	High	430 (40)	380 (35)	380 (35)
Northern North Sea	26-33	0-12	High	Moderate	180 (17)	90 (8)	120 (11)
Southern North Sea	26-33	0-12	High	Moderate	150 (14)	90 (8)	100 (9)
Arabian Gulf	15	30	Moderate	Low	130 (12)	65 (6))	90 (8)
Australia	23-30	12-18	High	Moderate	130 (12)	90 (8)	90 (8)
Brazil	20	15-20	Moderate	High	180 (17)	65 (6)	90 (8)
West Africa	20-30	5-21			130 (12)	65 (6)	90 (8)
Indonesia	19	24	Moderate	Moderate	110 (10)	55 (5)	75 (7)

(A) Typical values and ratings based on average conditions, remote from river discharge

(B) Water resistivities are a function of both chlorinity and temperature. In the Corrosion Handbook by H. H. Uhlig (New York, NY: John Wiley and Sons, Inc., 1948), the following resistivities are given for chlorinities of 19 and 20 parts per thousand:

Resistivities (ohm-cm) Temperature (ºC)

Chlorinity (ppt)	**0**	**5**	**10**	**15**	**20**	**25**
19	35.1	30.4	26.7	23.7	21.3	19.2
20	33.5	29.0	25.5	22.7	20.3	18.3

(C) In ordinary seawater, a current density less than the design value suffices to hold the platform at protective potential once polarization has been accomplished and calcareous coatings are built up by the design current density. CAUTION: Depolarization can result from storm action

(D) Conditions in the North Sea can vary greatly from the northern to the southern area, winter to summer, and storm periods.

(E) Initial current densities are calculated using Ohm's Law and a resistance equation such as Dwight's or Crennell's (McCoy;s) equation with the original dimensions of the anode. An example of this calculation is given in Appendix D, using an assumed cathode potential of -0.80 V (Ag/AgCl $^{[sw]}$).

(F) Mean current densities are used to calculate the total weight of anodes required to maintain the protective current to the platform over the design life. An example of this calculation is given in Appendix D.

(G) Final current densities are calculated in a manner similar to the initial current density, except that the depleted anode dimensions are used. An example of this calculation is given in Appendix D.

Table 1 - *Design Criteria for Cathodic Protection Systems*

A new design approach based on the slope parameter concept eliminates the requirement that an initial current be defined at some potential[11]. However, the initial current density concept is contained in the slope factor. If a quick and effective polarization is desired, a proper slope should be chosen in order to achieve a high initial polarization current and hence a protective calcareous deposit. However, for the reliable application of this new approach in deep water systems more data about steel polarization behavior in cold water is needed.

The definition of an optimal slope parameter for design requires information regarding the shape of the long term polarization curve because only on this basis is the minimum maintenance current density generally achieved[1]. An example of the sigmoidal polarization behavior observed in warm waters is shown in Figure 1[12]. In contrast, little data is available regarding the long term polarization behavior in conditions typical for deep waters. It is believed that for high water velocity or low water temperatures the polarization behavior does not exhibit a pronounced sigmoidal curve[1]. This lack of information potentially makes it difficult to apply the slope parameter concept in cathodic protection designs for deep waters.

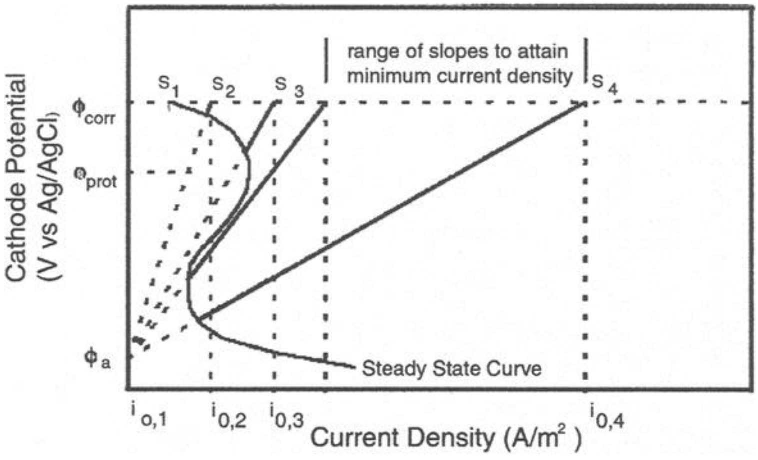

Figure 1 - *Sigmoidal polarization behavior typical for warm waters.*

Coatings and Cathodic Protection

Several designers are planning to use coatings to cover the steel and to decrease the current required to protect the structure [5,13,14]. This is, of course, the same technology that has been used for pipelines for many years. With the current requirement for cold waters increasing to very high levels, coatings are becoming more attractive economically. The designer that combines coatings with cathodic protection will also be required to make a decision regarding the effectiveness of the coating system with time as the coating ages. Goolsby [*14*], for example used a final "percent bare" factor of 45% at the end of 35 years service. This figure is, at best, an estimate. There are little hard data that documents this condition; test data and experience is needed.

Anode Material

In designing CP systems for deep water structures, anode material selection is one of the key elements. It is important from the economical point of view and a necessity to meet design expectations (i.e., platform weight limits). More data is needed for anodes operating in typical deep water conditions. This is the reason for initiating our current testing program. Goolsby[*14*] recommends the use of an Al anode near the sea floor that contains 5% Zn instead of the usual 3%. This recommendation is based on a costly field testing program. The advantages of this higher Zn content should be examined further to see if it has proven merit under varying service conditions.

Environmental Factors

Based on a survey of experience, the major environmental factors that affect cathodic protection are dissolved oxygen, temperature, salinity, pH, water velocity from sea currents, and fouling. Among these, the more obvious factors appear to be temperature and pH because they affect the deposition of calcareous deposits. However, other factors can also contribute greatly to CP design.

Dissolved Oxygen

The dissolved oxygen concentration, salinity, resistivity, and temperature gradients for the Gulf of Mexico (GOM) were determined in an extensive test program conducted over a period of 20 years by Shell. The data includes information from over 7000 sites located primarily in the gulf waters off of the coast of Louisiana [*2*]. Testing and reporting of environmental factors has also been conducted in Brazil[*6*], Norway[*15*], and in other areas of the world[*16*].

Figure 2 shows variations of oxygen concentration, temperature and salinity as a function of depth at one location in the GOM[3]. Dissolved oxygen content in the GOM has been found to be approximately 4.8 ppm at the surface and to decrease to 2.8 ppm at 1000 ft (305 m) and then to increase to 4.8 ppm at 4000 ft (1219 m)[*2*].

---

[3] Griffin, R., "Private Communication," Mechanical Engineering Department, Texas A&M University, April 1995

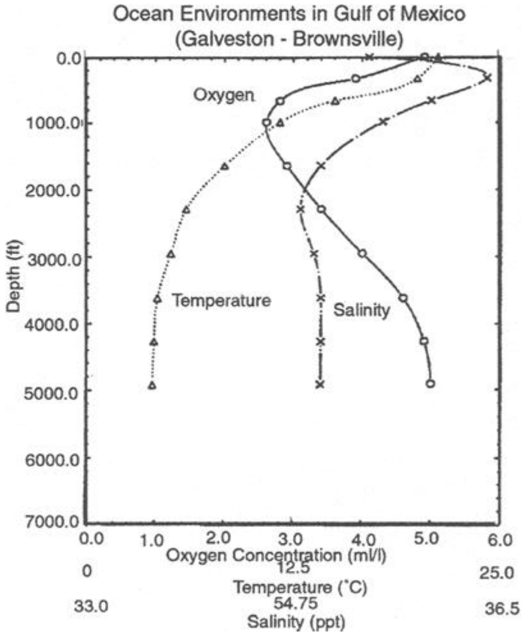

Figure 2 - *Ocean Environments in the Gulf of Mexico*

For other areas of the world like the Atlantic and Pacific Oceans, the oxygen concentration profiles are different. At some North Pacific locations dissolved oxygen content can be lower than 1 ppm at depths from 1000 to 3000 ft (305 to 915 m)[*3,16*], 2 ppm around 6000 ft (1829 m) and 6 ppm at the surface. Analysis of sea water from various depths in the Atlantic indicate that the oxygen concentration decreases from 4.5 ppm at the surface to approximately 3.5 ppm around 1000 ft (305 m) and then recovers a value close to 6 ppm at depths of 5000 to 19000 ft (1524 to 5791 m)[*3*].

Oxygen is the main depolarizing agent and its concentration is a principal factor that governs the minimum design current density at which polarization necessary for complete cathodic protection can be achieved. However its availability is linked to the hydrodynamic conditions that apply to the particular submerged structure. Neither oxygen concentration nor hydrodynamic conditions alone appear to be decisive factors. It is their interaction that should be taken into account and subjected to further study

Temperature

Temperatures in the GOM were found to decrease from ambient at the surface to approximately 5°C at a water depth of 2000 ft (610 m), as is shown in Figure 2. These same low temperatures in deep water were found in Norway[*12*], in both the Atlantic and Pacific[*16*], and even in more tropical regions such as Brazil and West Africa[*7,17*].

Temperature has an indirect influence on CP requirements. In fact, it does affect seawater resistivity and formation of calcareous deposits both of which are critical to CP design[*15*]. The process of formation of calcareous deposits is determined by the solubility of calcium carbonates and magnesium hydroxide in water. Figure 3 shows the temperature dependence for the solubility of these compounds in water. Temperature may also affect the limiting current density through its effect on the diffusion coefficient of oxygen. The diffusion coefficient of oxygen exhibits an exponential dependence on temperature. The colder the water is, the lower is the diffusion coefficient of oxygen[*18*].

Salinity and pH

In the GOM, salinity and pH were found to be fairly constant with respect to depth[2]. The salinity was found to be approximately 35 ppt and the pH was found to be in the range of 8 to 8.2. Off western Africa, pH measurements were found to be lower than most other areas. The lower pH was attributed to a greater amount of organic matter in the water which reduced the dissolved oxygen content as a result of organic decomposition processes. Organic decomposition produces CO_2 which in turn makes pH lower[16]. A lower pH increases the dissolution rate of calcium carbonate calcareous deposits. Hence, pH and oxygen concentration in deepwaters appear to be factors strongly dependent on biological activity. Additionally, the mentioned effect has been thought to be conditioned to a greater water residence time at depth in the Pacific Ocean than in the Atlantic[*16*].

Water Velocity

Water velocity from ocean currents is an important factor prior to formation of a calcareous coating on the metal surface but, in most cases, is of little significance thereafter[*4*]. Current density and potential varied directly with the sea current velocity during the first week or two of the testing, but velocity had little effect after a calcareous deposit had formed[4]. Nisancioglu et al[*19*] performed very detailed work to study the polarization of steel as a function of velocity.

Velocity affects the stability of the films that result from the reduction of oxygen and hydrogen on the steel surface. With increasing velocities, the resultant formation and stability of the OH^- ion layer is delayed, as is the subsequent formation of calcareous coatings.

Data regarding velocity at the GOM seems to be very scarce and more is needed. Velocities up to 0.4 m/s were reported at depth in Norway[*4*] and 0.1 m/s in the Atlantic off Brazil[*17*].

Fouling

High oxygen concentrations found at depths in the Atlantic as compared to the Pacific have been attributed to the lower biological oxygen demand in the Atlantic. In other words, decaying organisms in the Atlantic do not exhaust the available oxygen supply[*3*]. Thomason reported that organic matter (fouling potential) reduces the rate of precipitation of calcite. In the waters off Africa and Asia, the water contains much biomatter that is degrading. This process will consume oxygen and also causes pH to be lower[*7*]. A lower pH in turn will increase the solubility of the calcareous deposits.

Calcareous Deposits

Calcareous deposits are the precipitates that form on the surface of the steel in sea water that is being protected from corrosion by cathodic protection. When a current flows to the steel the water and dissolved oxygen are reduced and form hydroxyl ions. These ions cause the alkalinity to increase and the pH adjacent to the metal surface to rise. As a result of the increased pH, calcium and magnesium carbonates are less soluble and precipitate from the solution.

The calcium carbonate in the calcareous deposit is in the form of both calcite and aragonite. Calcite crystallizes in the hexagonal form while aragonite forms rhombic crystals. Aragonite is unstable, and gradually changes to calcite, but the transition is extremely slow at ordinary temperatures.

Figure 3 shows the temperature dependence for the solubility of calcium carbonate and magnesium hydroxide in water[*18*].The solubility of calcium carbonate increases as the temperature decreases, whereas the magnesium hydroxide exhibits the opposite behavior. Solubility of calcium carbonate also increases with pressure. At 5°C and at 1000 m the solubility of calcium carbonate will increase by nearly 500%[*7*]. Thus, at some depth, the sea water will become undersaturated with respect to calcium carbonate. This would limit precipitation and make cathodic protection at great depths much more difficult.

In both cold and warm waters, deposition of magnesium hydroxide is rapid. However, magnesium deposits afford little reduction in current density[*18*]. One explanation is that the magnesium hydroxide has higher water content and also has a more open structure compared to that of calcium carbonate deposits. Magnesium also inhibits the nucleation of both calcite and aragonite, and also interferes with the crystal growth of calcite.

In warm waters, the calcium is primarily in the form of aragonite. While magnesium inhibits the nucleation of aragonite, once some aragonite is formed it continues to grow at a rapid rate. At colder temperatures calcite is formed preferentially and because magnesium inhibits both nucleation and crystal growth rate of calcite, less deposits form on the metal surface[*20*]. Near the surface of the water the calcareous deposits will therefore be mostly aragonite and at greater depths the calcareous deposits will be richer in calcite.

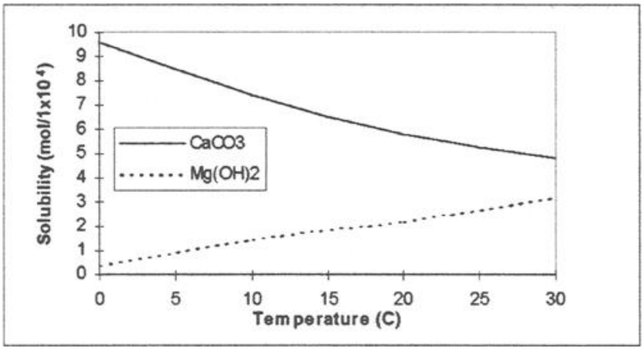

Figure 3 - *Solubility of calcium carbonate and magnesium hydroxide in water.*

Experimental Design

An experimental facility has been developed to simulate low temperatures, various levels of dissolved oxygen and velocities typical for deep waters. The experimental apparatus is shown in Figure 4.This apparatus was developed within a program currently underway which has expanded to include joint industrial sponsorship. This facility is provided with fresh sea water obtained from an offshore site in the GOM.

A computerized acquisition system collects current and potential data while the carbon steel cathodes are in electrical contact through an external resistor with Al-Zn-In anodes. The measurements are conducted using a constant high initial polarization current density which is set at the start of the experiment. The potential data is measured versus a Ag/AgCl electrode. A special board carries out the analog-digital conversion of the current signal measured using a zero impedance ammeter. As seen in Figure 4, velocity can be set using a stirring unit located at the edge of a plexiglass tube contained in the electrochemical cell. The cathodes and anodes are located inside the aforementioned tube, thus, under the action of a laminar flow.

The effects of temperature, oxygen and velocity typical for deep waters, on current and polarization characteristics of various Al based anodes are being studied using statistical experimental design. The principal experimental responses that will be subjected to statistical analysis are the cathode current density, cathode potential and weight loss of the anodes after one month of testing.

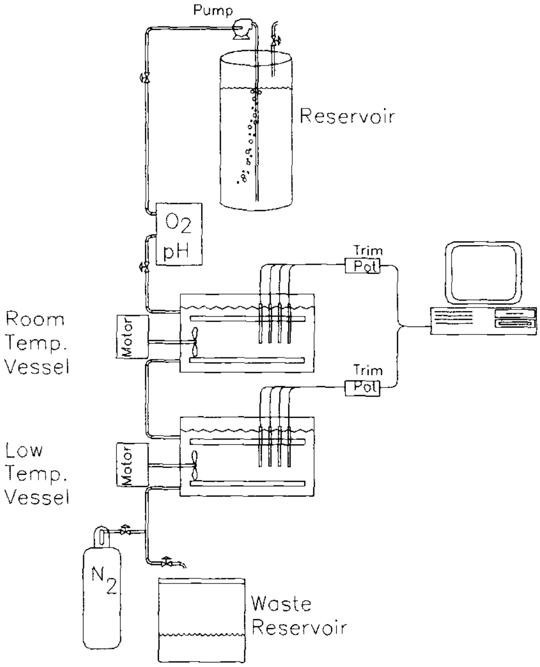

Figure 4 - *Experimental facility*

Correlation of Laboratory Test Results with Service Documented Experiences

Preliminary results based on weight loss data and final current densities indicated differences in anode performance for Al-Zn-In anodes with a Zn content of 5.5, 6.1 and 4.8%, respectively. Table 2 and Figure 5 and 6 contain weight loss and electrochemical data from where some trends can be illustrated. For 5 ppm of dissolved oxygen and stagnant conditions, the 5.5% Zn anode had the lowest consumption rate and exhibited the smallest increase in protection current density for the temperature transition from 25°C to 5°C.

On the other hand, for 50 ppb of dissolved oxygen and flowing conditions, the 6.1% Zn anode had the lowest consumption rate and exhibited the smallest increase in protection current density for the same temperature transition. The 4.8% Zn anode exhibited an intermediate behavior when tested with 5 ppm of dissolved oxygen under stagnant conditions. With 50 ppb of dissolved oxygen and flowing conditions, the 4.8% Zn anode exhibited a behavior that was closer to that of the 6.1%.Zn anode.

Test Conditions	**Anode**	**Anode Consumption Rate (mpy)**	**Cathode Corrosion Rate (mpy)**
5 ppm O_2 and No Flow	A[1]	383	0.26
	B[2]	351	0.30
	C[3]	294	0.24
50 ppb O_2 and Flow	A	143	0.10
	B	142	0.15
	C	174	0.26

[1] Al-Zn-In anode with 6.10% Zn

[2] Al-Zn-In anode with 4.81% Zn

[3] Al-Zn-In anode with 5.51% Zn

Table 2 - *Weight loss data for Anodes and Cathodes at 5°C*

Al-Zn-Si-In results of field tests cited by Goolsby[*14*] have shown that an alloy containing 3% Zn had inferior potential performance in cold deep water relative to the Al-Zn-Si-In alloy containing 5% Zn. The cited field tests program lasted for eight years and much of the data was obtained using very expensive ROV's[*14,21*].The results obtained in this study are very encouraging. After testing in the laboratory for only 30 days at a nominal cost, the results showed that there can be substantial differences in anode behavior in cold waters relative to small variations of the Al-Zn-In alloy Zn concentration and such environmental factors as the level of dissolved oxygen and velocity.

Figure 6 shows data indicating the influence of oxygen availability on short-term polarization behavior of carbon steel cathodes protected by one of the studied anode compositions in cold water over a seven day period. Three initial current densities were used in the range of 100 to 300 mA/m^2. The cathodes represented by the curves 1 and 2 were tested with the lowest dissolved oxygen concentration and the lowest high initial polarization current, respectively. As shown in Figure 6, these cathodes were the least polarized. The next polarized cathode is represented by curve 3. This cathode was tested without flow. The most polarized cathodes are represented by curves 4 and 5. In this case, the cathodes were tested with high initial polarization currents, flow and a high concentration of dissolved oxygen thus producing the highest polarization effect.

Oxygen availability depends on the dissolved oxygen concentration and velocity, however as shown in Figure 6, since a higher initial high polarization current in curve 3 than in curve 2 was used, the cathode represented in curve 3 was more polarized. The specific combination of initial current density, dissolved oxygen concentration and water velocity determines the speed of the oxygen reduction reaction and consequently the pH at the steel interface and the protective nature of the calcareous deposits.

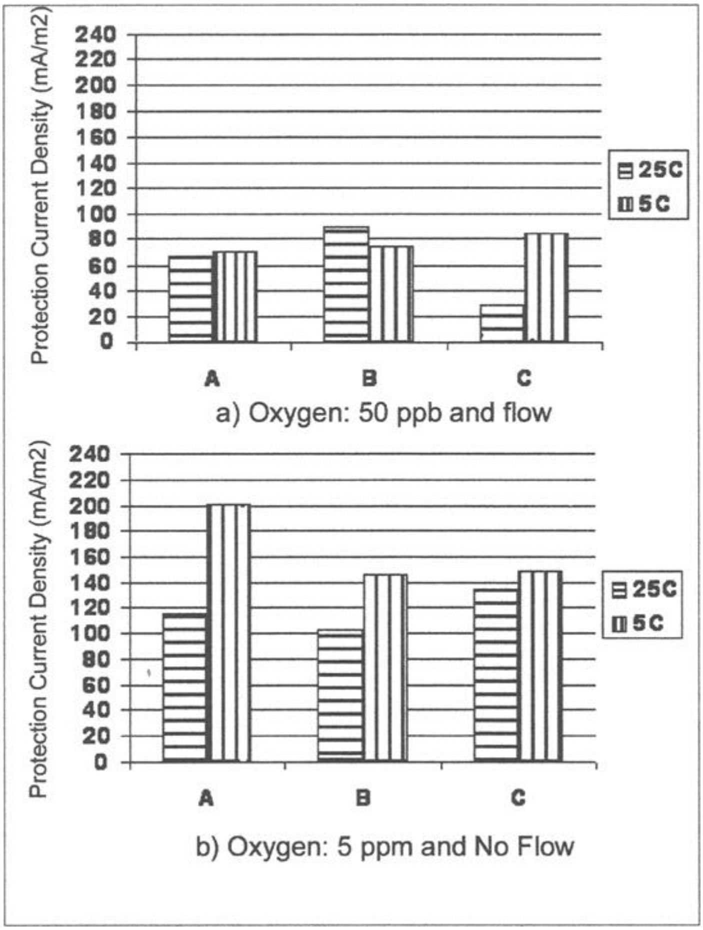

Figure 5 - *Influence of temperature on protection current densities for cathodes protected by anodes A, B and C.*

General Summary

1. As the oil production industry moved into deeper waters (~ 1000 ft (305 m)), design criteria that had been used in shallow waters to provide cathodic protection proved less than effective. In cold waters calcium carbonates were more soluble (less stable), making the calcareous coating less effective, and higher CP current was required to cause the structure to polarize.

2. Oxygen availability is a main factor governing the minimum design protection current density for deep waters and it is the result of the interaction of environmental factors such as the dissolved oxygen concentration and water velocity. The optimum value of the high initial polarization current appears to depend on the specific dissolved oxygen concentration and water velocity.

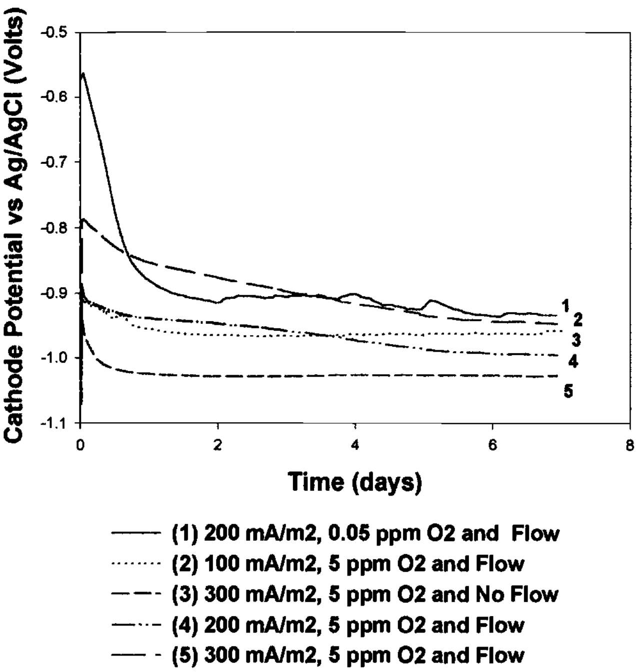

Figure 6 - *Influence of oxygen availability, on the short term polarization behavior of cathodes protected by the anode C during 7 days at a temperature of 5°C.*

Conclusions

1. Short-term polarization data obtained for an Al-Zn-In anode, with a Zn content around 5.5% and various levels of oxygen availability in cold water, showed evident differences in the value of initial polarization. The best polarization results were obtained for conditions of high dissolved oxygen concentration and flow with a high initial polarization current, and the worst ones were obtained when test conditions

comprised either the lowest high initial polarization current (100 mA/m^2), a low dissolved oxygen concentration (50 ppb), or the absence of flow.

2. Preliminary laboratory data indicate that small variations in anode composition can produce substantial differences in anode performance in cold waters when testing various combinations of such environmental factors as dissolved oxygen concentration and velocity. A high initial polarization current density was also shown to be a critical factor to achieve high polarization.
3. Preliminary results obtained in this program also showed that it is possible to get, on a short-term basis, meaningful data that can be applied to the design of deepwater cathodic protection systems.

Recommendations

1. More field and laboratory data on the behavior of galvanic anode materials is necessary in order to select an optimum anode composition and CP design that meets the current requirements encountered for deep waters

References

[1] "Design of Galvanic Anode Cathodic Protection Systems for Offshore Structures", NACE International Publication 7L198, July 1998.

[2] Goolsby, A. D. and Ruggles, B. M., "Development of a Water Property Database for Deep Water Cathodic Protection Design", *Corrosion*, Vol. 47, No. 5, May 1991, p 387.

[3] Beavers, J. A. Koch, G. H. and Berry, W. E., "Corrosion of Metals in Marine Environments", MCIC Report/ July 1986.

[4] Fisher, K. P., Sydberger, T. and Lye, R., "Field Testing of Deep Water Cathodic Protection on the Norwegian Continental Shelf", Corrosion 87, paper 67, NACE International, Houston, Texas.

[5] Evans, S., "Deep Water Platform Protection Using Coatings Combined with Cathodic Protection", *Materials Protection*, April 1992.

[6] Benedict, R. L., "Cathodic Protection in Natural Waters", Corrosion 93, paper 531, NACE International, Houston, Texas.

[7] Fisher, K. P., Thomason, W. H. and Eliassen, S., "CP in Deep Water: the Importance of Calcareous Deposits and the Environmental Conditions", Corrosion 96, paper 548, NACE International, Houston, Texas.

[8] Cox, G. C., U.S. Patent 2,200,469, 1940.

[9] Humble, H. A., *Corrosion*, Vol. 4, No. 7, 1948, p 358.

[10] Kennelley, K. J. and Mateer, M. W. "Evaluation of the Performance of Bi-Metallic Anodes on a Deep Water Production Platform", Corrosion 93, paper 523, NACE International, Houston, Texas.

[11] Hartt, W. H, Chen, S. and Townley, D. W. "Sacrificial Anode Cathodic Polarization of Steel in Sea Water: Part 2 - Design and Data Analysis", *Corrosion*, Vol. 54, No. 4, 1998.

[12] Gartland, P., Strommen, R. and Bardal, E. "Current Density Requirements for Cathodic Protection of Steel Structures in the North Sea", *Materials Performance*, 23, 6, June 1983.

[13] Osvill, H. and Gartland, P. O., "Computer Modeling to Evaluate Cathodic Protection of Tendon/Risers for Deep Water Structures", Corrosion 94, paper 502, NACE International, Houston , Texas.

[14] Goolsby, A. D. and Smith, J. D., "Auger Tension Leg Platform Cathodic Protection System", Corrosion 95, paper 313, NACE International, Houston, Texas.

[15] Fischer, K. P., "Cathodic Protection in Deep Water", Corrosion 89, paper 577, NACE International, Houston, Texas.

[16] Hartt, W. H., Wang, W. and Chen, T. Y., "Critical Questions Pertaining to Deep Water Cathodic Protection", Corrosion 89, paper 576, NACE International, Houston, Texas.

[17] Vianna, R. O. and Pimenta, G. S., "An Initial Investigation of Calcareous Deposits upon Cathodically Polarized Steel in Brazilian Deepwaters", Proceedings of 12th SPE/NACE International Congress, Vol.4, p.2278, 1993, Houston, Texas.

[18] Hartt, W. H., Kunjapur, M. M. and Smith, S. W., "The Influence of Temperature and Exposure Time Upon Calcareous Deposits", Corrosion 86, paper 291, NACE International, Houston, Texas.

[19] Nisancioglu, K., Gartland, P. O., Dahl, Turid and Sander, Elisabeth, "The Role of Surface Structure and Flow Rate on the Polarization of Cathodically Protected Steel in Sea Water", Corrosion 86, paper 296, NACE International, Houston, Texas.

[20] Lin, S. H. and Dexter, S. C., "Effects of Temperature and Magnesium Ions on Calcareous Deposition", *Corrosion*, Vol. 44, No. 9, September 1988, p 615.

[21] Britton, J. N., "Monitoring of Cathodic Protection System Performance in Deep Water Production Systems", Corrosion 89, paper 578, NACE International, Houston, Texas.

V. G. DeGiorgi[1] and K. E. Lucas[2]

Computational Design of ICCP Systems: Lessons Learned and Future Directions

---

Reference: DeGiorgi, V. G. and Lucas, K. E., **"Computational Design of ICCP Systems: Lessons Learned and Future Directions,"** *Designing Cathodic Protection Systems for Marine Structures and Vehicles, ASTM STP 1370,* H. P. Hack, Ed., American Society for Testing and Materials, West Conshohocken, PA, 1999.

Abstract: Computational modeling using boundary element techniques has been proposed for design and evaluation of shipboard impressed current cathodic protection (ICCP) systems. LaPlace's equation, the governing differential equation for electrochemical corrosion, is well suited for solution by the boundary element method. There has been much work performed in this field during the past two decades. Computational modeling efforts designed to validate boundary element procedures are reviewed. U. S. Navy ship systems discussed are CG-59, CG-66 and CVN-68. Computational analysis accuracy is determined by comparison with physical scale modeling experimental results. Lessons learned from the analyses described are summarized. Advantages and disadvantages of boundary element modeling are discussed.

Keywords: boundary element, cathodic protection, computational modeling, physical scale modeling, impressed current

The performance of cathodic protection systems, such as shipboard impressed current cathodic protection (ICCP) systems, is a complex response to a variety of factors including, but not limited to, geometry, conductivity of surrounding medium, material polarization response and material interactions. Changes in system configuration and service conditions can occur. System configuration changes can be due to damage or aging. Service condition changes can occur due to changes in deployment location. The ability to predict performance under a variety of changing conditions is becoming increasingly important in this era of time and cost consciousness. Past reliance on simple

---

[1] Engineer, Multifunctional Materials Branch, Naval Research Laboratory, Washington, DC 20375

[2] Section Head, Marine Corrosion Facility, Naval Research Laboratory, Key West, FL 33041

design models is not sufficient to meet today's performance requirements. There are candidate methodologies, experimental and computational, that provide a rational basis for design.

Preliminary work on computational modeling procedures for corrosion problems was completed by the late 1980s as documented in review articles by Adey and Niku [1], Munn [2] and Gartland et al. [3]. Results of work performed during the past decade have shown significant advances in the application of boundary element procedures to cathodic protection. Boundary element work completed from 1987 to 1997 has been reviewed [4]. While there have been significant advances in boundary element modeling applications there are still areas in which computational modeling approach can be further developed and improved.

This paper reviews major computational analysis efforts at The Naval Research Laboratory (NRL) which were designed to validate boundary element techniques for design and evaluation of shipboard ICCP systems. The analyses discussed focused on two U. S. Navy ship hull forms; the CG cruiser class and the CVN aircraft carrier class. Computational results were compared with experimental results to determine accuracy of the boundary element analyses. Major findings of these studies are highlighted. References are provided for more detailed examination of the studies and supporting documentation. These findings are not unique to the boundary element software used and the usefulness of boundary element methods is discussed.

Mathematical Basis for Computational Approach

The equation governing electrochemical corrosion for the wetted surface of a ship hull is:

$$k\nabla^2\Phi = 0 \tag{1}$$

where Φ is the potential and k is the conductivity of the electrolyte. Eqn. 1 is valid if the electrolyte is homogeneous, there are no electrical sources or sinks and the system is electroneutral. A shipboard ICCP system can be modeled in such a way to meet these conditions. Seawater is often represented as a uniform mixture of multiple components, i.e. a homogeneous electrolyte. Current source points and exposed metal can be represented by boundary conditions eliminating the need to include sources and sinks in the model. Electroneutrality maintains charge equilibrium for the ship, surrounding water and ICCP system.

The solution space for problem defined by eqn. 1 used in the boundary element approach is the surface Γ which bounds the domain Ω as defined by:

$$\Gamma = \Gamma_A + \Gamma_C + \Gamma_I \tag{2}$$

where Γ_A is the anodic surface, Γ_C is the cathodic surface and Γ_I is the insulated surface. Γ must be continuous but all sections of one surface type do not have to be contiguous.

The surface represented is the wetted hull surface. The domain is the seawater region surrounding the ship.

An ICCP system consists of the surfaces to be protected, the anodes, the reference cells and the power supply. Anodes are defined by maintaining the potential at a constant value, Φ_A:

$$\Phi(x,y)=\Phi_A \tag{3}$$

or defining the current density as a constant, q_A, on a surface:

$$\frac{\partial\Phi(x,y)}{\partial n(x,y)}=q_A \tag{4}$$

where $\Phi(x,y)$ is the electrical potential at the point (x, y) and n(x,y) is the normal to the surface at the point (x, y). Reference cells are defined as specific points on the hull where the solution is obtained.

Power supply amperage is the sum of the current for the anodes connected to the power supply. This total must be equal to or less than the defined rating of the power supply.

Damaged paint is modeled as exposed metal surfaces. The current density on the surface of a cathodic material, Γ_C, is defined as:

$$\frac{\partial\Phi(x,y)}{\partial n(x,y)}=f_c\left[\Phi(x,y)\right] \tag{5}$$

where f_C is the cathodic polarization function, i.e. the material polarization response.

Undamaged painted surfaces are defined as perfect electrical insulation:

$$\frac{\partial\Phi(x,y)}{\partial n(x,y)}=0 \tag{6}$$

Eqns. (1) through (6) are combined to solve for the potential and current density at all points on the wetted surface. Details on the boundary element method and solution procedures can be found in many textbooks such as ref. 5.

Experimental Process

A key feature in validation of boundary element method is the comparison of experimental and calculated results. This section briefly describes physical scale (PS) modeling, an experimental method used to evaluate and design shipboard ICCP systems. In PS modeling the structural dimensions and the conductivity of the electrolyte are scaled by the same factor. The theoretical basis for this mechanical scaling is presented by Ditchfield et al. [6]. In this process the scaled model and the full size structure maintain identical current density values at points, identical potential differences at points, identical polarization potentials at the anode and cathode and an identical potential drop across the electrolyte. Detailed verification of the procedure involved comparison with sea trial data from an U. S. Navy CG cruiser class system [7,8].

PS modeling of CG and CVN hulls and associated ICCP systems was completed at NRL's Marine Corrosion Facility. Detailed current and potential information was obtained from embedded sensors for a variety of damage and service conditions including those modeled in the boundary element analysis.

Computational Analyses

Boundary Element Analyses

Detailed computational solutions have been obtained for 2 different ship geometries and 3 different ICCP systems. The goal of these analyses is to validate the use of boundary element based computational procedures for the design and evaluation of shipboard ICCP systems. Factors common to all analyses performed are presented here.

The portion of the ship modeled is the underwater hull up to the design water line. Propellers and rudders are included in the model. Propellers are attached to the hull by a single connecting solid beam representing the main strut for the support system. The propellers are modeled as uniform thickness solid disks. The disks are defined so that there is sufficient thickness to avoid numerical problems that can result from solid sections that are too thin. The boundary element mesh defined represents the interface of the ship hull and surrounding seawater. This mesh is enclosed in an outer box that represents a large but finite volume of seawater. The domain is bounded by edges sufficiently far away from the ship hull so that edge effects on the potential profile of the surface ship are negligible. In all cases symmetry conditions were invoked and only half of the hull was modeled. The commercial boundary element code BEASY-CP [9] was used for all analyses.

Minimum and maximum paint damage conditions that include bare propellers were considered. Location of damaged paint regions was defined by protocols provided by Naval Sea Systems Command. Minimum damage has 2.8% of the hull surface and the propeller area defined as damaged paint. Maximum damage has 15% of the hull surface including the propellers defined as damaged paint areas. These correspond to beginning of service and end of service life conditions. Damaged paint areas are defined as exposed metal surfaces in the boundary element models. This duplicates the conditions for the PS model where painted surface is represented by fiberglass and damaged paint areas are represented by strips of uncoated metal attached to the PS model hull.

The design condition matrix is created by the pairing of two service flow conditions, static and dynamic, with each damage condition. Static flow represents ship at rest or in port conditions. Dynamic flow condition represents ship underway conditions. The design matrix consists of 4 cases; static minimum damage, static maximum damage, dynamic minimum damage and dynamic maximum damage.

Reference cells and anode locations in the computational model duplicate as closely as possible the locations of these features in the physical scale models. In cases where port and starboard anode locations are not strictly symmetric, the boundary element model anode is placed at the average of the port and starboard locations.

In all cases the potential levels of the impressed anodes are defined as fixed input potential values. The resulting potentials on the hull, current density values and total current values are determined by boundary element procedures. A solution consists of a computer run in which the potential of the mesh points representing the reference cell locations on the hull are at the target potential -0.85 Volts with respect to the Ag/AgCl reference electrode. Reference cell readings are calculated potential values at the mesh point at the reference cell location. The calculated total anode current associated with a power supply is compared to the limits of that power supply. This is a feasible solution check. The power supply capacity is defined as part of the ICCP system design. The solution is determined through a multiple run process in which anode values are varied. Each change in anode potential values results in a separate boundary element solution.

Results of computational and physical scale modeling were compared to establish the level of accuracy obtainable by the computational model. Results of interest are the potential profiles along sections of the hull and the amperages required to achieve the target potential at the reference electrodes.

CG Hull Class

The purpose of the CG cruiser hull analysis was to determine whether boundary element techniques could be used to accurately predict system performance [10-12]. The hull geometry investigated is that of a U S Navy CG hull class cruiser. ICCP systems of the CG-47 [10], 59 and 66 [11,12] were evaluated. The CG-47 ICCP system is a single power zone, 6 anode system. This analysis investigated the feasibility of creating a working model. Results were of importance in identification of areas of concern for further investigation. The CG-59 and 66 are 2 power supply zone systems and have 6 and 7 anodes, respectively. Issues of mesh refinement, geometric features and material characterization dominated these analyses. The CG-59 and 66 analyses will be summarized in this article.

The model used in the CG-47 analysis consisted of 573 rectangular elements. This mesh was determined to be insufficient for accurate system evaluation. A mesh refinement study was performed [11] and demonstrated that a significantly higher degree of mesh refinement was required than is typically considered necessary for boundary element analysis. Typical boundary element meshes are relatively coarse when compared to finite element meshes as can be seen in Ref. 5. The final mesh determined to be adequate for ICCP modeling appears more like a finite element mesh with a higher level of resolution than one would expect in a boundary element mesh. Once the mesh study was completed, a 3D representation of the bilge keel was added to the model. This model was used in the CG-59 and 66 work and consists of 1583 8-noded rectangular elements

(Figure 1). The boundary element program used allows for a linear geometry option for the 8-noded elements effectively eliminating element curvature. This option was chosen due to computer memory limitations. The resulting hull geometry is a faceted surface.

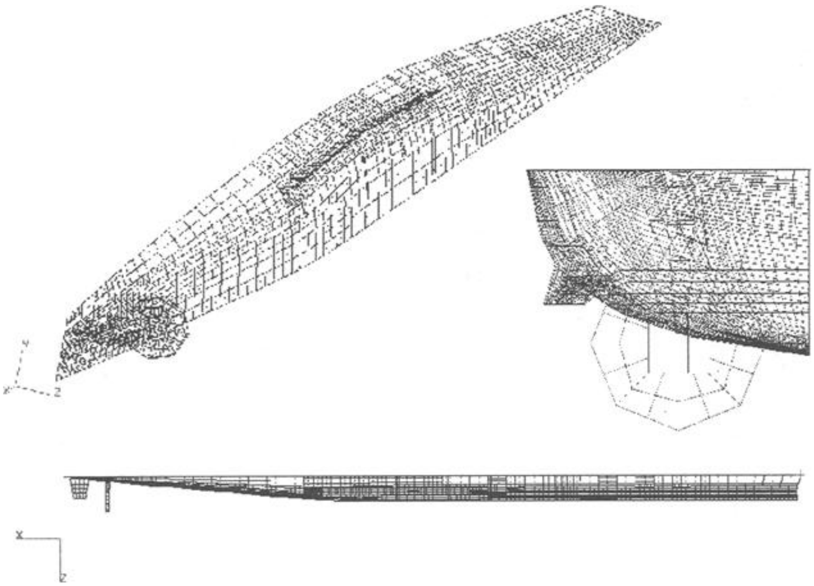

Figure 1 - Boundary Element Mesh used in CG-59 and CG-66 Analyses

Two sources of polarization data were used in the CG analyses. Polarization data from laboratory testing using small specimens (13 to 25 mm^2) [13] provided unsatisfactory boundary element results. Experimental and computer calculated potential profile yielded similar trends. However, current magnitudes showed poor agreement. Mesh refinement alone did not improve the agreement between calculated and measured results. Polarization response was therefore identified as a critical issue. Accuracy of computational results is directly related to the accuracy of the polarization response. Larger specimens (309 cm^2) tested in open seawater were the second source of polarization data [14]. This testing process resulted in polarization response for an open sea environment. Two issues were introduced by the change in polarization response; larger specimens vs. small laboratory specimens and open seawater vs. laboratory environment. The open sea polarization responses when used with the refined CG model resulted in better agreement with PS modeling results than laboratory small scale specimen based polarization response. Typical potential profile results are dynamic-maximum damage condition results for CG-66 (Figure 2). Potential spikes occur in the vicinity of anode locations and represent the general increase in voltage associated with an electrical source. Current totals for dynamic conditions, the more severe design condition, show good agreement as seen in Table 1

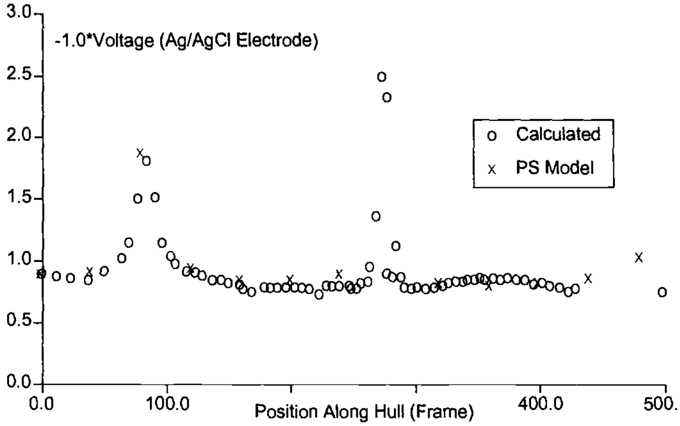

Figure 2- Potential Profile for CG-66, Dynamic Flow-Maximum Damage Conditions. Potential values at 3 m below waterline.

Table 1 - Current Demand (Amps) for CG-66 System, Dynamic Flow Conditions Reference Cell Reading=-0.85 V Ag/AgCl

	Propellers	Docking Blocks	Other Bare Steel	System Total
Min. Damage				
Calculated	50.3	14.9	NA	65.2
PS Model	44.5	14.1	NA	64.9
Max. Damage				
Calculated	51.3	13.7	264.5	329.5
PS Model	52.3	13.0	177.9	260.3

In summary major results from the CG hull class analyses are:

1. A greater degree of mesh refinement was required for accurate current results than traditionally recognized for boundary element techniques
2. Less refinement in mesh and relatively crude polarization response data can be used to approximate potential response of the structure (i.e. potential contours for such crude modeling show good and bad protection areas but should not be used for detailed design)
3. Detailed modeling of relatively small geometric features (e.g. the bilge keel) are essential for correct potential profile response

CVN Hull Class

The purpose of the CVN analysis [15] was to determine if the expertise gained in the previous work could be used to create an accurate ICCP system boundary element model. Once model development guidelines are established as appropriate for any geometry and system configuration, the boundary element models can be generated for any ship hull form with confidence.

A boundary element model was created of the U S Navy CVN aircraft carrier (Figure 3). The boundary element mesh consists of 1884 linear-quadratic displacement 9-noded rectangular elements. The 9-node configuration consists of 8 exterior mesh points that define the element geometry and 1 mesh point placed at the centroid of the element. The boundary element code used this centroidal node to create element curvature while maintaining linear or constant characteristics for the solution parameters. This element type was not available for the earlier work. The 9-noded element allows for more accurate modeling of the curved hull surface. Choice of element is critical and will depend on features available in the boundary element code used. Knowledge of element features for a specific code is essential for development of the mesh.

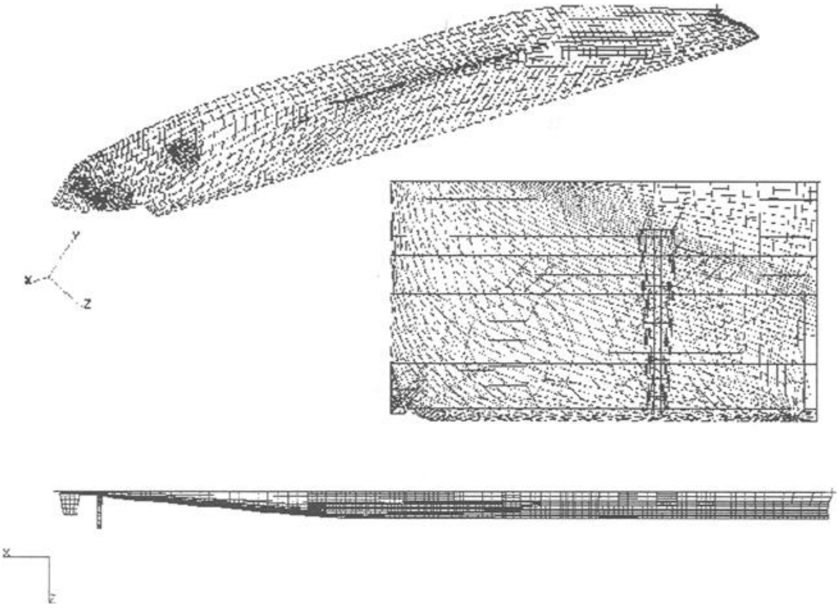

Figure 3 - Boundary Element Mesh used in CVN-68 Analysis

The CVN ICCP system consists of 3 independent power supplies and 17 anodes. The forward power supply is attached to 2 port anodes, 2 starboard anodes. The midship power supply is attached to 4 port anodes, 4 starboard anodes. The aft power supply provides current for 2 port anodes, 2 starboard anodes and 1 mid-line anode.

The polarization response used was generated from small scale laboratory test procedures using the scaled conductivity water used in PS modeling. This source of polarization data was chosen so that PS modeling testing procedures would be represented by the polarization response. In this analysis an attempt was made to duplicate PS modeling test conditions rather than actual ship service conditions. Therefore polarization data based on scaled conductivity seawater was used instead of polarization data based on full strength seawater. The objective was to eliminate sources of differences in material response between PS modeling and computational modeling. This was done with the intent to refine and gain insight into the selection of appropriate material response. Previous work did not consider the variation in electrolyte for polarization testing, computational model and PS model. This study matched electrolyte composition for polarization testing, computational model and PS model.

Typical of potential predictions are the profiles for dynamic-maximum damage conditions shown in Figure 4. Potential spikes occur in the vicinity of anode locations and represent the general increase in voltage associated with an electrical source. Total current requirements for dynamic conditions are shown in Table 2. Ref. 15 contains a detailed comparison of calculated and experimental results. While potential profiles and magnitudes were accurately predicted, there was a larger degree of variation in amperage values than for the CG analysis. Past work identified mesh refinement, model simplification and polarization response as likely causes of differences between experimental and boundary element results. Each of these in relationship with the CVN analysis will be discussed.

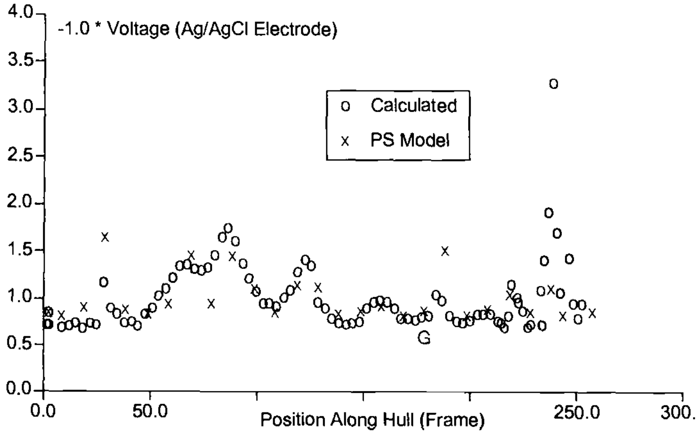

Figure 4 - Potential Profile for CVN-68, Dynamic Flow-Maximum Damage Conditions. Potential values at 3 m below waterline.

Table 2 - Current Demand (Amps) for CVN-68 System, Dynamic Flow Conditions Reference Cell Reading=-0.85 V Ag/AgCl

	Propellers	Docking Blocks	Rudder	Bilge Keel	Water Line	Struts	Hull	Total
Min.Damage								
Calculated	118.9	71.7	NA	NA	NA	NA	NA	190.6
PS Model	201.1	110.6	NA	NA	NA	NA	NA	314.7
Max.Damage								
Calculated	189.8	185.2	85.0	174.4	206.8	85.8	791.0	1718.0
PS Model	228.2	181.8	43.0	290.8	229.8	104.4	759.5	1837.7

The degree of mesh refinement in the CVN model was consistent with the final mesh configurations in the CG mesh refinement study. Based on past experience a larger variation between experimental and calculated potential values would have been observed if mesh refinement had been insufficient.

The primary model simplification in the CVN analysis involves the bilge keel. There were difficulties adding this geometric feature to both PS and boundary element models. The bilge keel on the boundary element model has a different profile and attachment angle to the hull than that of the PS model. Best effort was made to match the two geometries in the modeling effort. Other model simplifications are use of constant thickness disks to represent the propellers, use of one major connection between the propeller and hull and use of single connector between the rudder and the hull. It is felt that the variations in bilge keel geometry are a contributing factor in variations observed for amperage required for mid-hull damaged areas.

Small scale single material specimens were the source of the polarization response used in the boundary element analysis. While the conductivity of the water matched that of the PS model environment, there were other significant differences between the PS modeling test environment and the laboratory polarization experiments. All factors that contribute to the polarization response are not included in the experimental data. Material interaction was not included in the polarization experiments but occurs due to the physical proximity of different materials on the PS models. Film coatings are observed to form on some metal surfaces in the PS modeling but are not considered the polarization response used. In high current conditions, i.e. dynamic flow, current levels are greater than those used in the determination of polarization response. Extrapolation of polarization response to high current levels may or may not be valid. Each of these factors could have significant effects on the polarization response. For example, film formation has been observed to reduce conductivity by an order of magnitude or more [16]. It is felt that the variation in calculated and experimental results is due largely to the inexactness of the polarization response used in the boundary element model analysis.

Major findings of the CVN analysis are:

(1) Mesh refinement guidelines based on CG hull geometry can be translated to other hull geometries.
(2) Small scale features such as the bilge keel are essential to correctly determine potential contours regardless of hull dimensional scale.
(3) Geometric simplifications and modifications can have a significant affect on results even when applied to small scale features such as the bilge keel.
(4) Polarization response that accurately represents the service conditions, including material interaction effects, film formation and high current regime response, is necessary for accurate current calculations.
(5) Potential profiles and trends can be accurately predicted even without the most accurate polarization data.

Advantages and Disadvantages of Boundary Element Modeling

It has been demonstrated that boundary element modeling using boundary element methods can accurately predict experimental results. A major issue for accurate predictions is the availability of accurate polarization data [10-12,15,17]. However, the lack of availability of accurate polarization data for a particular design condition does not eliminate all advantages associated with boundary element modeling. Reasonable polarization data can be used to obtain potential maps that identify good and bad regions of protection.

Boundary element methods also can be used to evaluate the effect of a single parameter on system performance. In this way basic understanding of electrochemical corrosion and parameter interactions can be obtained. Several parametric studies have been completed to date. Effects evaluated are damage levels in the propeller area [18], seawater conductivity [19] and finite paint resistance [20]. Work by Trevelyan and Hack investigated the influence of stray current source on system performance [21].

Another advantage of computational analyses is that different system configurations and conditions can be evaluated. Today it is possible that ships will be deployed in environments different from ICCP system design conditions. Computational analyses can be customized so current deployment environment is duplicated. Another issue that occurs with time in service is damage and lost of anodes. Variations in anode count and strengths can be readily evaluated.

There are many advantages of computational modeling. However polarization accuracy is a major concern. It is possible to design experiments that would account for the majority, if not all, of factors that influence polarization response for the materials in question. However, this approach quickly leads to impracticably large experimental programs. The computational method becomes cost effective when laboratory or existing polarization data can be used and meaningful results obtained. There are two processes for ICCP system design, which relay on boundary elements but which eliminate the need for a high degree of accuracy in polarization response.

One proposed method defines the polarization response as an unknown to be solved in the boundary element process [22]. Sensors provide potential information at specific locations. An inverse problem is defined in which the potential map of the ship hull is defined from the measure data and assumptions of behavior in the regions between sensor points. The solution obtained through a series of boundary element evaluations is the polarization data. Discrete areas of damage can be located based on differences in calculated potentials and measured values at the sensor locations. Once the polarization response is determined for a given ship geometry and service condition, anode strengths and power requirements can be readily obtained. This approach is intriguing but has not been demonstrated for complex ICCP system designs. Computer resources may become an issue for complex ICCP systems such as the CVN-68 system.

The second proposed approach is a hybrid design combining boundary element and PS modeling techniques [23]. In the first stage boundary element modeling is used to develop best estimates of the layout of an ICCP system. Anode locations, anode numbers, reference cell locations and reference cell numbers are factors that can be varied using computational analyses. The polarization response used in this phase does not have to duplicate service conditions but only has to be a reasonable approximation. The second stage of the ICCP design used PS modeling. Final design changes to the best estimate system obtained from computational modeling are made based on results of PS modeling. The use of a best estimate design would eliminate multiple cycles of PS modeling. This approach enables the designer to exploit the advantages of both boundary element and PS modeling approaches.

Summary

Computational modeling is a viable method for design and evaluation of shipboard ICCP systems. Considerable effort has been expended by a variety of researchers in the validation of this process. There are unique aspects of the application of boundary element methods to shipboard ICCP systems that must be understood in order to generate accurate calculated results.

While there is considerable evidence that the use of boundary element modeling can provide advantages in the design and evaluation of ICCP systems, it is not a complete solution to design issues associated with these systems. Computational analysis is well suited for determining optimum anode location and number. It provides a rational basis for the initial design of new systems. It can provide insight into the operation of existing systems, especially in the case where anodes have ceased to function. It has been established that the process can be used to obtain information on protection levels even with less than accurate polarization response data. A major weakness in boundary element modeling is the determination of amperages to anodes to maintain protection levels. This is largely due to the uncertainty of polarization response. Calculated amperages are sensitive to polarization data accuracy. In closing, much information on ICCP system performance and electrochemical corrosion behavior can be obtained from computational modeling but it would be in error to rely totally on boundary element analyses.

Acknowledgments

The support of Dr. A. I. Kaznoff, Naval Sea Systems Command, is gratefully acknowledged.

References

[1] Adey, R. A. and Niku, S. M., "Computer Modeling of Corrosion Using the Boundary Element Method," *Computer Modeling in Corrosion*, STP-1154, American Society of Testing and Materials, pp. 248-264, 1992.

[2] Munn, R. S., "A Review of the Development of Computational Corrosion Analysis for Spatial Modeling Through It's Maturity in the Mid 1980's," *Computer Modeling in Corrosion*, STP-1154, American Society for Testing and Materials, pp. 215-228, 1992.

[3] Gartland, P. O. et al, "Innovations Developed Through the 1980'ies in Offshore CP Design Computer Modeling and CP Inspection," *Corrosion 93*, Paper 522, National Assc. of Corrosion Engineers, 1993.

[4] DeGiorgi, V. G., "A Review Of Computational Analyses Of Ship Cathodic Protection Systems," *Boundary Elements XIX*, Computational Mechanics Pub., pp. 829-838, 1997.

[5] Trevelyan, J., *Boundary Elements for Engineers*, Computational Mechanics Pub., Boston MA, 1994.

[6] Ditchfield, R. W., McGrath, J. N. and Tighe-Ford, D. J., "Theoretical Validation of The Physical Scale Modeling Of The Electrical Potential Characteristics of Marine Impressed Current Cathodic Protection," *J. of Applied Electrochemistry*, 25, pp. 54-60, 1995.

[7] Thomas, E. D. and Parks, A. R., "Physical Scale Modeling of Impressed Current Cathodic Protection Systems," *Corrosion 89*, Paper No. 274, National Assc. of Corrosion Engineers, 1989.

[8] Parks, A. R., Thomas, E. D., and Lucas, K. E., "Verification of Physical Scale Modeling with Shipboard Trials," *Corrosion 90*, Paper 370, National Assc. of Corrosion Engineers, 1990.

[9] Computational Mechanics, *BEASY-CP Users Manual*, Computational Mechanics International, Billerica, MA, 1990.

[10] DeGiorgi, V. G., Thomas, E. D. and Kaznoff, A. I., "Numerical Simulation of Impressed Current Cathodic Protection (ICCP) Systems Using Boundary Element Methods," *Computer Modeling in Corrosion*, ASTM STP-1154, pp. 265-276, 1992.

[11] DeGiorgi, V. G et al, "Boundary Element Evaluation of ICCP Systems Under Simulated Service Conditions," *Boundary Element Technology VII*, Computational Mechanics Pub., pp. 405-422, 1992.

[12] DeGiorgi, V. G., Kee, A., and Thomas, E. D., "Characterization Accuracy in Modeling of Corrosion Systems," *Boundary Elements XV*, Computational Mechanics Pub., pp. 679-694, 1993.

[13] Hack, H. P., "Galvanic Corrosion Prediction Using Long Term Potentiostatic Polarization Curves," David W. Taylor Naval Research and Development Center, Bethesda, MD, DTNSRDC/SME-82/88, Dec. 1982.

[14] Thomas, E. D. and R. L. Foster, "Instrumented Plate Velocity Study Preliminary Report," NRL Marine Corrosion Facility, Key West, FL, Sept. 1992.

[15] DeGiorgi, V. G., Thomas, E. D. and Lucas, K. E., "Scale Effects and Verification of Modeling Ship Cathodic Protection Systems," *Engineering Analysis with Boundary Elements*, 22, pp. 41-49 1998.

[16] Ulhig, H. H. and Revie, R. W., Corrosion and Corrosion Control, John Wiley and Sons 1985.

[17] Hack, H. P. and Janeczko, R. M., "Verification of the Boundary Element Modeling Technique for Cathodic Protection of Large Ship Structures," *CARDIVNSWC-TR-61-93/02*, Carderock Division NSWC Report, Dec. 1993.

[18] DeGiorgi, V. G. and Hamilton, C. P., "Coating integrity effects on ICCP system parameters," *Boundary Elements XVII*, Computational Mechanics Pub., pp. 395-403, 1995.

[19] DeGiorgi, V. G., "Influence of Seawater Composition on Corrosion Prevention System Parameters," *Boundary Element Technology XII*, Computational Mechanics Pub., pp. 475-583, 1997.

[20] DeGiorgi, V. G., "Finite Resistivity and Shipboard Corrosion Prevention System Performance", *Boundary Element Method XX*, Computational Mechanics Pub., pp. 555-564 1998.

[21] Trevelyan, J. and Hack, H. P., "Analysis of stray current corrosion problems using the boundary element method," *Boundary Element Technology IX*, Computational Mechanics Pub., pp. 347-356, 1994.

[22] Aoki, S., Amaya, K. and Gouka, K., "Optimal cathodic protection of ship," *Boundary Element Technology XI*, Computational Mechanics Publications, pp. 345-356, 1996.

[23] DeGiorgi, V. G., Thomas E. D. and Lucas, K. E., "A Combined Design Methodology for ICCP Systems," *Boundary Element Technology XI*, Computational Mechanics Pub., pp. 335-345, 1996.

Lee M. Zook[1]

Cathodic Protection Deployment on Space Shuttle Solid Rocket Boosters

---

Reference: Zook, L. M., "**Cathodic Protection Deployment on Space Shuttle Solid Rocket Boosters,**" *Designing Cathodic Protection Systems for Marine Structures and Vehicles, ASTM STP 1370*, H. P. Hack, Ed., American Society for Testing and Materials, West Conshohocken, PA, 1999.

Abstract: Corrosion protection of the space shuttle solid rocket boosters incorporates the use of cathodic protection (anodes) in concert with several coatings systems. The SRB design has large carbon/carbon composite (motor nozzle) electrically connected to an aluminum alloy structure. Early in the STS program, the aluminum structures incurred tremendous corrosive attack at coating damage locations due primarily to galvanic coupling with the carbon/carbon nozzle. Also contributing to the galvanic corrosion problem were stainless steel and titanium alloy components housed within the aluminum structures and electrically connected to the aluminum structures. This paper highlights the evolution in the protection of the aluminum structures, providing historical information and summary data from the operation of the corrosion protection systems. Also, data and information are included regarding the evaluation and application of inorganic zinc rich primers to provide anode area on the aluminum structures.

Keywords: cathodic protection, aluminum, airframes, anode

Background

With the launch of the Space Shuttle *Columbia* in 1981 NASA entered into a new paradigm of reusing space flight hardware. One of the major challenges among hardware designated for reuse was the Space Shuttle and the solid rocket boosters (SRB). While the space shuttle would land on a runway, like an airplane, the SRB was not so fortunate. The SRB drops into the ocean at a velocity approaching 27 m/s. The SRB is towed through the ocean to a slip where it is removed from the water. This process takes between 24 and 72 hours depending on launch time and weather conditions. Figure 1 shows the SRB major components. The structure of greatest interest (where the greatest corrosion problems have occurred) is the aft skirt (Figure 1).

SRB Design

The large-scale reuse of space flight hardware began with the shuttle program. With regard to the SRB, NASA had little experience with the effects on the hardware of the descent, splashdown and tow back environments. The SRB aft skirt structure is constructed of welded aluminum alloy (AA) 2219-T87 with bolted in AA 2219-T87

---

[1] Senior Materials Engineer, USBI Co., P.O. Box 21212, Kennedy Space Center, FL 32815.

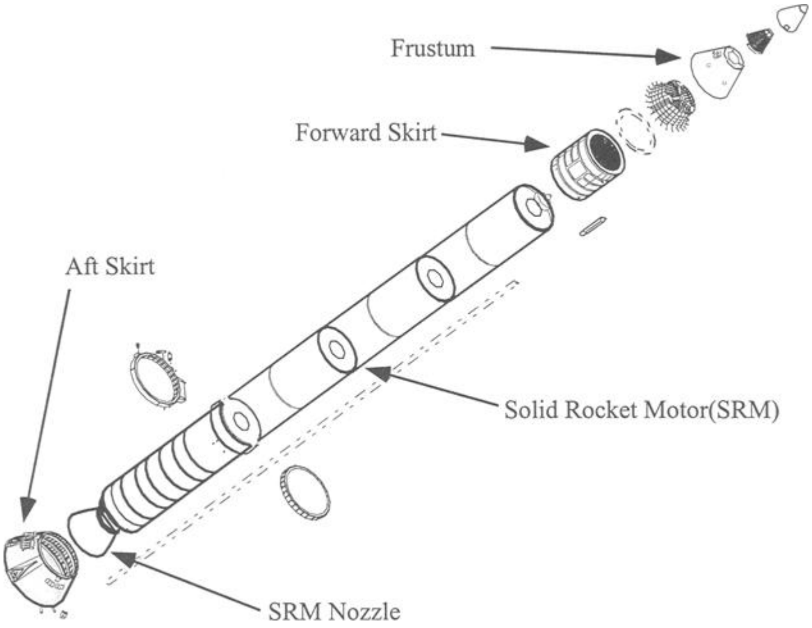

Figure 1- *Solid Rocket Booster (SRB) view.*

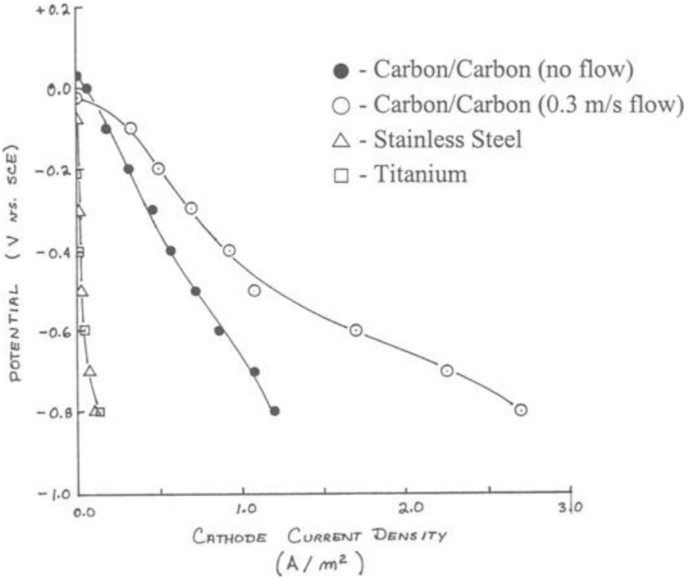

Figure 2- *Polarization of cathode materials.*

reinforcements. Housed within the aft skirt is the thrust vector control system (TVC). The TVC system provides the directional control for the Space Shuttle during the first two minutes of flight. The TVC system is constructed of many alloy types including, stainless steels, titanium and nickel alloys. Most of these alloys are left uncoated (bare). Table 1 lists the TVC system alloys which provide the majority of the uncoated cathode surface areas. The solid rocket motor (SRM) cases are high strength low alloy steel (painted) while the nozzle has a carbon/carbon liner bonded to a steel structure (painted). All components are electrically bonded for lightning protection grounding. On the exterior of the aft skirt a thermal protective coating is applied to protect the structure from thermal loads during ascent. To protect the aft skirt interior and TVC system from radiant heating, a thermal blanket made from quartz glass and fiberglass is attached between the aft skirt and SRM nozzle.

Table 1-*Summary of TVC System Exposed Surface Areas.*

Alloy*	Exposed Surface Area(m^2)
Titanium, Ti6Al4V	2.9
Austenitic Stainless Steel	2.5
UNS N06625, N07718	0.8
UNS R30188	0.4
17-4 PH	0.1
Other Nickel Alloys	0.1

* AA 2219 is anodic when coupled with these alloys.

The original corrosion protection system for the aluminum components consisted of a chromate conversion coating surface treatment ,epoxy primer and epoxy topcoat. Bolted joints are sealed with a 2 component polysulfide sealant and all fasteners were oversealed. The original evaluation of corrosion protection materials for the aluminum alloys was performed by NASA. The coupons used for these evaluations were painted without being scribed or intentionally damaged. The evaluation included coastal(beach) exposure, sea water (ocean and Gulf of Mexico) immersion and limited galvanic evaluations (ocean) of the coated aluminum with the TVC system alloys [1]. The result of the evaluation was the recommendation to use these systems because they performed well in all evaluations. The original coating system was recently replaced with a chromate conversion coating, barium chromate epoxy primer and polyurethane topcoat. A significant design change which had a positive affect on the aft skirt corrosion was the addition of polyurethane foam to the interior surfaces (except behind the TVC system) of the aft skirt on flight STS-5 (11/11/82).

Initial Flight Results

The corrosion which resulted from the first flights of the SRB exceeded most expectations. Corrosion primarily occurred at locations where the coatings had been damaged during the descent and splashdown of the SRB. Damage sources included propellant slag, thermal blanket debris, water impact force and SRM exhaust hot gases. Also noted as contributing to the problem was poor coating application technique. A committee was formed to formally evaluate the postflight condition of the hardware and

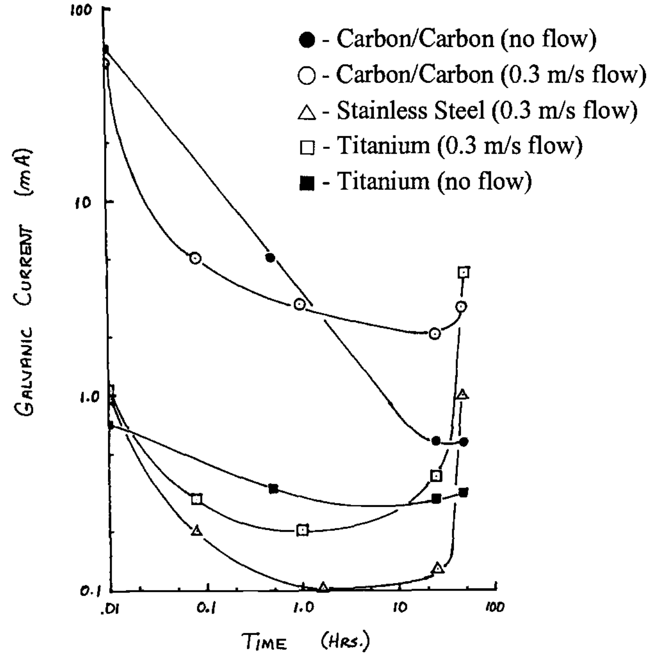

Figure 3- *Galvanic couple currents for AA 2219 during a 48 hour exposure period.*

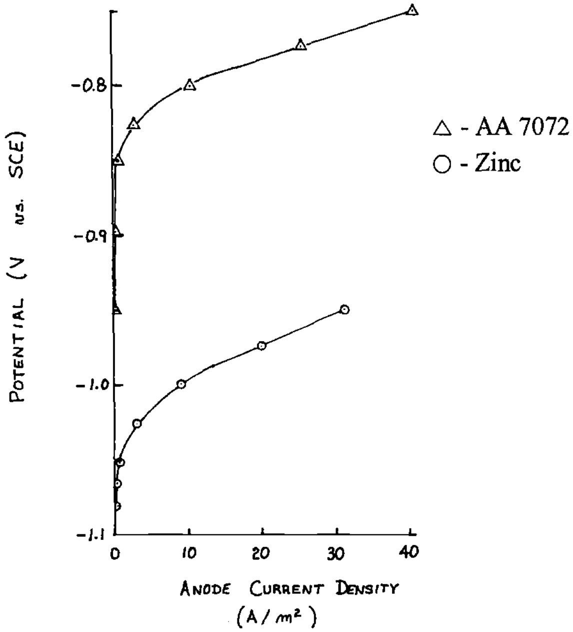

Figure 4- *Polarization of anode materials (0.3 m/s flow).*

provide recommendations for effective corrosion control activities. Problems noted during the investigation included dissimilar metal and crevice corrosion, coating damage during descent and a number of workmanship issues. The committee provided recommendations that included addressing the galvanic, pitting and crevice corrosion situations. These recommendations provided the foundation for subsequent corrosion control and cathodic protection activities for the aft skirt structure.

SRB Cathodic Protection System Design

The approach for cathodic protection focused upon the use of sacrificial anodes instead of impressed current systems. This was due to the relative simplicity of anodes and the fact that anodes could be deployed with minimal flight hardware design changes. Initial anode system design focused on understanding the contributions of the cathodic materials to the overall corrosion problem, evaluating anode alloys, determining anode effectiveness under a special foam coating, and developing a systematic approach to reduce the overall galvanic damage to the aluminum aft skirt structure. To address the first three issues, a series of experiments were conducted with the alloy to be protected (AA 2219), the primary cathode areas (18-8 stainless steel, Ti6Al4V titanium alloy and carbon/carbon phenolic composite) and the anode candidates (zinc and AA 7072). The experiments conducted included polarization of the cathode and candidate anode materials and a determination of the sacrificial response of the anode materials for each of the primary cathode materials. The electrolyte was aerated seawater.

Experimental Results

The testing confirmed that the carbon/carbon material was the greatest contributor to the galvanic problems (Figure 2) and that a great amount of current would be required to polarize this material to reach a potential near that of the 2219 AA (-0.82 V vs. saturated calomel electrode (SCE) [2]). A surprising result was that flowing seawater on the carbon/carbon material more than doubled the current required to polarize the cathode to -0.8 V (vs. SCE). Also, the stainless steel and titanium alloys would require very little current to be polarized to the same potential. In evaluating the corrosion currents of the primary cathode materials, it was determined (Figure 3) that the carbon/carbon material initially had a high current which continued to decrease with exposure time. The stainless steel and titanium materials' corrosion current acted similar to that of the carbon/carbon, except the magnitude of the current was significantly less.

The anode polarization data (Figure 4) shows that the 7072 alloy would not be able to polarize the cathode-anode pair as easily as the zinc anode material. To determine the relative amount of anode area that would be required to polarize the respective cathode surface the amount of anode area was varied in relation to the cathode area (Figure 5). From these results (Figure 5) it was decided that for the stainless steel and titanium surfaces the anode area should be about 20-25% of the cathode area and for the carbon/carbon material the anode area should be about 30-40% of the cathode area. Additional anode area beyond these percentages would provide minimal benefit to the aluminum protection. Testing of anode performance under the polyurethane foam indicated that once the foam was saturated with water the anodes performed normally.

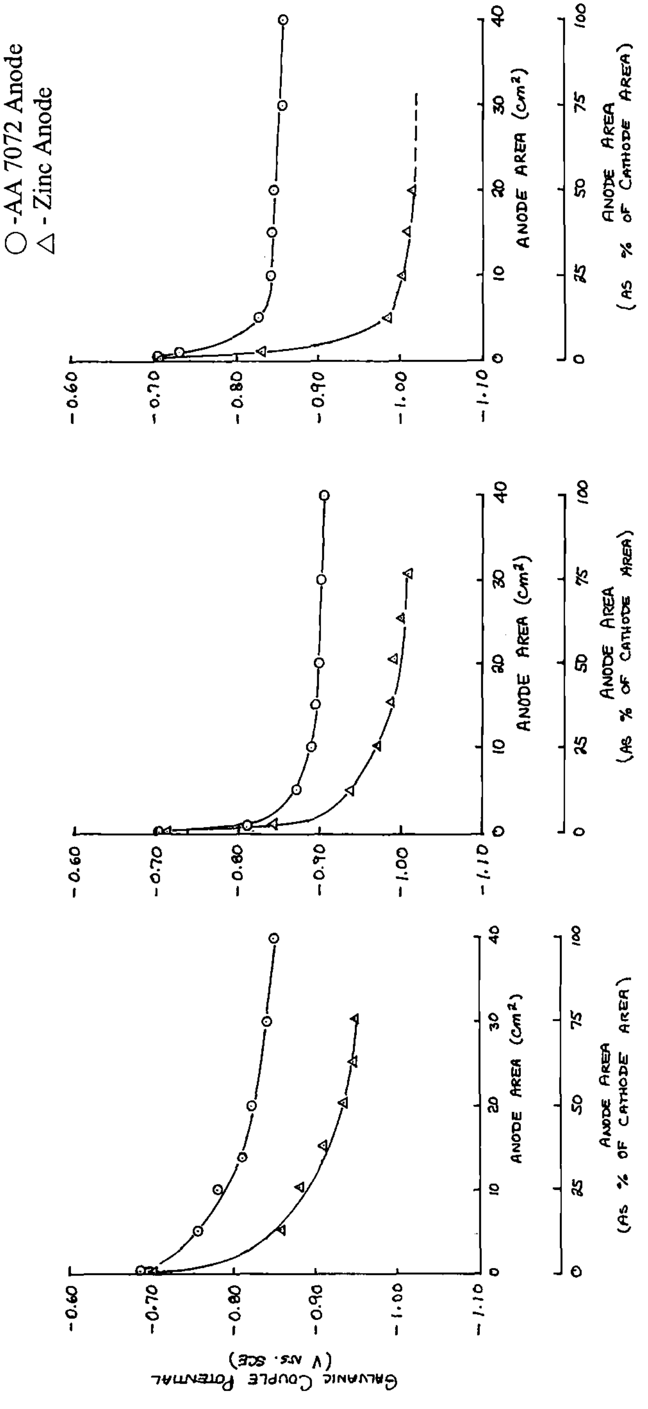

Carbon/Carbon Cathode

Stainless Steel Cathode

Titanium Cathode

Figure 5 - *Galvanic couple potential of the cathode materials with AA 2219 in 0.3 m/s flowing seawater (40 cm² cathode area).*

However, the length of time required to obtain water saturation could vary. Due to the unknown water saturation rate of the foam, it was decided not to deploy anodes under foam.

Protection Approach

The original plan for corrosion protection of the aft skirts included the incorporation of zinc anode area, coating of cathodic surface area and isolating the SRM nozzle. The exposed cathode areas within the aft skirt (including alloys listed in Table 1) total to approximately 23 m^2. Based upon the galvanic couple potential results (Figure 5) it was planned to deploy a total of 6.5 m^2 of zinc area to negate the cathode affects on the aluminum structure. This amount of zinc could be reduced as the cathode areas were coated (planned cathode area reduction of 5.4 m^2) and when nozzle isolation was incorporated (planned cathode area reduction of 16.1 m^2) into the design. The hardware areas targeted for anode deployment were within the TVC system and on the SRM nozzle. The goal was to achieve a galvanic potential of -1.0 V vs. SCE on the aluminum structure and components.

Protection System Implementation

Anode deployment occurred over a two year period beginning with STS-6 (April 4, 1983) and completed with STS-23 (April 21, 1985). The anode deployment schedule is shown in Table 2. The anode area was obtained through the use of solid zinc anodes and thermally applied (flame spray) zinc coatings. The initial location of anode deployment was on 2 TVC components. The next deployment was through the use of a diver installed anode (DIA). The anode is usually installed within four hours of SRB splashdown. It should be noted that both of these deployments were made prior to the testing program discussed under the System Design. The total deployed anode area was 3.09 m^2. While additional surface areas were planned for thermally applied zinc, new post Challenger accident non-destructive evaluation requirements halted the implementation.

The other actions from the original plan, the coating of cathodic surface area and isolating the SRM nozzle, were pursued with little success. The application of coatings to cathodic areas was met with tremendous resistance from the design engineering and operations organizations. They believed that since the cathodic components would not corrode they did not need to be "painted". They could not be convinced of the benefits of coating the cathode areas and stopped this part of the plan. Regarding the isolation of the SRM nozzle, several meetings were held with representatives of Thiokol Corporation (contractor for the SRM). The result of the meetings was that there were several paths which provided electrical grounding and that it would require a major redesign of the nozzle to motorcase interface to allow for severing the electrical ground. This aspect of the plan was halted. One positive item which came out of the meetings was that a more accurate calculation of the active carbon/carbon nozzle liner area was obtained from the Thiokol engineers. Based upon the nozzle design, they determined the active area to be approximately 5.2 m^2 as opposed to the 16.1 m^2 area originally calculated.

Table 2-*SRB Anode Deployment Schedule.*

Deployment Date / Flight	Location	Anode Surface Area(m^2)
April 4, 1983 / STS-6	TVC System-components	0.13
August 30, 1983 / STS-8	Diver attached to aft skirt HDP	0.61
April 6, 1984 / STS-13	DOP	0.35
November 8, 1984 / STS-19	Nozzle-Thermal Curtain Brackets	0.32
January 24, 1985 / STS-20	TVC System-covers	1.03
April 21, 1985 / STS-23	Nozzle-Thermal Curtain Brackets	0.65

Data Collection

To evaluate the effectiveness of the anodes, potential measurement surveys were conducted. The survey was performed while the SRB was in the port. This is usually between 24-48 hours after SRB splash down. Representative results from the potential surveys conducted during the anode deployment activities are presented in Tables 3a and 3b.

Table 3a -*Galvanic Potential Measurements (-V vs. SCE).*

Flight	Total Anode Area(m^2)	Measurement Location			
		Nozzle carbon/ carbon	Aft Skirt Interior Structure	TVC Frame	TVC Exhaust Duct
STS-5 11/11/82	0	-	0.71	-	0.72
STS-11 2/3/84	0.74	0.34	0.85	-	0.81
STS-17 10/5/84	1.10	0.31	0.84	0.85	0.85
STS-19 11/8/84	1.42	0.41	0.86	0.88	0.85
STS-20 1/24/85	2.45	0.15	0.89	0.92	0.88
STS-26 7/29/85	3.10	0.42	0.90	0.96	0.91
STS-27 8/27/85	3.10	0.38	0.93	0.96	0.89
STS-31 11/26/85	3.10	0.36	0.93	0.97	0.89

Table 3b -*Galvanic Potential Measurements (-V vs. SCE).*

Flight	Total Anode Area(m^2)	Measurement Location		
		Blast Container	Diver Operated Plug	Diver Installed Anode
STS-5 11/11/82	0	0.71	-	-
STS-11 2/3/84	0.74	0.85	-	0.95
STS-17 10/5/84	1.10	0.84	0.74	0.96
STS-19 11/8/84	1.42	0.83	0.81	0.95
STS-20 1/24/85	2.45	-	0.92	1.01
STS-26 7/29/85	3.10	0.80	0.86	0.98
STS-27 8/27/85	3.10	0.85	0.89	1.00
STS-31 11/26/85	3.10	0.86	0.92	1.00

As can be observed from the potential measurements, the aluminum structure potential has been shifted - 0.22 V from the pre-anode condition. Also, the aluminum TVC frame is almost at the -1.0 V goal. Visual inspection of the aluminum components after removal from the water confirmed that the anodes were performing well, with minimal pitting observed at coating damage locations. While these results are good, several significant issues have arisen with the use of the anodes. The most significant is the desire to stop installing the DIA.

The use of a DIA has been controversial from the beginning of the effort to protect the aft skirt from corrosion. The DIA was chosen because it was the quickest way to get anode area on to the SRB. During the cathodic protection design studies the galvanic current of the AA 2219 to cathode couples were evaluated (Figures 3a and 3b) with the finding that the cathode areas generate high corrosion currents initially (within the first 4-5 hours). This would indicate that the zinc anode area needs to be available immediately upon water impact. The DIA is the last item installed on the SRB during recovery. Historically the DIA is usually installed within 6.5 hours of water impact. However, there is no guarantee that the DIA will be installed at all (especially during rough seas). Recently, concerns have been raised about diver safety during the recovery operations and used as justification for elimination of the DIA. As a result of the planned elimination of the DIA there is a renewed interest in adding more anode area directly to the aft skirt structure.

New Approaches to Anode Area

The original plan developed for the skirt protection emphasized applying zinc directly to the TVC frames and aft skirt interior using thermal spray. Since the plan was approved, new constraints have been placed on these locations. Current postflight hardware evaluations include the use of dye penetrant and ultrasonic nondestructive inspections. When several zinc coated TVC covers required NDE after being straightened, we found that removing the metallic zinc safely and quickly was very difficult. Since the zinc is not easily removed, the structural design group would not allow the application of metallic zinc directly to the structural components. As a result of this situation, two different approaches are being investigated to increase the anode areas.

To achieve the originally recommended 6.5 m^2 of zinc surface area without enduring a significant weight penalty, it was conceptualized that an inorganic zinc rich primer (IZRP) could possibly provide the required protection. An additional concept that was recently introduced was to deploy anode area by using an expanded zinc (metal foam) product. Both of these approaches will be discussed in greater detail beginning with the IZRP.

Inorganic Zinc Rich Primer Anode Area

The advantages of using the primer included that it could be easily removed using conventional blasting techniques with plastic media, the primer could replace the coating system currently applied to the structures, the coating would offer better abrasion and heat resistance than the current coating system and that no special processes/equipment would be required to apply the IZRP to the hardware. While these advantages are important, several significant issues have to be addressed to assure that the hardware will be adequately protected. Issues raised included adhesion of the IZRP to aluminum, coating reuse and the anode performance of the coating. To determine the feasibility of the concept, limited adhesion and corrosion evaluations were performed.

AA 2219-T87 panels were prepared by cleaning the surface, abrasive blasting (anchor profile of 25-40 μm) or applying a pretreatment and applying a solvent borne, environmentally compliant IZRP to achieve a dry film thickness of approximately 75 μm. After completion of cure, pull off adhesion tests were performed. The results of these tests are shown in Table 4. It should be noted that the zinc rich primer flaked off of the conversion coated surface prior to bonding anvils to the painted surface. This testing established that the IZRP could meet the minimum flight coating adhesion requirements of 4826 kPa.

Table 4-*Inorganic Zinc Rich Primer Applied to Aluminum Adhesion Testing Results.*

Surface Preparation Technique	Coating Adhesion(kPa)
Chromate Conversion Coating	N/A*
glass bead(MIL-G-9954, #6) blast	5592
Aluminum oxide(20-30 mesh) blast	6433
sodium bicarbonate blast	7267

*Coating debonded from surface prior to performing adhesion test.

The initial anode performance of the IZRP was assessed through the use of electrochemical impedance spectroscopy (EIS) and polarization resistance techniques [3]. The evaluation compared the performance of an epoxy zinc rich primer currently used on the SRB with a solvent based inorganic zinc rich primer. The results indicated that the IZRP would provide sufficient protection to the aft skirt, however, it was recommended that additional testing be performed to simulate the aft skirt use conditions.

Metal Zinc Foam

The concept of using a zinc foam for anode material came from work that was being performed using aluminum foam for energy absorption on the aft skirt hold down post frangible nuts. Discussions were held with the aluminum foam vendor to determine their ability to process zinc metal into foam. They reported that they have made zinc foam material for a battery company and were interested in our possible use of zinc foam material. They reported that with a foam density of 1.2 pores per mm, it was possible to obtain 4.2 m^2 surface area with a volume of 0.23 m^3 and weight of 3.2 kg. Samples are being obtained to further evaluate the performance of this anode material.

Summary

The as-implemented cathodic protection system has performed well in actual use. While the deployed anode area is approximately 50% of the original recommendation, no signs of aggressive corrosive attack have been observed in damaged coating locations. The disparity between theory and real life may be explained by the fact that the cathode areas were calculated on a worst-case basis: all of the carbon/carbon nozzle liner completely intact and active. In reality, the splashdown/water impact loads tend to cause flexing of the nozzle and debonding of the carbon/carbon material. The only planned improvement of the cathodic protection system will occur in conjunction with the deletion of the DIA. While the DIA accounts for 20% of the deployed anode area, the planned new area will attempt to fully implement the original recommendation of 6.5 m^2 total anode area. Evaluation of the IZRP and zinc metal foam solutions is underway and the new application will be ready for deployment before the DIA is deleted.

References

[1] "SRB Materials and Processes Assessment From Laboratory and Ocean Environmental Tests", NASA TM-78187, National Aeronautics and Space Administration, Washington, DC, 1978.

[2] Hollingsworth, E. H. and Hunsicker, H. Y., "Corrosion of Aluminum and Aluminum Alloys", *Metals Handbook*, 9th Ed., Vol. 13, Corrosion, ASM International, Metals Park, OH, 1987, p. 584.

[3] Danford, M. D., Walsh, D. W., and Mendrek, M. J., "The Corrosion Protection of 2219-T87 Aluminum by Organic and Inorganic Zinc-Rich Primers", NASA TP-3534, National Aeronautics and Space Administration, Washington, DC, February 1, 1995.

ISBN 0-8031-2623-9